CHAPTER 14

SERVOACTUATORS FOR CLOSED-LOOP CONTROL

Karl N. Reid
College of Engineering, Architecture and Technology
Oklahoma State University
Stillwater, Oklahoma

Syed Hamid
Halliburton Services
Duncan, Oklahoma

1 INTRODUCTION **543**
1.1 Definitions 543
1.2 Applications 543
1.3 Mathematical Models 544

2 ELECTRICAL SERVOMOTORS **544**

3 DIRECT-CURRENT SERVOMOTORS **546**
3.1 Brushed dc Servomotors 546
3.2 Brushless dc Servomotors 552

4 ALTERNATING-CURRENT SERVOMOTORS **557**
4.1 Types of ac servomotors 557
4.2 Mathematical Model 559

5 STEPPER MOTORS **562**
5.1 Operation 563
5.2 Types of Stepper Motors 564
5.3 Mathematical Model of a Permanent-Magnet Stepper Motor 567
5.4 Numerical Example 567

6 ELECTRICAL MODULATORS **569**
6.1 Direct-Current Motor Modulators 569
6.2 Stepper Motor Modulators 573

7 HYDRAULIC SERVOMOTORS **574**
7.1 Linear-Motion Servomotors 574
7.2 Rotary-Motion Servomotors 575
7.3 Mathemtical Models 576

8 HYDRAULIC MODULATORS **582**
8.1 Servovalve Design and Operation 582
8.2 Mathematical Model of a Spool-Type Valve 584
8.3 Mathematical Models for an Electrohydraulic Servovalve 588

9 ELECTROMECHANICAL AND ELECTROHYDRAULIC SERVOSYSTEMS **590**
9.1 Typical Configurations of Electromechanical Servosystems 590
9.2 Typical Configurations of Electrohydraulic Servosystems 590
9.3 Comparison of Electromechanical and Electrohydraulic Servosystems 592

10 STEADY-STATE AND DYNAMIC BEHAVIOR OF SERVOACTUATORS AND SERVOSYSTEMS **596**
10.1 Electromechanical Servoactuators 596
10.2 Electromechanical Servosystems 602
10.3 Electrohydraulic Servoactuators 604
10.4 Electrohydraulic Servosystems 606
10.5 Hydraulic Compensation 610
10.6 Range of Control for Electrodydraulic and Electromechanical Servosystems 616

REFERENCES **617**

BIBLIOGRAPHY **618**

Reprinted from *Instrumentation and Control,* Wiley, New York, 1990 by permission of the publisher.

1 INTRODUCTION

1.1 Definitions

A servoactuator is an open-loop system that controls the linear or rotary motion of a load in response to an input command (Fig. 1*a*). Feedback may be used with a servoactuator to produce a closed-loop system referred to as a servosystem (Fig. 1*b*). Servoactuators are normally "rate-type" systems, in that an input command results in an output velocity for steady-state operation. Position feedback must be used with the rate-type system to produce a servosystem for position control. If high-accuracy velocity control is required, velocity feedback may be used with the servoactuator. Or, if high-accuracy force (or torque) control is required, force (or torque) feedback may be used.

The term "servomotor" designates the various types of higher level energy converters such as electrical and hydraulic motors. The servomotor provides the muscle function of the servoactuator. The "modulator" provides a conversion of the low-power input command (for the servoactuator) or the error signal (for the servosystem) to a high-power output that operates the servomotor. The "transducer" provides the feedback in the case of the servosystem. The input to the servoactuator or servosystem can be electronic, mechanical, hydraulic, or pneumatic. And depending on the energy conversion medium, servoactuators can be of the electromechanical, electrohydraulic, electropneumatic, or hydromechanical types.

1.2 Applications

Early development of servoactuators and servosystems was predominantly in electropneumatics (in the process control industry).[1] With the advent of microprocessors and the development of high-coercive-strength magnetic materials (such as samarium cobalt and neodium). electromechanical servosystems find the largest applications in modem industry.[2] Table 1 describes the servocomponents (modulator, servomotor, and transducer) for the various implementations. Applications range from fairly simple open-loop systems such as the hydraulic

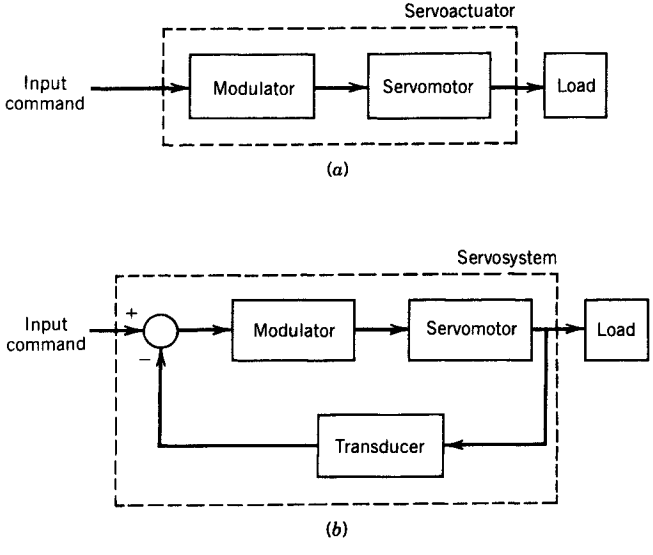


Figure 1 (*a*) Servoactuator (open loop); (*b*) servosystem (closed loop).

Table 1 Servosystem Components

System Type	Modulator	Servomotor	Transducer
Electromechanical	Amplifier	Servomotor ac, dc Linear/Rotary	Position, velocity, torque
	Driver	Brushless servomotor	
	Translator/driver	Stepper motor	
Electrohydraulic	Servovalve	Hydraulic motor cylinder	Position, velocity force, pressure torque
Electropneumatic	Servovalve	Airmotor, cylinder	Position, velocity, force, pressure torque,

controls on a backhoe to complex feedback systems in robotics and aerospace vehicles. Figure 2 shows a typical linear output servosystem designed for use in a wide variety of motion control applications. A threephase brushless motor is modulated by a pulse-width-modulated controller (not shown in Fig. 2; see Ref. 3). A ballscrew is used to convert rotary motion to linear motion. Feedback is provided by a tachometer.

1.3 Mathematical Models

Mathematical models of the various components of a servoactuator are needed for component selection to meet a given set of performance specifications. These specifications may consist of moving a given load through a given displacement or velocity profile in a specified time or, equivalently, following displacement or velocity commands generated by other subsystems or by an operator. The mathematical model of a component describes the steady-state and/or dynamic performance characteristics of that component. Mathematical models are presented in this chapter for the components typically used in high-performance servoactuators and servosystems. Examples are presented to illustrate the use of mathematical models in the prediction of steady-state and dynamic performance of servoactuators and servosystems.

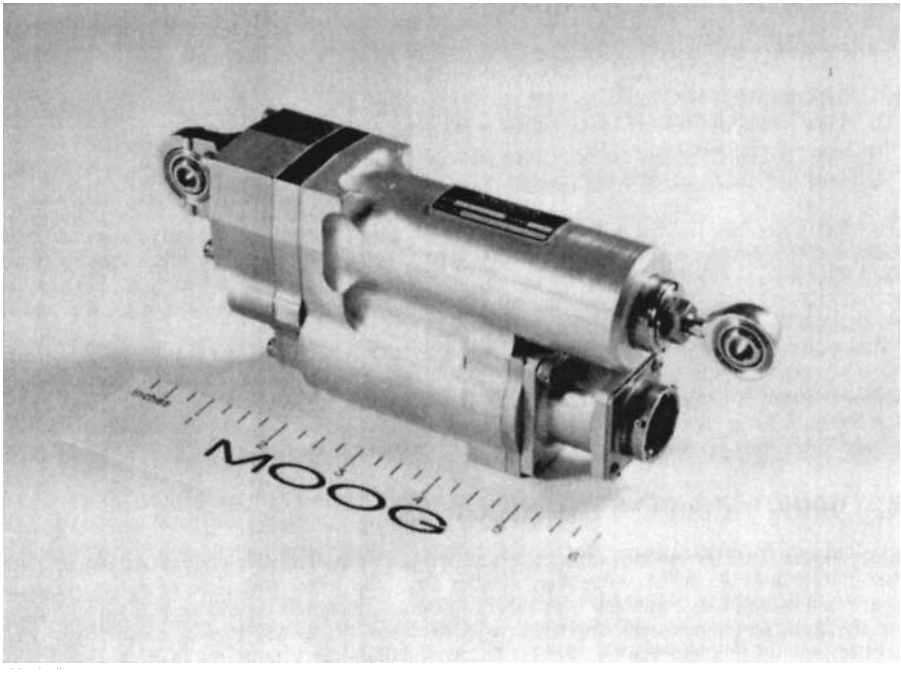
2 ELECTRICAL SERVOMOTORS

Electrical servomotors may be classified by the following characteristics:

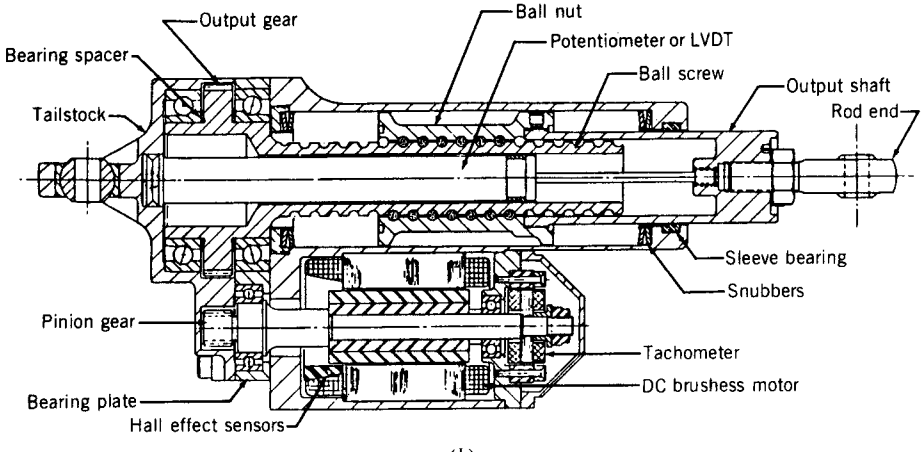
1. Type of power [direct current (dc) or alternating current (ac)]
2. Type of motion executed (continuous or discrete, rotary or translatory)
3. Type of commutation (mechanical or electronic)
4. Method of magnetic field generation (permanent magnet or electromagnetic)

Accordingly there are dc and ac servomotors of both the permanent-magnet and field-wound types. Stepper motors belong to the discrete motion type. The rather uncommon linear motor executes translatory motion. Brushless dc motors are of the electronic commutation type. For the sake of simplicity, electrical servomotors are broadly classified here into four categories: dc and ac servomotors, stepper motors, and linear servomotors.

Electrical servomotors offer several advantages over their hydraulic and pneumatic counterparts. These advantages include (a) compactness (facilitated by availability of high-coercive-strength magnetic materials such as samarium–cobalt or neodium), (b) low cost, (c)



(*a*)



(*b*)

Figure 2 (*a*) Electromechanical servosystem; (*b*) cross section of an electromechanical servosystem. (Courtesy of Moog, Inc., East Aurora, NY.)

high reliability, (d) cleanliness, (e) ease of control function implementation, (f) portability due to operation at low dc voltage levels, and (g) large bandwidth due to high torque/inertia ratios.

3 DIRECT-CURRENT SERVOMOTORS

Direct-current servomotors offer certain advantages over ac servomotors. These advantages are higher reliability, smaller size, and lower cost. Use of epoxy resins and improved brush designs combined with superior magnetic materials contribute to these advantages. Direct-current servomotors are compatible with thyristors (silicon controlled rectifiers, SCR) and transistor amplifiers, which facilitates control implementation. Typical dc servomotors range in power from fractional horsepower to several thousand horsepower. Conventional brushed dc motors theoretically can be used as servomotors. However, in lower horsepower levels (10 hp or less) they are not preferred.

3.1 Brushed dc Servomotors

In the dc servomotor, the interaction of two magnetic fields (either one or both generated electrically) results in mechanical motion of an armature. A typical permanent-magnet dc motor is illustrated in Fig. 3. The permanent magnet is sometimes replaced by a field winding to generate the magnetic field. The field winding may be connected in three different ways to the armature winding: series, shunt, or compound. Table 2 summarizes the basic features of the various configurations along with the resultant performance characteristics. Table 3 shows typical upper limits of dc servomotor performance.[4]

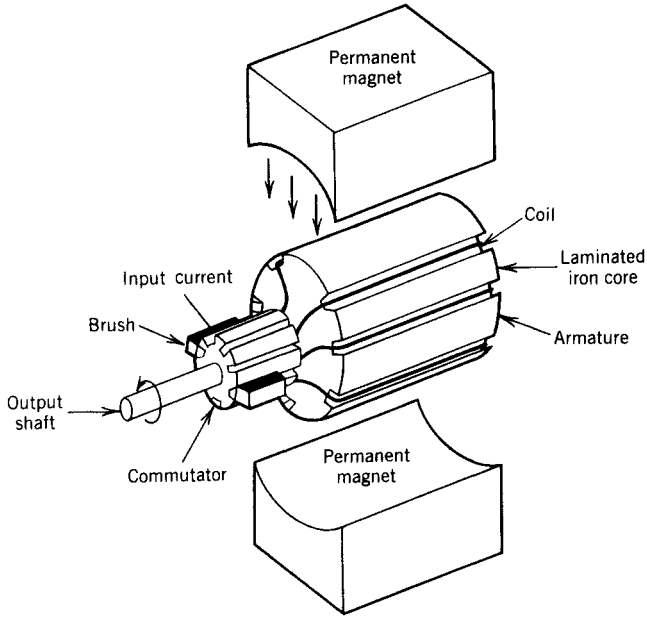


Figure 3 Conventional permanent-magnet motor.

Table 2 dc Servomotor Classification

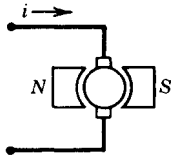
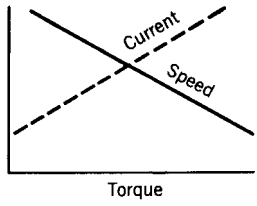
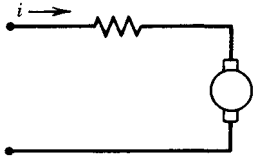
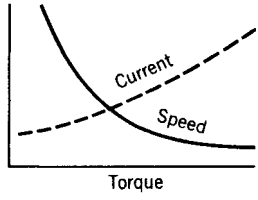
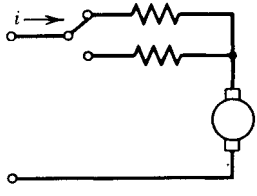
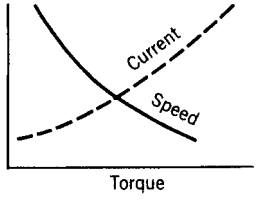
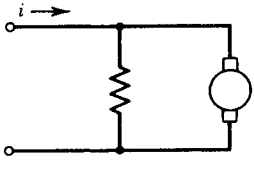
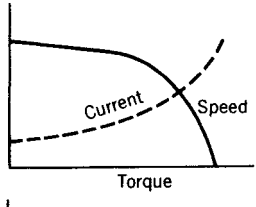
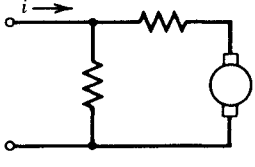
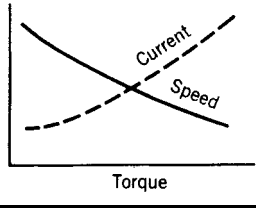
Motor Type	Configuration	Typical Steady-State Characteristics	Salient Features
Permanent magnet			No power required for field generation Runs Cooler Torque-speed characteristics is linear Compactness
Straight series			Large starting torque
Split series			Allows quick reversing
Shunt			Low starting torque Finite speed at zero torque
Compound			High starting torque Complex circuitry required for reversing

Table 3 Upper Limits of dc Servomotor Performance

Motor Type	Maximum Power (hp)	Maximum Speed (rmp)	Torque/Inertia Ratio (rad/s^2)	Maximum Bandwidth (rad/s)
Moving coil	0.5–1	4500–5500	200–250	1500
Printed circuit	7	3000–4000	130–220	1000
Permanent magnet	10–15	850–3000	15–30	100

Source: From Ref. 4.

The split-series field-wound motor has two windings, one for each direction of rotation. A manual switch is usually employed to activate the appropriate winding. The two windings of the compound motor are always excited and result in a high starting torque with good linearity. All of the fieldwound motors are self-excited with the residual magnetism.

Permanent-Magnet Motors

Permanent-magnet (PM) motors are the most extensively used for servomotors because they generate less heat and have higher efficiency and more compactness than field-excited motors. There are three types of PM motors with mechanical commutation: (1) iron core, (2) surface wound, and (3) moving coil. Figure 4 shows the construction of the three types. Details of the advantages and disadvantages of each type may be found in Ref. 5.

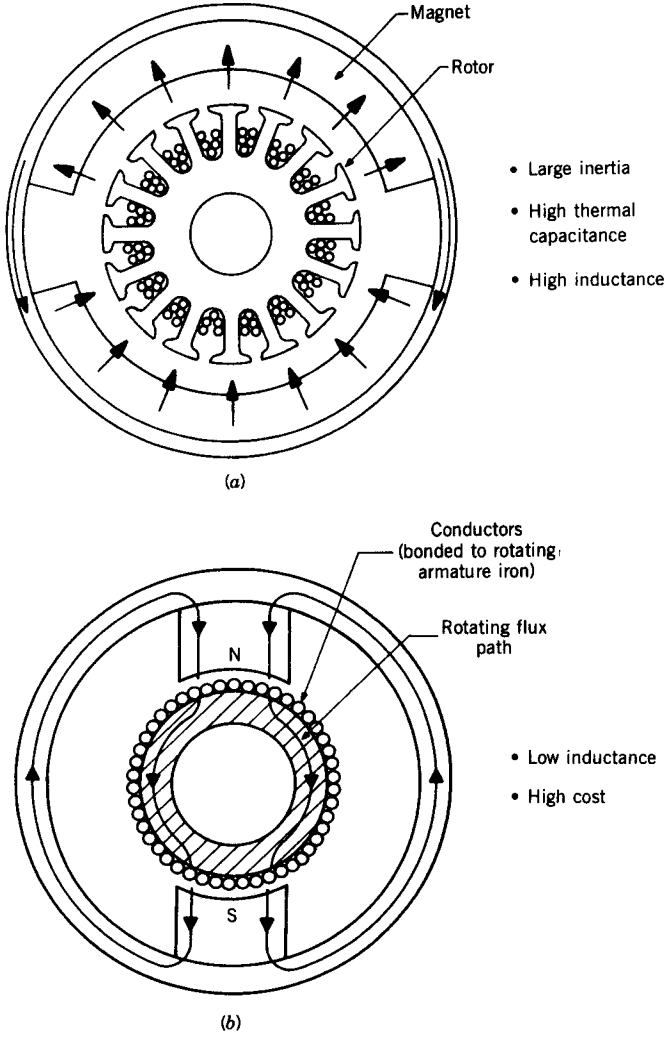


Figure 4 (*a*) Iron core; (*b*) surface wound.

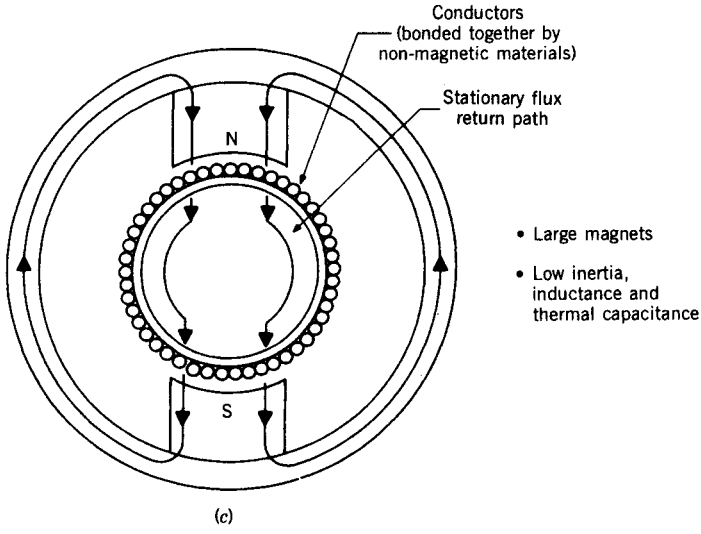


Figure 4 (*Continued*) (*c*) Moving coil. (From Ref. 5.)

Mathematical Model of a Permanent-Magnet Servomotor

Comprehensive presentations on mathematical modeling of dc servomotors are given in Refs. 6–9. A simplified dynamic model is presented here.

The mathematical model of a permanent-magnet dc motor is obtained by lumping the inductance and resistance of the armature winding as shown in Fig. 5. The resulting equations are given:

Voltage equations:

$$v_a = L_a \frac{di}{dt} + R_a i + e_b \tag{1}$$

$$e_b = K_E \Omega_m \tag{2}$$

Torque balance equation:

$$K_T i = J_m \frac{d\Omega_m}{dt} + B_m \Omega_m + T_{fm} + T_L \tag{3}$$

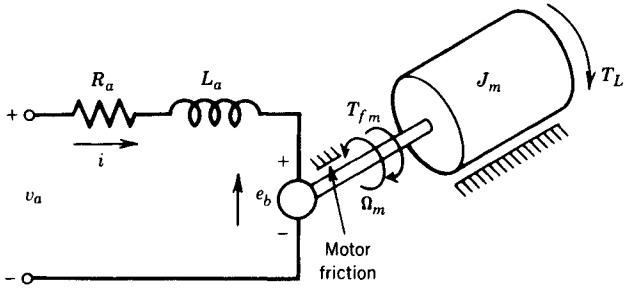


Figure 5 Lumped-parameter model of a permanent motor.

Taking Laplace transforms of Eqs. (1)–(3) gives, after algebraic manipulation,

$$\Omega_m(s) = G_1(s)V_a(s) - G_2(s)\,[T_{fm}(s) + T_L(s)] \tag{4}$$

where the transfer functions G_1 and G_2 are given by

$$G_1(s) = \frac{K_T}{R_aB_m(\tau_e s + 1)(\tau_m s + 1) + K_T K_E} \tag{5}$$

$$G_2(s) = \frac{R_a(\tau_e s + 1)}{R_aB_m(\tau_e s + 1)(\tau_m s + 1) + K_T K_E} \tag{6}$$

and the parameters are defined as follows:

B_m = viscous damping in motor (N·m·s/rad)
e_b = back electromotive force (emf) (V)
i = current through armature (A)
J_m = polar moment of inertia of armature (N·m·s^2/rad)
$K_E = z'\phi P/60$ = motor voltage constant or back emf constant (V·s/rad)
$K_T = z'\phi P/2\pi$ = motor torque constant (N·m/A)
L_a = armature inductance (H)
P = number of poles
R_a = armature resistance (Ω)
s = Laplace operator
t = time (s)
T_{fm} = Coulomb friction torque in motor (N·m)
T_L = external load torque
v_a = voltage applied to armature (V)
$V_a(s)$ = Laplace transform of armature voltage $v_a(t)$
z' = number of conductors per parallel path in armature
θ_m = angular position of motor shaft (rad)
ϕ = magnetic flux per pole (Wb)
$\tau_e = L_a/R_a$ = electrical time constant (s)
$\tau_m = J_m/B_m$ = mechanical time constant (s)†
Ω_m = angular velocity of motor (rad/s)
$\Omega_m(s)$ = laplace transform of motor angular velocity

Equation (4) can be simplified if the armature inductance is small (making the electrical time constant τ_e negligible) and the Coulomb friction and load torque are assumed zero. The result is

$$\frac{\Omega_m(s)}{V_a(s)} = \frac{K_m}{\tau s + 1} \tag{7}$$

where

$$K_m = \frac{K_T}{R_aB_m + K_T K_E} \quad \text{(motor constant)} \tag{8}$$

and

† Some servomotor manufacturers define τ_m differently. For example, Electro-Craft[9] defines the mechanical time constant as $\tau_m = (R_aJ_m)/(K_T K_E)$.

$$\tau = \frac{R_a J_m}{R_a B_m + K_T K_E} \tag{9}$$

Reference 9 discusses cases where the electrical time constant cannot be neglected.

The preceding mathematical models assume a voltage input. For applications where a current amplifier is used, the following approximate model should be used:

$$\frac{\Omega_m(s)}{I(s)} = \frac{K'_m}{\tau_m s + 1} \tag{10}$$

where $I(s)$ is the Laplace transform of the current input i. The motor constant in this case is

$$K'_m = \frac{K_T}{B_m} \tag{11}$$

In principle, the models developed can be applied to all of the dc motors of the various types with the appropriate input conditions. These models describe the open-loop response. For closed-loop systems with velocity or position feedback, an appropriate closed-loop transfer function can be derived easily by making use of the motor dynamic model. An example of a closed-loop system is given in Section 10.2.

Numerical Example

For Motomatic PM servomotor model number E350-MG,[10] the following specifications are given:

K_T = 3.4 in.·oz/A (0.024 N·m/A)
K_E = 2.5 V/krpm (0.024 V·s/rad)
R_a = 12.4 Ω
J_m = 2.5×10^{-4} in.·oz·s^2/rad (1.8×10^{-6} N·m·s^2/rad)
B_m = 0.015 in.·oz/krpm (1.01×10^{-6} N·m·s/rad)
T_{fm} = 0.5 in.·oz (3.5×10^{-3} N·m)
$T_{\max}$ = 2.5 in.·oz (1.8×10^{-2} N·m)
$I_{\max}$ = 0.75 A
$\Omega_{\max}$ = 10,500 rpm at no load (1099 rad/s)
L_a = 3.1 mH
τ_e = 0.25×10^{-3} s
R_{th} = thermal resistance = 13°C/W

The mechanical time constant can be computed as

$$\tau_m = \frac{J_m}{B_m} = 1.75 \text{ s} \tag{12}$$

Since $\tau_e \ll \tau_m$, Eq. (7) can be used to determine the dynamic response if the Coulomb friction and load torque are neglected. In this case, the time constant is

$$\tau = \frac{R_a J_m}{R_a B_m + K_T K_E} = 0.037 \text{ s} \tag{13}$$

and the motor constant is

$$K_m = \frac{K_T}{R_a B_m + K_T K_E} = 0.39 \text{ krpm/V} \quad (40.8 \text{ rad/V·s}) \tag{14}$$

The transfer function of Eq. 7 becomes

$$\frac{\Omega_m(s)}{V_a(s)} = \frac{40.8}{0.037s + 1} \tag{15}$$

For a step input of 1 V, the motor speed is given by

$$\Omega_m(s) = \frac{1}{s}\left(\frac{40.8}{0.037s + 1}\right) \tag{16}$$

The inverse Laplace transform gives the step response as

$$\Omega_m(t) = 40.8(1 - e^{-t/0.037}) \tag{17}$$

3.2 Brushless dc Servomotors

The development of brushless dc servomotors was an outgrowth of semiconductor devices even though the first patent was obtained with vacuum tube technology.[11] The basic construction of a brushless dc motor eliminates mechanical commutation. Instead, the commutation process is accomplished electronically with no moving contacts. Hence, the problems associated with mechanical commutation such as brush wear particles, electromagnetic interference (EMI), or arcing are eliminated. Elimination of arcing makes dc servomotors excellent candidates for applications requiring explosion-proof safety classification.

Construction

Typically, brushless motors have an inner rotor and outer stator and a configuration such as the one shown in Fig. 6*a*. However, the other configuration (i.e., inner stator and outer rotor) is also possible (see Fig. 6*b*). The former configuration with the outer stator carrying electrical windings provides excellent thermal dissipation characteristics, since both the iron and copper losses occur in the stator and the stator is better exposed to the ambient for convective heat transfer. This feature allows brushless motors to be operated at higher speeds and hence provides higher power-to-weight ratio.

Brushless dc motors range from 1 to 40 in. (0.025 to 1.02 m) in diameter with 6 in·oz (4.24×10^{-2} N·m) to 1650 ft·lb (2237 N·m) of torque capability (see Table 4). Typical applications include memory disk drives, videotape recorders, and position servos in cryogenic compressors and fuel pumps.

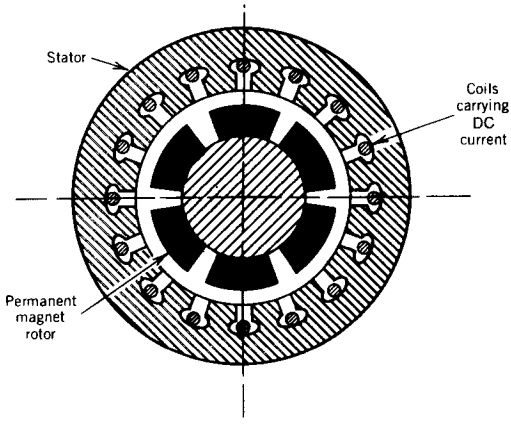
The rotors are permanent magnets made from one of three primary materials: ceramic, AlNiCo, and rare earth (such as samarium cobalt). Ceramic rotors are used in applications where cost consideration is important. Rare-earth magnets are the most expensive but provide exceptional performance. AlNiCo magnets are of medium cost and provide medium magnetic strengths.

Operation

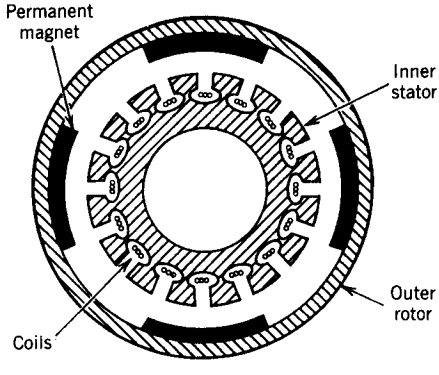
The brushless motor is operated by generating a rotating magnetic field that is 90° (electrical) out of phase with the rotor. Position sensors are used to determine the rotor position. These position sensors are of three types: phototransistor, electromagnetic, and Hall effect generators.

Commutation

An electronic module consisting of logic circuits and power amplification circuits is used to drive the motor.[3,4,12,13] This module receives rotor position information from the position sensors. The angle through which the rotor turns during the firing of a winding is called the "conduction angle." Figure 7 shows schematically a two-phase brushless motor with the driver electronics.



(*a*)



(*b*)

Figure 6 Cross section of typical brushless dc motors: (*a*) inner rotor–outer stator type; (*b*) inner stator–outer rotor type. (From Ref. 5.)

Table 4 Brushless dc Motor Performance Data

Magnet Type	Power (W)	Peak Torque (in.·oz)	Electrical Time Constant (s)	Mechanical Time Constant (s)	Torque/Inertia ratio (rad/s^2)
Ceramic	25–900	10–600	0.0002–0.0016	0.0221–0.7400	413–11,400
AlNiCo	20–280	6–5,000	0.0001–0.0030	0.0065–0.1330	465–57,500
Rare earth	25–6000	10–316,000	0.0001–0.0140	0.0024–0.0291	137–100,000

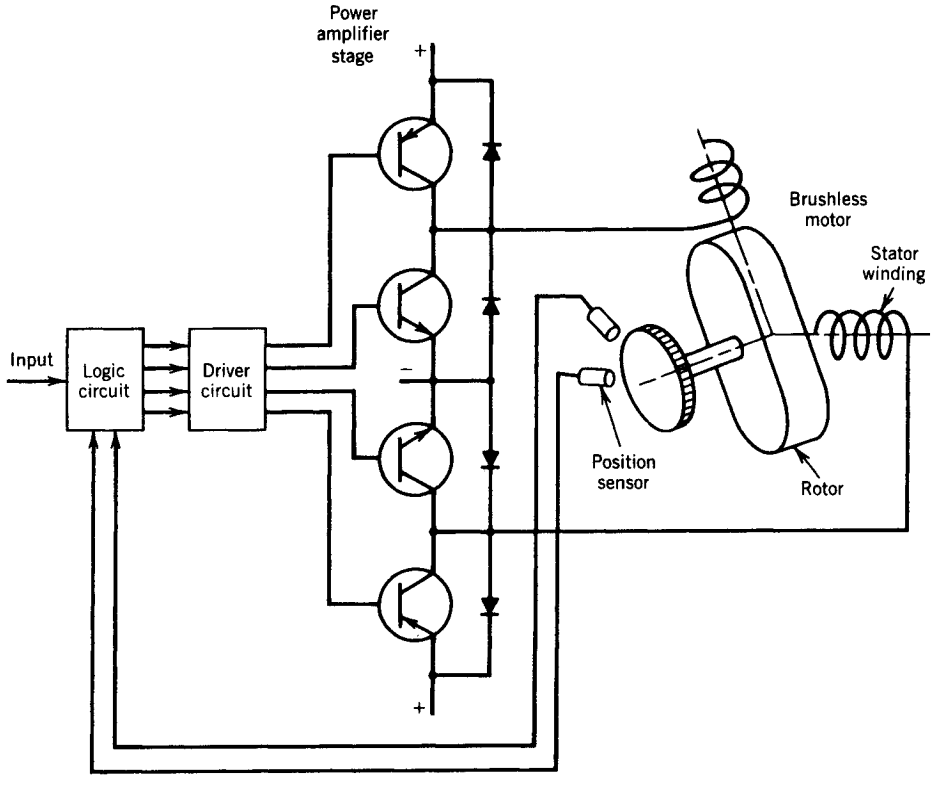


Figure 7 Two-phase brushless motor with driver electronics.

Figure 8 shows the controller circuit for a three-phase brushless motor. Each phase requires a pair of switches for commutation. Since the cost of the motor is dependent on the number of switches, there is a tendency to keep the number of phases to a minimum. Typically, three-phase motors with six switches are used. The current through the windings may be varied in a sinusoidal or a square-wave manner. The latter excitation results in a small torque ripple (17% average to peak for a two-phase motor and 7% for a three-phase motor).

Ideally, a sinusoidal torque function results in a constant torque. But sinusoidal torque function generation is technically difficult and uneconomical. An alternate approach is to design the spatial variation of the magnetic field (possible by means of high-coercive-strength magnets) to obtain a trapezoidal torque function while the input current has a square waveform (easily generated by simple transistor control circuitry, such as shown in Fig. 8). The motor torque is then approximately constant and is proportional to the maximum value of current during each cycle. The trapezoidal torque generation scheme also results in higher efficiency.

The locations of the position sensors relative to the rotor are aligned to result in appropriate timing for proper commutation. When properly commutated, a brushless motor duplicates the torque–speed characteristics of a brush-type dc motor.

The power output of the brushless motor is effectively controlled by pulse-width modulation (PWM) or pulse-frequency modulation (PFM) methods. A linear (i.e., class A) power amplifier can also be used for power control. However, use of this type of amplifier produces

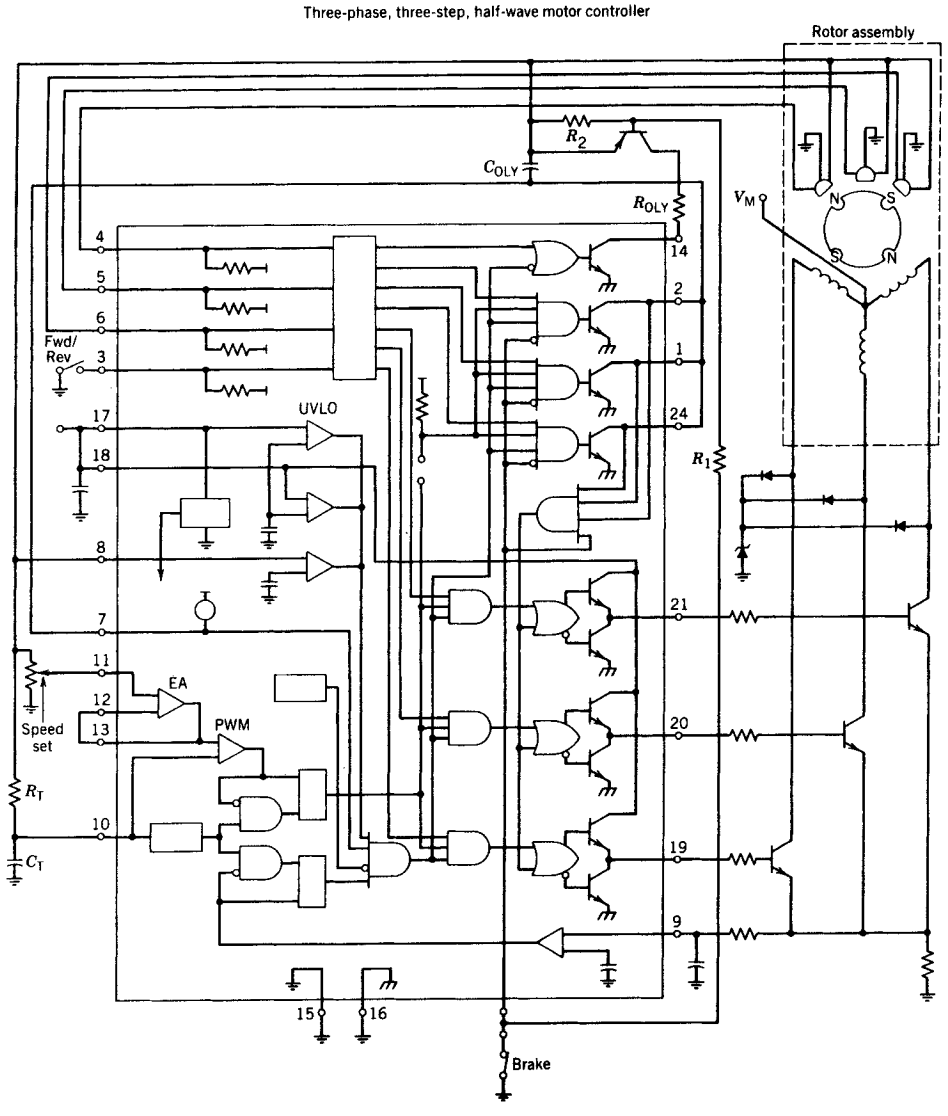


Figure 8 Three-phase brushless motor controller circuit. (From *Machine Design,* June 9, 1988, p. 140.)

back-emf conduction during the zero-voltage portions of the voltage modulation and thereby increases viscous damping. This effect can be eliminated by using a current amplifier rather than a voltage amplifier.[9]

Figure 9 shows a cross section of a brushless motor developed for use as a fin actuator. Hall effect sensors are used for position measurement.

Mathematical Model

The mathematical model required to represent a brushless dc motor is identical to that of a brush-type dc motor. Therefore the equations given in Section 3.1 are applicable.

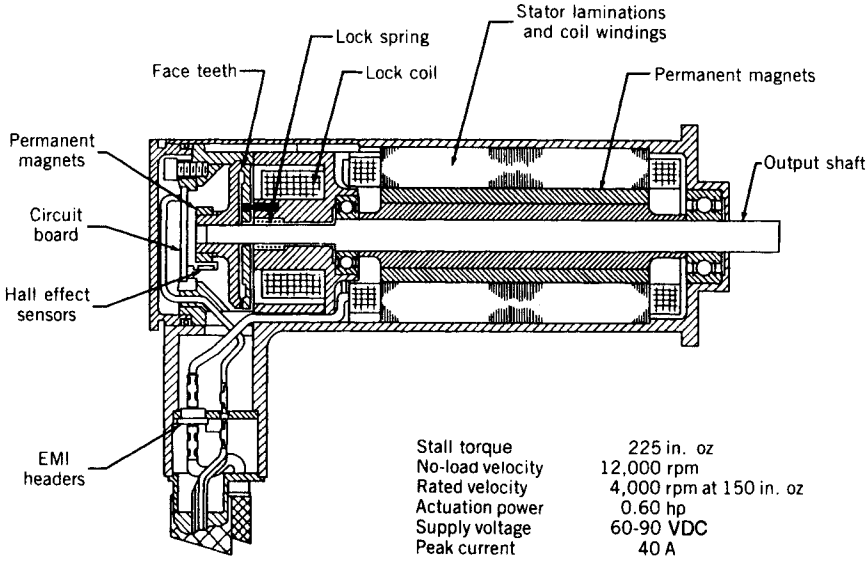


Figure 9 Cross section of a brushless dc motor. (Courtesy of Moog, Inc., East Aurora, NY.)

Numerical Example

Table 5 shows the specifications for a ceramic magnet, inside rotation-type dc brushless motor manufactured by Magnetic Technology.[14,15]

If this motor is operating at peak torque, the steady-state motor speed is given by [from Eq. (4), dropping the dynamic terms]

Table 5 Performance Data for Magnetic Technology Model 2800-153-084 Brushless dc Motor

Peak torque	40 in.·oz
Power at peak torque	175 W
Electrical time constant	0.0005 s
Mechanical time constant	0.054 s
Damping factor	0.064 in.·oz·s/rad
Moment of inertia	0.0035 in.·oz·s^2/rad
Total breakaway torque	1.5 in.·oz
Temperature rise	2°C/W
Maximum allowable winding temperature	155°C
Weight	19 oz
Number of poles	8
Number of phases	2
Resistance	8.4 Ω
Inductance	4.2 mH
Voltage at peak torque	38.2 V
Current at peak torque	4.57 A
Torque constant	8.7 in.·oz/A
Voltage constant	0.0617 V·s/rad

$$\Omega_m = \frac{K_T v_a}{R_a B_m + K_T K_E} = 309 \text{ rad/s} = 2953 \text{ rpm} \tag{18}$$

and the temperature rise is

$$\Delta T = (2°\text{C/W})\ (175 \text{ W}) = 350°\text{C} \tag{19}$$

This temperature rise is greater than the 155°C maximum allowable winding temperature. Thus the motor cannot be operated at peak torque indefinitely. The ambient temperature should be added to the temperature rise to arrive at the operating temperature of the winding.

4 ALTERNATING-CURRENT SERVOMOTORS

Alternating-current servomotors are used in applications requiring smooth speed control. These motors find widespread use in stationary industrial applications due to the ready availability of ac power.[16,17] In a majority of these applications, two-phase ac servomotors are used because of simplicity of the associated controls. Figure 10 shows a schematic of a two-phase ac servomotor. The operation of the two-phase ac servomotor is similar to an induction motor except the voltages applied to the two windings (fixed phase and control phase) are generally unequal and out of phase. The ac voltage applied to the fixed phase is held constant, and the one applied to the control phase is varied to control the motor speed. The two phases are generally 90° out of phase. Changing the phase angle from $+90°$ to $-90°$ reverses the direction of rotation of the motor. The appropriate phase angle is achieved through capacitors or other phase-shift circuits.

4.1 Types of ac Servomotors

Depending on the rotor construction, ac servomotors are classified into three types: (1) squirrel cage, (2) solid iron, and (3) drag cup (see Fig. 11). The squirrel-cage construction of the rotor is exactly the same as that of a standard induction motor. The inherent disadvantage of the squirrel-cage construction is cogging, or nonuniform armature rotation, which is minimized by skewing the bars of the cage relative to the rotor axis. The solid-iron rotor eliminates cogging. However, this configuration has a low torque-to-inertia ratio. The torque-

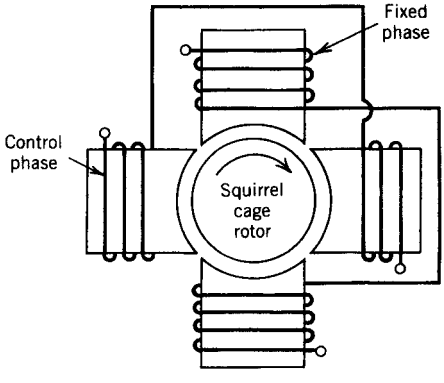
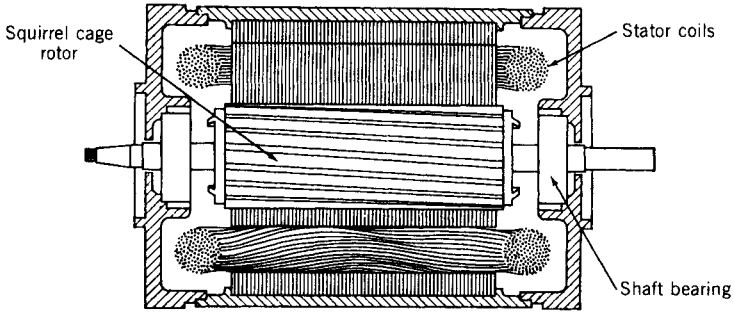
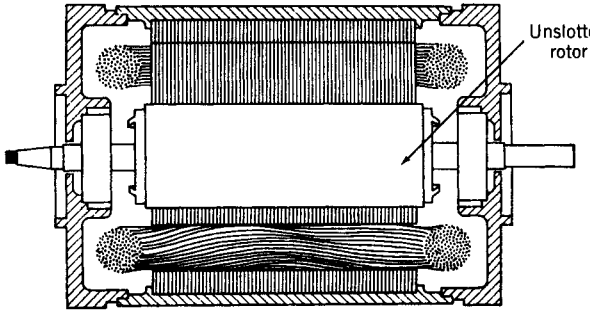


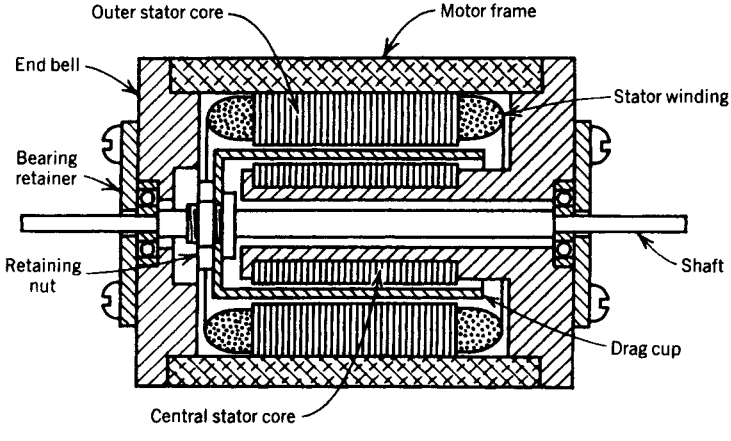
Figure 10 Two-phase ac servomotor.



(*a*)



(*b*)



(*c*)

Figure 11 Types of ac servomotors; (*a*) squirrel-case rotor; (*b*) solid-iron rotor; (*c*) drag-cup rotor. (From J. E. Gibson and F. B. Tuteur, *Control System Components,* McGraw-Hill, New York, pp. 279–280.)

to-inertia ratio is improved by the use of drag-cup construction (see Fig. 11*c*). The efficiency of ac servomotors is fairly low (5–20%), which necessitates external cooling.

4.2 Mathematical Model

Steady-State Model

Assuming linearity (i.e., operation without magnetic saturation) and using the method of symmetrical components,[18] mathematical models can be developed for the ac servomotor. Figure 12 shows an equivalent circuit of one phase of the ac servomotor. The torque developed by a two-phase servomotor in which the control phase lags the reference phase by an angle θ is given by

$$T_m = \tfrac{1}{4}\,[F_1(1 + 2k \sin\theta + k^2) - F_2(1 - 2k \sin\theta + k^2)]|v_m|^2 \tag{20}$$

The functions F_1 and F_2 are defined as follows:

$$F_1 = \frac{2}{\Omega_s}\left|\frac{Z_m}{Z_1(Z_2 + Z_m) + Z_2 Z_m}\right|^2 \frac{R_2'}{S_R} \tag{21}$$

$$F_2 = \frac{2}{\Omega_s}\left|\frac{Z_m}{Z_1(Z_2' + Z_m) + Z_2' Z_m}\right|^2 \frac{R_2'}{2 - S_R} \tag{22}$$

where f = frequency of ac voltages (Hz)
$k = v_c/v_m$
n_1 = number of turns in winding of one pole of the stator
n_2 = number of turns of rotor winding ($n_2 = 1$ for squirrel-cage rotor)
R_1 = resistance of stator (Ω)
R_2 = resistance of rotor (Ω)
$R_2' = R_2(n_1/n_2)^2$
R_m = resistance due to magnetic field (Ω)
S_R = slip ratio $= (\Omega_s - \Omega_m)/\Omega_s$
v_c = voltage applied to control phase (V)
v_m = voltage applied to fixed phase (V)
X_1 = inductive reactance of stator
X_2 = inductive reactance of rotor

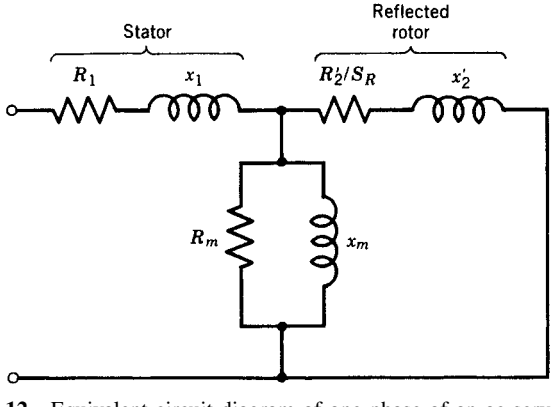


Figure 12 Equivalent circuit diagram of one phase of an ac servomotor.

$X_2' = X_2(n_1/n_2)^2$
X_m = inductive reactance due to magnetic field
Z_1 = stator impedance = $R_1 + jX_1$
Z_2 = reflected impedance of rotor at $S_R = (R_2'/S_R) + jX_2'$
Z_2' = reflected impedance of rotor at $(2 - S_R) = R_2'/(2 - S_R) + jX_2'$
Z_m = impedance due to magnetic field generation in the stator = $[(1/R_m) + (1/jX_m)]^{-1}$
θ = phase angle between fixed and control voltages
Ω_m = motor speed (rad/s)
Ω_s = synchronous speed (rad/s)

Figure 13 shows typical torque–speed characteristics for a two-phase ac motor. The characteristics are clearly nonlinear. However, about the origin they may be treated as linear.

Dynamic Model

Combining the equation of motion, the electrical lag (due to stator inductance and resistance), and the torque–speed characteristic of Eq. (20) yields a nonlinear dynamic model. For an approximate static analysis, Eq. (20) may be linearized about an operating point. For many servosystem applications the most interesting and useful operating point is $k = 0$ and $S_R = 1.0$. This linearization yields

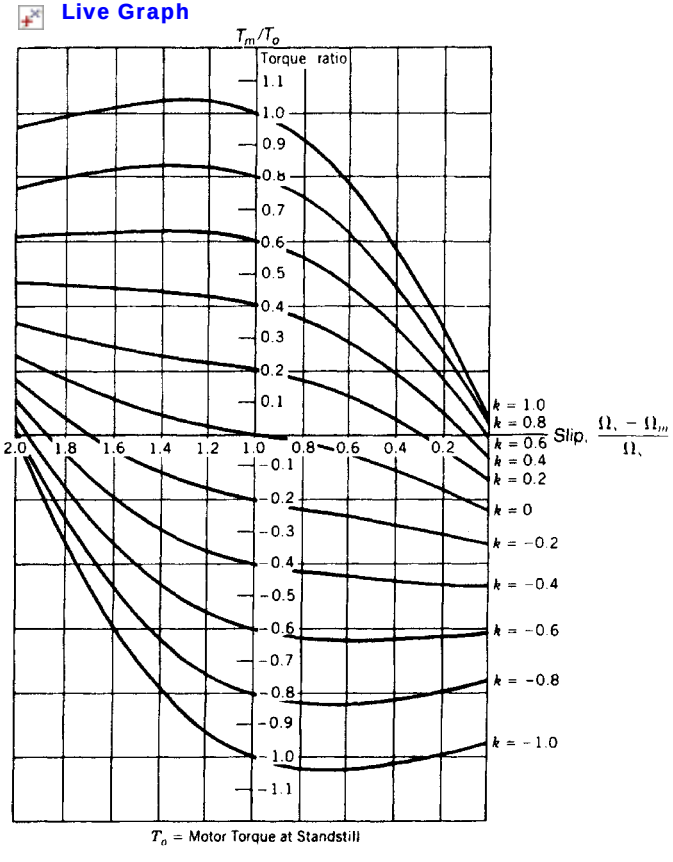


Figure 13 Torque–speed characteristics of a two-phase ac servomotor. (From J. E. Gibson and F. B. Tueter, *Control System Components,* McGraw-Hill, New York, 1958, p. 288.)

$$\Delta\Omega_m = A\ \Delta v_c - \frac{1}{B}\Delta T_m \tag{23}$$

where

$$A = \frac{\partial\Omega_m}{\partial v_c} \tag{24}$$

$$\frac{1}{B} = -\frac{\partial\Omega_m}{\partial T_m} \tag{25}$$

The symbol Δ indicates small variations from the steady-state operating point. Including the electrical and mechanical dynamics gives the transfer function

$$\Delta\Omega_m(s) = \frac{A\ \Delta V_c(s) - (1/B)\ \Delta T_m(s)}{(\tau_e s + 1)(\tau_m s + 1)} \tag{26}$$

where B_m = damping coefficient of motor (N·m·s)
J_m = polar moment of inertia of rotor (N·m·s^2/rad)
L_1 = inductance of stator (H)
R_1 = resistance of stator (Ω)
s = Laplace variable
ΔT_m = change in load torque reflected to motor shaft
$\Delta T_m(s)$ = Laplace transform of change in load torque reflected to motor shaft
$\tau_e = L_1/R_1$ = electrical time constant (s)
$\tau_m = J_m/B_m$ = mechanical time constant (s)
$\Delta\Omega_m(s)$ = Laplace transform of change in motor speed

Computation of the constants A and B of Eq. (26) from the torque expression of Eq. (20) is rather tedious and requires measurements of the rotor impedances over a speed range of $-\Omega_s$ to $+\Omega_s$. As an alternative, an approximate expression for the torque has been developed[18] as follows:

$$T_m = \frac{S_R}{C_1 + C_2 S_R^2} \tag{27}$$

where C_1 and C_2 are constants which are determined from two points on an experimentally measured torque–speed characteristic. The constants A and B in Eq. (23) are related to C_1 and C_2 as follows:

$$A = \frac{2\Omega_s}{v_m}\frac{(C_1 + C_2)}{(C_1 - C_2)}\sin\theta \tag{28}$$

$$B = \frac{1}{2\Omega_s}\frac{(C_1 - C_2)}{(C_1 + C_2)^2} \tag{29}$$

Numerical Example

Specifications for a typical two-phase ac servomotor are given as follows:

Number of poles = $P = 4$
Stator resistance = $R_1 = 10\ \Omega$
Stator inductance = $L_1 = 3$ mH
Moment of inertia of rotor = $J_m = 5.4 \times 10^{-5}$ in.·oz·s^2/rad (3.8×10^{-7} N·m·s^2/rad)
Locked torque = 9.5 in.·oz (6.71×10^{-2} N·m)

Torque at 1000 rpm = 5.4 in.·oz (3.8×10^{-2} N·m)
Voltages: v_c = 110 V at 90°; v_m = 110 V at 0°
Frequency = 60 Hz
Synchronous speed $\Omega_s = 120f/P$ = 1800 rpm (188.3 rad/s)
Slip ratio at standstill = $S_{R1} = 1$
Slip ratio at 1000 rpm = $S_{R2} = (\Omega_s - \Omega_m)/\Omega_s = 0.44$

Substituting T = 9.5 in.·oz at $S_R = 1$ in Eq. (27) gives

$$\frac{1}{C_1 + C_2} = 9.5 \tag{30}$$

Similarly, substituting T = 5.4 in.·oz at $S_R = 0.44$ gives

$$\frac{0.44}{C_1 + C_2(0.44^2)} = 5.4 \tag{31}$$

Solving Eqs. (30) and (31) gives

$$C_1 = 0.076 \text{ 1/in.·oz (11 1/N·m)} \qquad C_2 = 0.029 \text{ 1/in.·oz (4.1 1/N·m)}$$

Substituting numerical values in Eqs. (28) and (29) gives

$$A = 7.79 \text{ rad/V·s}$$

$$B = 1.59 \times 10^{-2} \text{ in.·oz·s/rad } (1.12 \times 10^{-4} \text{ N·m·s/rad})$$

From the definitions for the motor time constants

$$\tau_e = 3 \times 10^{-4} \text{ s} \qquad \tau_m = 4.6 \times 10^{-2} \text{ s}$$

From Eq. (26), the motor transfer function is given as

$$\Delta\Omega_m(s) = \frac{7.79\ \Delta V_c(s) - 62.9\ \Delta T_m(s)}{(3 \times 10^{-4}\ s + 1)(4.6 \times 10^{-2}\ s + 1)} \tag{32}$$

Generally the mechanical time constant is much greater than the electrical time constant, as is the case for this example. The term $\tau_e s + 1$ in the transfer function of Eq. (26) often may be neglected without introducing significant error.

5 STEPPER MOTORS

Stepper motors (also called step motors) represent a significant breakthrough in the area of electromechanical actuation. These are incremental motors that by their very nature are compatible with digital systems. A stepper motor converts an electrical pulse into an equivalent rotary displacement. Since their introduction in the early 1930s, stepper motors have evolved into sophisticated designs.[19–22]

The stepper motor possesses some inherent advantages over a conventional servomotor: (1) it is compatible with digital processors; (2) open-loop control is possible, which eliminates stability problems associated with closed-loop servos; (3) the step error is noncumulative; and (4) the brushless design provides easy maintenance and ruggedness. As a result of these advantages, stepper motors find widespread usage in industrial applications such as drives for TV antennas, numerical control (NC) machines, computer drives, hydraulic valve positioning, and other high-performance feedback control systems. The primary dis-

advantage of stepper motors is their low efficiency, which restricts their use to fractional horsepower applications.

5.1 Operation

The principle of operation of a stepper motor is illustrated by the single-stack, variable-reluctance, three-phase motor shown in Fig. 14. The stator has six poles that are wound in a three-phase configuration. The soft-iron rotor has four poles. When phase 1 is powered by a dc voltage, one pair of rotor poles will line up with the phase 1 stator poles. When phase 1 is switched off and phase 2 is turned on, the rotor will turn clockwise through 30° until one pair of teeth align with the phase 2 poles at C. Similarly, if phase 2 is switched off and phase 3 is turned on, the rotor will rotate another 30° in the clockwise direction. Thus, with each switching the rotor advances through one step of 30°. So the "step angle" is 30°. (The most commonly used step angle is 1.8°.) The direction of rotation may be reversed by switching in a 1.3.2.1.3.2 . . . sequence.

In the preceding scheme only one phase winding is switched on at a time. This scheme is termed "one-phase-on" switching. An alternate switching scheme is called "two-phase-on" switching. In two-phase-on switching, two windings are turned on simultaneously. Referring to Fig. 14, if the switching sequence is 12.23.31.12 . . . , the rotor will rotate in a clockwise direction one step of 30° at a time. So, the two-phase-on scheme does not alter the step size for a three-phase stepper motor such as shown in Fig. 14. However, for a four-phase variable-reluctance (VR) motor a switching sequence such as 1.12.2.23.3.34.4.41.1 . . . results in reducing the step size in half. This sequence is called "half stepping." Half stepping results in about 41% more torque (for a four phase motor) compared to the single-stepping scheme. By varying the relative magnitude of the voltages applied to the two windings, the rotor can be made to rotate in fractional increments of a step. This scheme is termed "microstepping."

When the motor is energized, the holding torque of a stepper motor theoretically varies with the rotor position as a sinusoidal. Figure 15 shows a typical torque-speed characteristic for a stepper motor. The torque above which the stepper motor definitely loses steps is termed

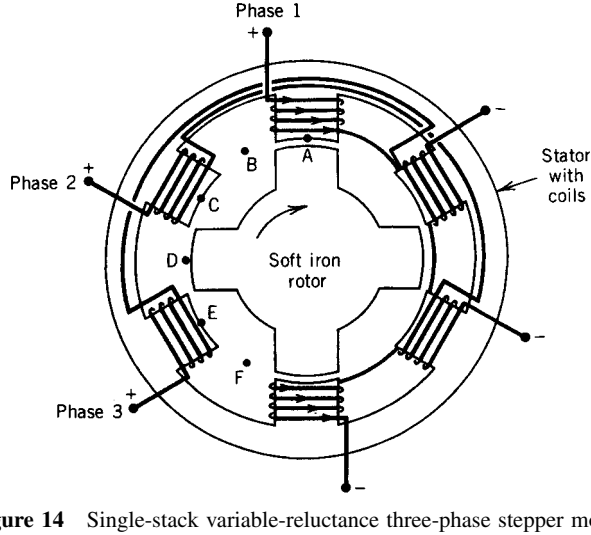


Figure 14 Single-stack variable-reluctance three-phase stepper motor.

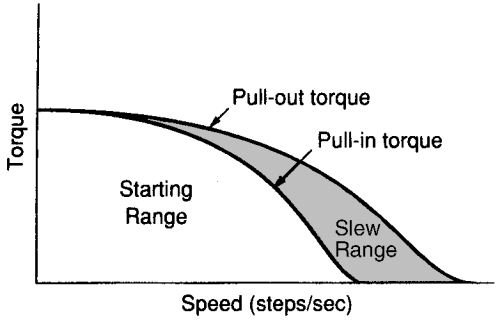


Figure 15 Typical relation between pull-in torque and pull-out torque of a stepper motor. (From B.C. Kuo, *Incremental Motion Control-Step Motors and Control Systems,* Vol. II, SRL Publishing, Champaign, IL, 1979, p. 101).

the "pull-out torque." The torque below which a stepper does not lose any steps (in an open-loop mode) is termed the "pull-in torque." The speed range between the pull-in and pull-out torques is called the "slew range." The slew range represents an unstable region of operation.

5.2 Types of Stepper Motors

In the early years of stepper motor development, stepper design included mechanical detenting and solenoid controls.[19] However, these designs have been replaced by more rugged and efficient designs. The latter designs may be broadly classified as (1) permanent-magnet steppers, (2) variable-reluctance steppers, (3) hybrid steppers, (4) electromechanical steppers, and (5) electrohydraulic steppers. Figure 16 shows configurations of each of these various types of stepper motors. The most commonly used are the permanent-magnet and the three-phase and four-phase variable-reluctance types of stepper motors.

The stator windings of variable-reluctance stepper motors sometimes are wound with two windings of opposite polarity per pole. This approach is termed a "bipolar winding." Figure 17 shows a bipolar-wound stepper motor. This arrangement provides more torque and improves damping, but the disadvantage is more complex circuitry.

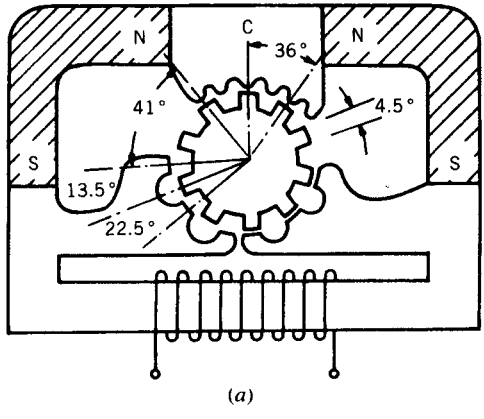
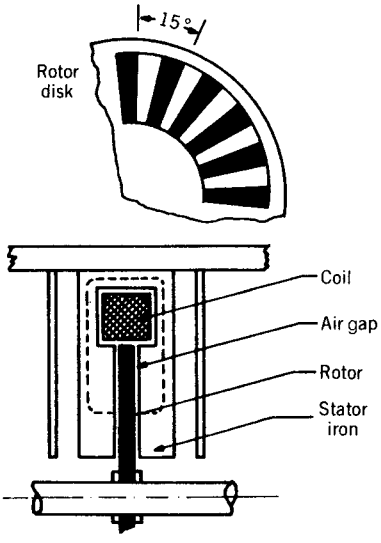
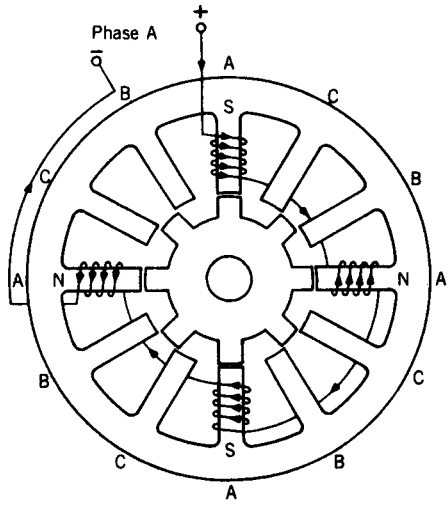


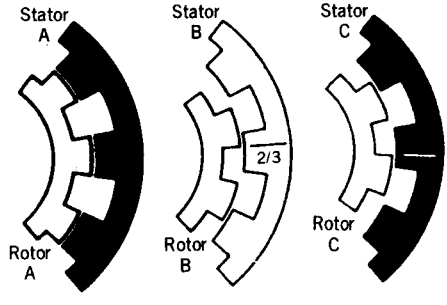
Figure 16 Stepper motor configurations. (From B. C. Kuo, *Incremental Motion Control-Step Motors and Control Systems,* Vol. II, SRL Publishing Co., Champaign, IL, 1979, pp. 12–14.): (*a*) permanent stator stepper motor.

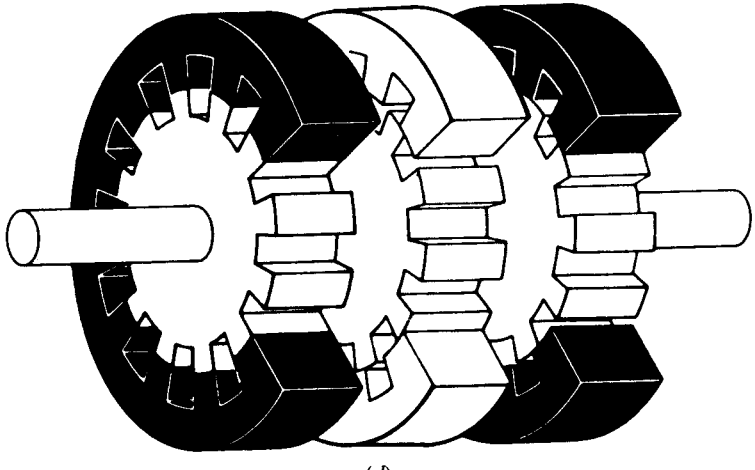


(*b*)



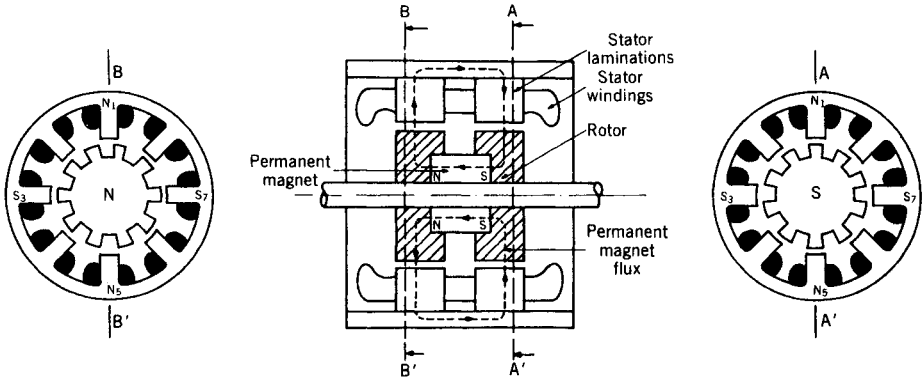
(*c*)



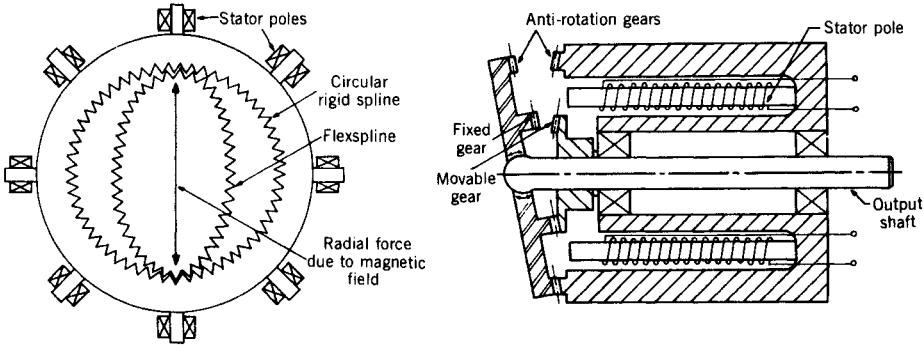


(*d*)

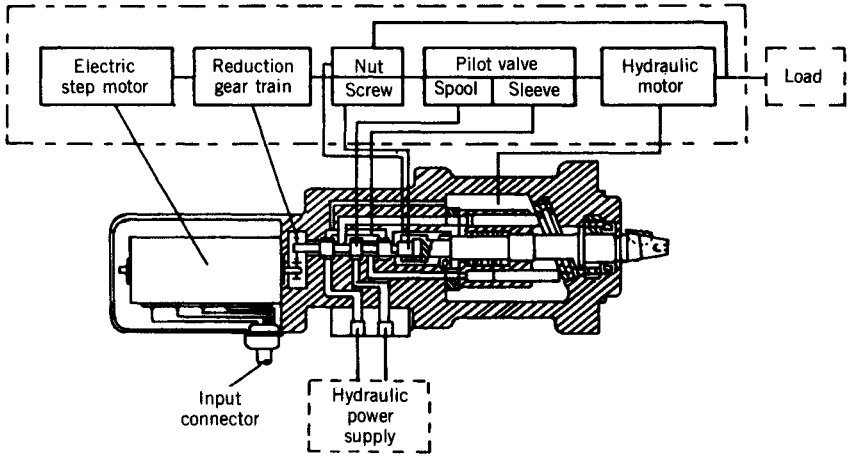
Figure 16 (*Continued*) (*b*) Single-stack, variable-reluctance, axial-gap stepper motor; (*c*) single-stack, variable-reluctance, radial-gap stepper motor; (*d*) multi stack, variable-reluctance, radial-gap stepper motor.



(*e*)



(*f*)



(*g*)

Figure 16 (*Continued*) (*e*) Hybrid stepper motor; (*f*) electromechanical stepper motor; (*g*) electrohydraulic stepper motor.

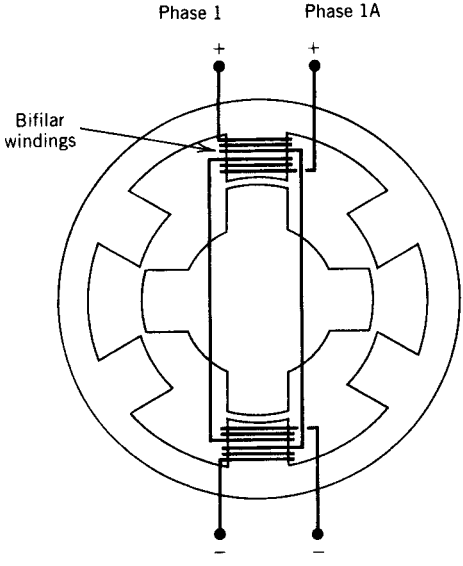


Figure 17 Bipolar-wound stepper motor.

5.3 Mathematical Model of a Permanent-Magnet Stepper Motor

The mathematical model of a stepper is generally much more complex than a conventional dc motor since the voltages applied to the various phases change in a discontinuous fashion. These discontinuities in the applied voltages result directly in corresponding discontinuities in the phase currents. This effect is further complicated by the spatial variation of the magnetic reluctance. Reference 20 gives detailed mathematical models for permanent-magnet and variable-reluctance stepper motors. Computer codes (in FORTRAN IV) are available in Ref. 20 for these stepper motors.

The mathematical models of stepper motors are inherently nonlinear due to discontinuities in input voltages and due to the transcendental spatial variation of the self and mutual inductances. Hence these models do not lend themselves to a frequency-domain analysis.

5.4 Numerical Example

Table 6 gives the specifications of a Crouzet model no. 82 940.0 stepper motor. The motor is to be used to drive a rotary viscometer that has a rotary inertia of 3.88×10^{-3} in.·oz·s^2/rad (2.74×10^{-5} N·m·s^2/rad), a constant frictional torque of 1.3 in.·oz (9.18×10^{-3} N·m). and a viscous damping coefficient of 0.96 in.·oz·s/rad (6.8×10^{-3} N·m·s/rad). The motor is required to accelerate the viscometer from 5.2 to 13.1 rad/s in a maximum of 0.1 s.

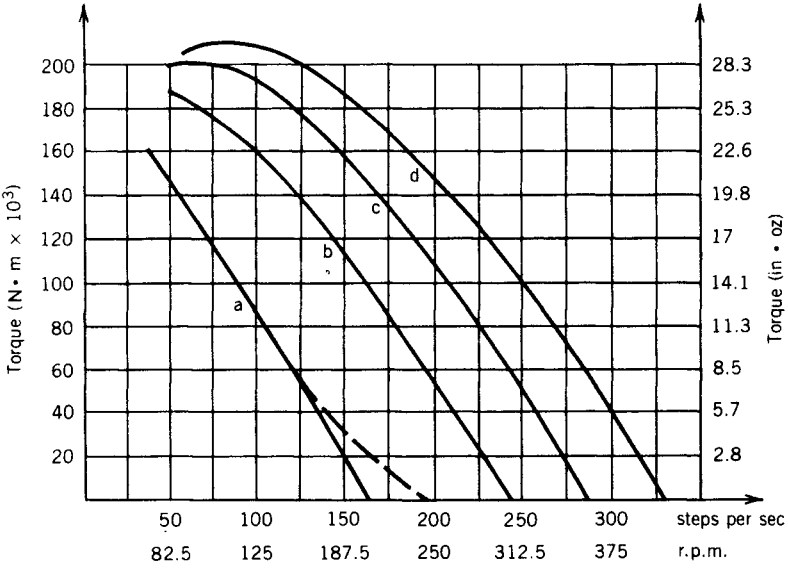
The maximum torque developed by the motor may be estimated as follows:

$$T_m = (J_m + J_L)\frac{d\Omega_m}{dt} + B_L\,\Omega_m + T_f \tag{33}$$

where B_L = rotary damping coefficient of viscometer cup
J_L = polar moment of inertia of viscometer cup
J_m = polar moment of inertia of motor

Table 6 Stepper Motor Specifications (Crouzet Model 82940.0)

Step angle	7.5°
Number of phases	2 (bipolar)
Resistance per phase	9 Ω
Inductance per phase	24 mH
Current per phase	0.55 A
Maximum input power	10 W
Maximum voltage	6.7 V (continuous duty)
Holding torque at 6 V	21.9 in.·oz
Detent torque	1.67 in.·oz
Rotor inertia	1.19×10^{-3} in.·oz·s^2/rad
Maximum coil temperature	248°F



a = Using constant voltage drive with Rs (series resistance) = 0 (L/R)
b = Using constant voltage drive with Rs (series resistance) = R *Motor* ($L/2R$)
c = Using constant voltage drive with Rs (series resistance) = $2R$ Motor ($L/3R$)
d = Using constant voltage drive with Rs (series resistance) = $3R$ Motor ($L/4R$)

T_f = friction torque on viscometer cup
Ω_m = motor shaft speed

From the specifications and Eq. (33): $d\Omega_m/dt = 78.5$ rad/s^2 and $T_m = 14.2$ in.·oz (0.10 N·m). From the torque–speed characteristics of Table 6 it can be seen that the characteristic labeled *b* can be used. So a series resistance of 9 Ω should be used to meet the torque requirements.

The electrical and mechanical time constants may be estimated as follows:

$$\tau_e \approx \frac{L}{R} = 2.7 \times 10^{-3} \text{ s}$$

$$\tau_m \approx \frac{J_m + J_L}{B_L} = 5.3 \times 10^{-3} \text{ s}$$

Since the time allowed for the acceleration of the load is 0. 1 s, which is more than an order of magnitude greater than either time constant, the motor should have adequate dynamic response.

For a more exact dynamic response determination, the motor parameters may be determined experimentally (as described in Chapter 6 of Ref. 20) and used in the dynamic models.

6 ELECTRICAL MODULATORS

This section describes electrical modulators used for the various types of servomotors described in Sections 3–5. The term ''modulator,'' as defined earlier, designates components employed for conversion of the command signal to appropriate means to modulate the power flow to the servomotor (see Fig. 1). Modulators for the various types of electrical servomotors differ significantly.

6.1 Direct-Current Motor Modulators

Modulators used in servoactuator applications with dc motors usually contain two stages of amplification: a first-stage voltage amplified followed by a second-stage power amplifier. Voltage amplifiers are generally quite linear in performance. Power amplifiers are used in two different configurations, type T and type H, as shown in Fig. 18. The type T configuration employs two power sources and only two power transistors. The type H configuration uses only one power source but four transistors. The type T configuration lends itself readily to current feedback schemes. However, the type H is more commonly used because of a single power source requirement. Type H configurations can be operated in two different modes, resulting in bipolar and unipolar drives.

Linear Amplifiers

Linear amplifiers that are dc amplifiers used in the output stage (as H or T configuration) provide gains typically in the range of 2–10. At power levels above 200 W, these amplifiers require external cooling (e.g., fans) to overcome excessive heat generation. This problem is particularly severe in high-performance servo applications that typically have low-impedance rotors operating at low-speed and high-torque conditions. Sometimes this problem is overcome by incorporating a dual-mode current-limiting device which permits high currents for short durations (for overcoming inertia) and then imposes a lower limit for longer durations.

Linear amplifiers are generally configured as voltage amplifiers, but in some applications a current source configuration is employed. Reference 5 discusses the details of voltage and current source configurations, the associated mathematical models, and the influence of the two configurations on the dynamic response of the motor.

Switching amplifiers overcome heat generation problems by switching the voltage on and off at high frequencies. This switching limits the maximum allowable inductance and results in shorter time constants and increased bandwidth. One drawback is that the RFI noise level generated is much higher than with linear amplifiers. There are predominantly two types of switching used in servoactuator applications: (1) PWM and (2) PFM. PWM amplifiers are most commonly used.

PWM Amplifiers

In PWM amplifiers, the voltage applied to the servomotor is varied by changing the pulse width of a high, constant-frequency (typically 10-kHz) train of pulses. Figure 19 shows a schematic of a PWM amplifier. Figure 20*a* shows a photograph of a typical PWM amplifier

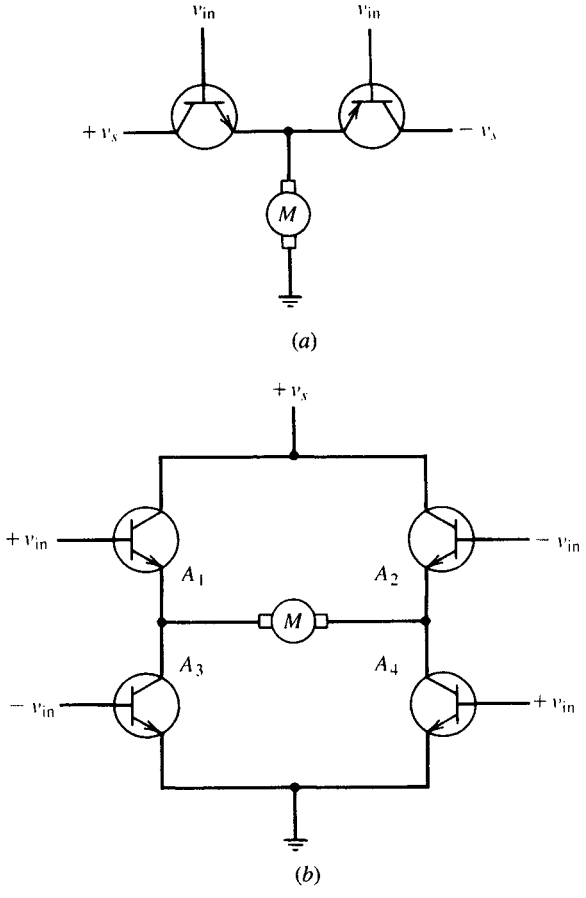


Figure 18 Electrical modulator configurations; (*a*) type T; (*b*) type H.

and Fig. 20*b* shows the associated circuit diagram. Figure 21 shows the firing sequence for unipolar and bipolar configurations.

Mathematical Model—Bipolar Drive PWM Amplifier

The average voltage v_{ma} applied over one cycle of the PWM signal is given by (see Ref. 9, Section 4.5.3)

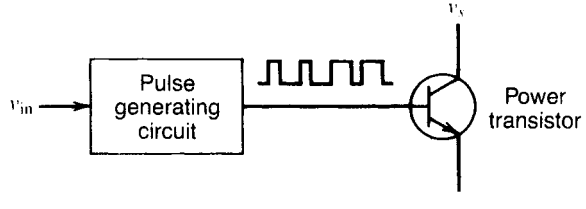
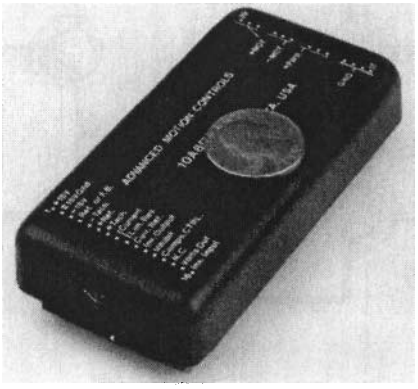
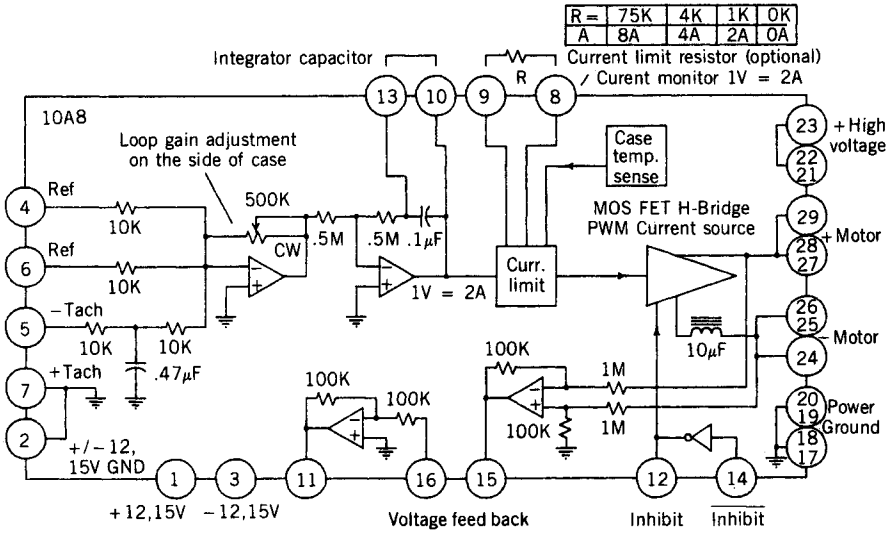


Figure 19 PWM amplifier configuration.



(*a*)



(*b*)

Figure 20 PWM servoamplifier IC: (*a*) PWM servoamplifier photograph; (*b*) PWM servoamplifier circuit diagram. (Courtesy of Advanced Motion Controls, Van Nuys, CA.)

$$v_{ma} = \frac{2v_s t_a}{t_p} - v_s \tag{34}$$

and the change in current over one cycle is given by

$$\Delta i = \frac{2v_s t_a}{L}\left(1 - \frac{t_a}{t_p}\right) \tag{35}$$

where i = current
L = inductance of armature winding
t_p = time period of PWM signal (see Fig. 21)
t_a = actuation time = $(t_p/2) - t_o - t_p v_{\text{in}}/v_c$ (see Fig. 21)

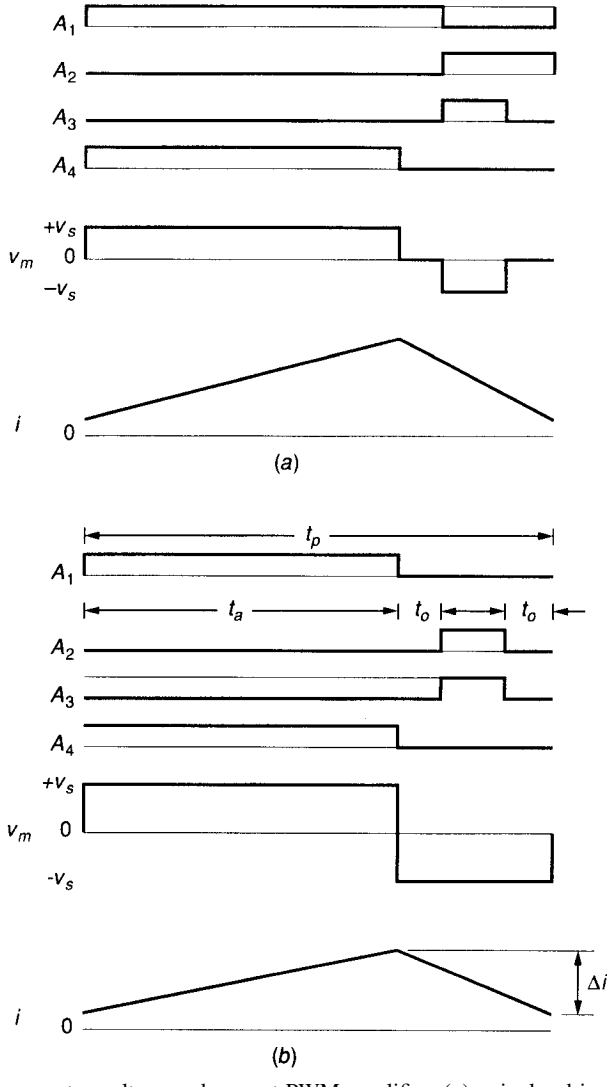


Figure 21 Phases, motor voltage and current PWM amplifier: (*a*) unipolar drive; (*b*) bipolar drive.

t_o = time delay (see Fig. 21)
v_c = peak-to-peak amplitude of a triangular wave voltage signal of time period t_p
v_{in} = input voltage signal applied to amplifier
v_s = supply voltage

Equations (34) and (35) are valid for operating conditions where the instantaneous motor current i remains positive throughout a cycle. The actuation time t_a is determined from the pulse generation circuit characteristics in conjunction with the input signal.[9]

Mathematical Model—Unipolar Drive PWM Amplifier

The average voltage and current amplitudes for a PWM amplifier in a unipolar drive mode are given by

$$v_{ma} = \frac{t_a v_s}{t_p} \tag{36}$$

and

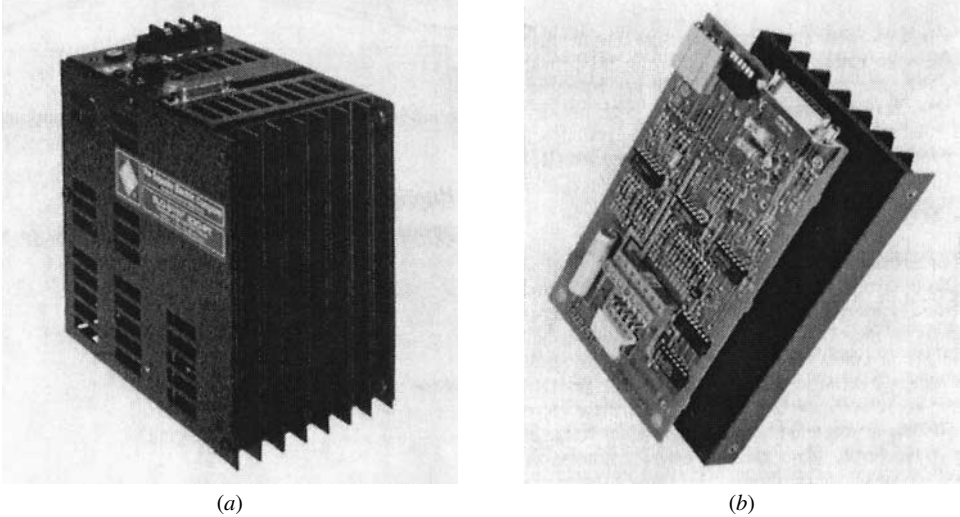
$$\Delta i = \frac{v_s t_a}{L}\left(1 + \frac{t_s}{t_p}\right) \tag{37}$$

For operating conditions where the instantaneous motor current becomes zero for a part of the cycle, the mathematical models can be found in Refs. 5, 20, 23, and 24.

6.2 Stepper Motor Modulators

Modulators for stepper motors are also called "drives." There are three types: oscillator-translators, indexers, and microstepping controls. Oscillators provide a variable-frequency pulse train to the translator. The function of the translator is to convert the pulse train into appropriate signals to operate the power transistors, thereby directing power to the stepper motor. The variable-frequency (3000–15,000 pulses per second) capability of the oscillators provides for accurate manual control of speed. Similarly, a pulse generator in conjunction with a translator provides manual position control. Figure 22 shows a typical oscillator-translator package. Most commercial units also provide for half-stepping and electronic damping.

Indexers are generally programmable microprocessors that perform the functions of the oscillator-translator package, in addition to providing features such as numerical processing, programming, and communications (RS232 and RS274) with computers. The software controls provide such features as setting upper and lower limits of stepper motion and controlling slewing rate. Figure 23 shows a typical indexer. Indexers generally operate on 20–100 V dc power.



(*a*) (*b*)

Figure 22 Oscillator-translator modulator for stepper motor control (courtesy of Superior Electric Co., Bristol, CT): (*a*) photograph of modulator; (*b*) Photograph of circuit card.

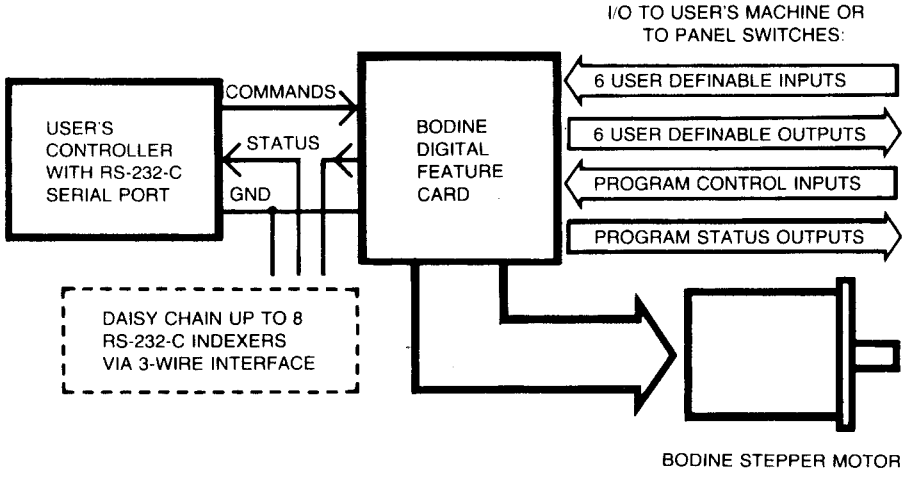


Figure 23 Linear-motion hydraulic servomotors (actuators); indexer-type modulator for stepper motor control. (Courtesy of Bodine Electric Co., Chicago, IL.)

Stepper motors suffer from mechanical resonances (generally in the range of 50–250 steps per minute) due to the excitation resulting from the square shape of the current pulses. Microstepping eliminates this problem by energizing multiple windings simultaneously and by controlling the currents. Hence, modulators for microstepping essentially control the simultaneous currents to the various phases achieving as high as 50,000 microsteps per revolution. Switching frequencies range from 20 to 200 kHz.

7 HYDRAULIC SERVOMOTORS

Hydraulic servomotors or "actuators" convert hydraulic power into mechanical motion. This mechanical motion can be either linear or rotary. Because hydraulic servomotors provide large actuating force or torque capabilities, they are commonly used in heavy-equipment industries. Also, due to their high mechanical stiffness, fast dynamic response, and high power-to-weight ratios, hydraulic servomotors find widespread use in aircraft, missiles, and space vehicles, as well as critical industrial systems where high performance and high-power control are needed.[25]

7.1 Linear-Motion Servomotors

Linear-motion servomotors or actuators provide a translatory motion of a load along a straight line. The motion of the load can be controlled by modulating the flow of hydraulic fluid into or out of the servomotor. There are two basic types of linear-motion servomotor designs: unbalanced and balanced designs, as shown schematically in Fig. 24. The unbalanced design is shorter, while the balanced design has equal extension and return rates when the servomotor is driven by a symmetrical modulator (control valve). High-performance hydraulic and electrohydraulic servosystems require servomotors with low leakage and low friction. Correspondingly, seals are critical elements in servomotor design. Construction details and mounting arrangements are discussed in Refs. 26–28.

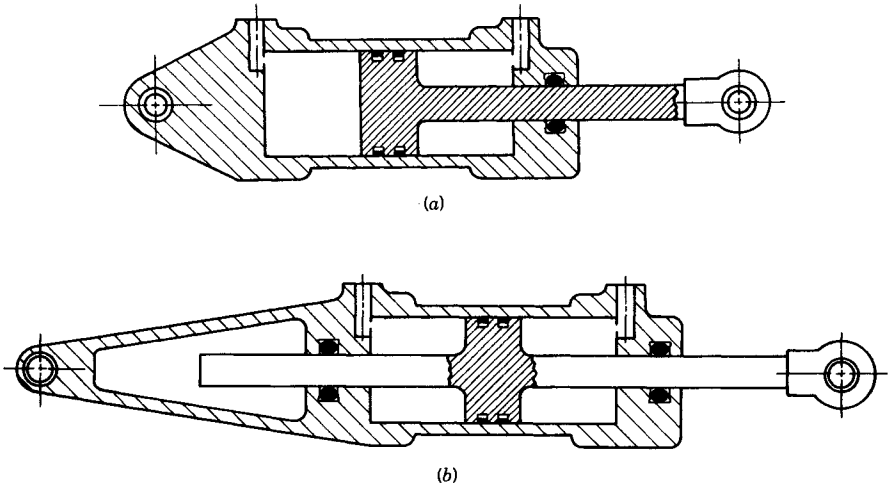


Figure 24 Linear-motion hydraulic servomotors (actuators): (*a*) double-acting unbalanced actuator; (*b*) double-acting balanced actuator.

Since servomotors must move heavy loads quickly and accurately, they should act as very stiff structural members. In a well-designed servomotor, the fluid columns on either side of the piston are the most compliant portions of the structure. The spring rate of one fluid column is given by $K = A\beta/L$ where A is the net column area, L is the column length, and β is the fluid bulk modulus of elasticity. Servomotors used for high-dynamic-performance systems are designed to have the minimum stroke and the shortest permissible connecting passages in order to minimize the volume of fluid under compression. Modulators often are integrated into the servomotor body to minimize lengths of connecting passages (see Section 9.2).

7.2 Rotary-Motion Servomotors

Rotary-motion servomotors are functionally more versatile than their linear counterparts. They are commonly employed even in linear-motion applications through a rack-and-pinion type kinematic conversion. However, linear-motion servomotors also are employed for rotary applications through corresponding kinematic conversion. Rotary actuators can be either simple reversible hydraulic motors of continuous-rotation type or high-performance type with limited angular displacement. Most rotary servomotors used in medium- and high-performance hydraulic and electrohydraulic servosystems are vane (continuous or limited rotation) or piston type (continuous rotation) servomotors.

Rotary-vane servomotors are commonly used in industrial applications where medium to high performance is required and size and weight are not at a high premium. Such applications include earth-moving equipment, agricultural machinery, and materials processing and handling equipment. Figure 25 shows a typical continuous-rotation rotary-vane servomotor capable of operating at speeds up to 4000 rpm (419 rad/s) and pressures up to 2500 psi (1.72×10^7 N·m^2).

In aircraft, missile, and spacecraft applications where high performance and small size and weight are required, piston-type servomotors are commonly used. Figure 26 shows a typical ''in-line'' piston-type servomotor and Fig. 27 shows a typical ''bent-axis'' piston-type

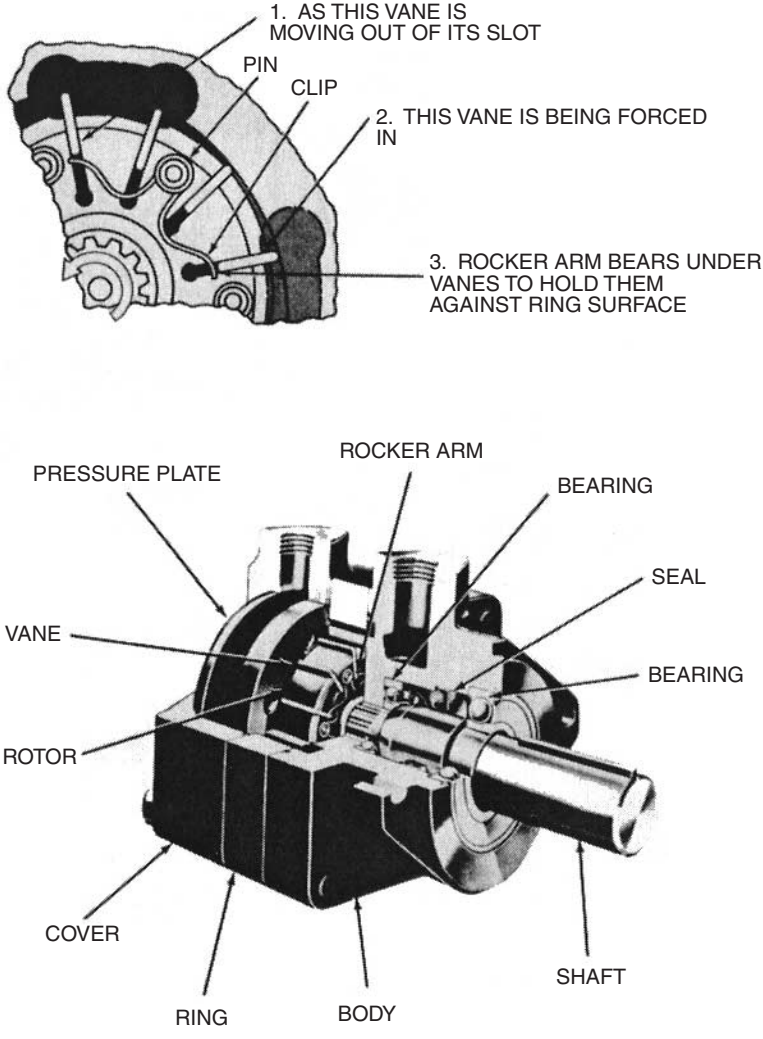


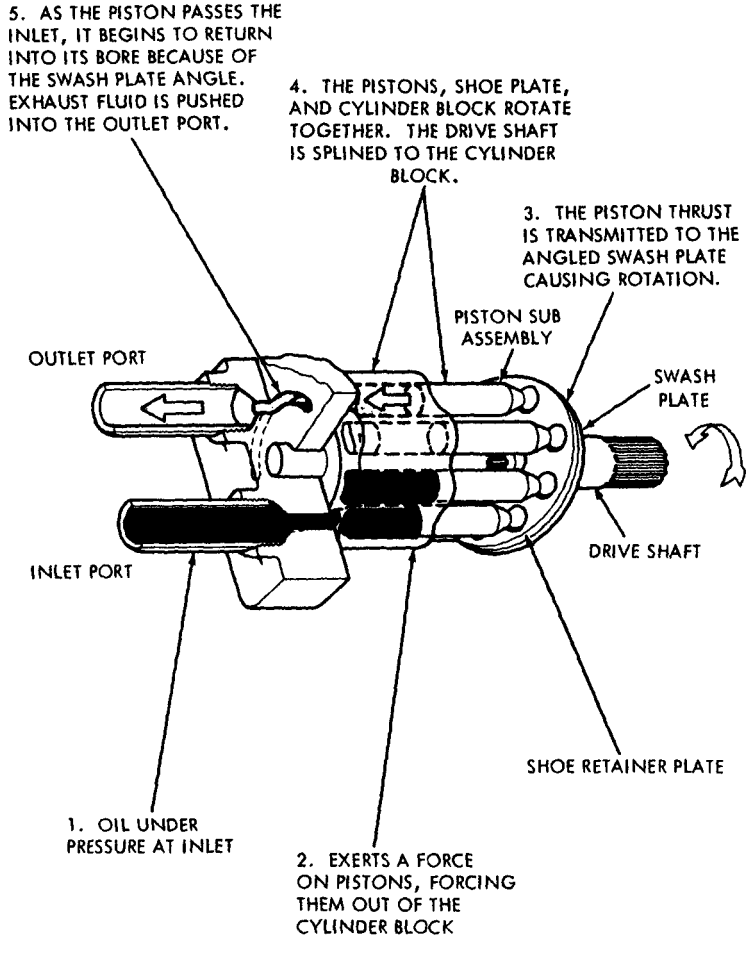
Figure 25 Balanced vane-type hydraulic servomotor. (Courtesy of Vickers, Inc., Troy, MI.)

servomotor. Such servomotors are capable of operating at speeds up to 8000 rpm (838 rad/s) and pressures up to 5000 psi (3.44×10^7 N/m^2).

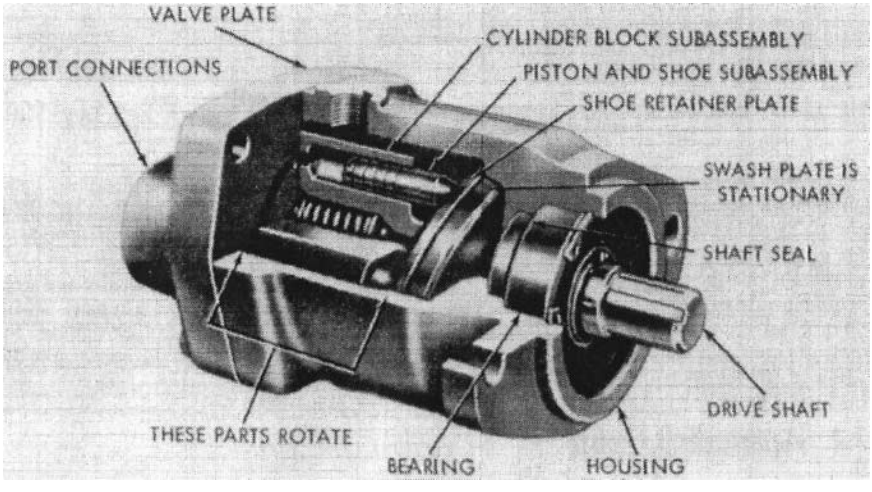
7.3 Mathematical Models

A hydraulic servomotor (either linear- or rotary-motion type) is a rate-type device. That is, a given flow rate into the servomotor results in a certain velocity (or speed for a rotary servomotor).

Figure 28 shows schematics of linear and rotary servomotors with definitions of the variables. Dynamic models are given in the following descriptions. It is assumed that all structural components are rigid and that external leakage to the environment is negligible. Models that include external leakage effects are presented in Ref. 29.

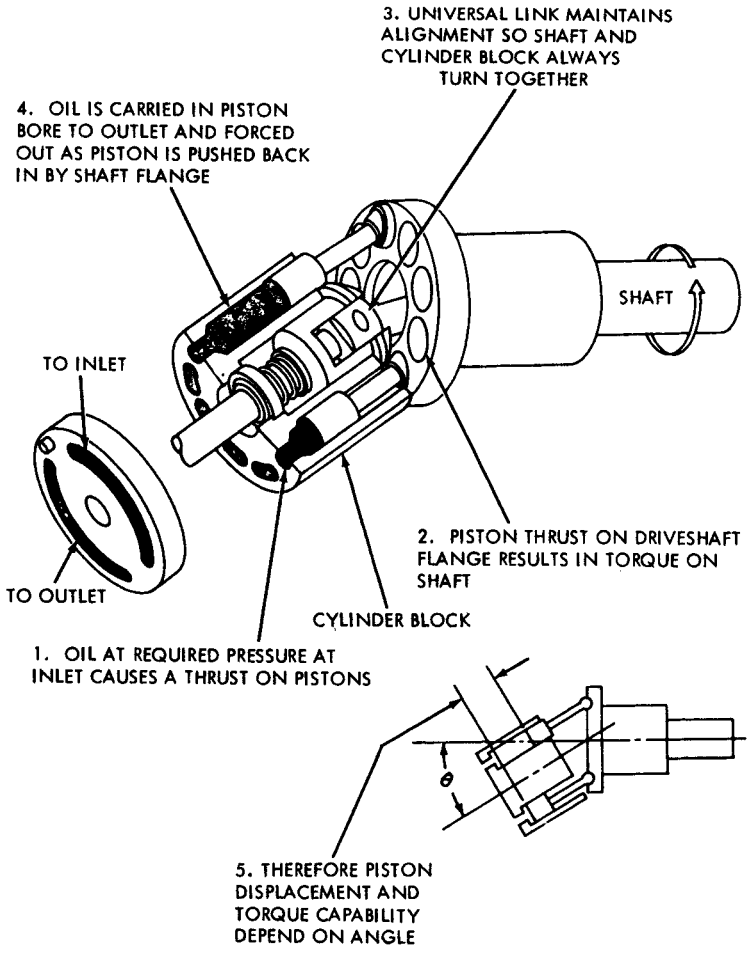


(*a*)

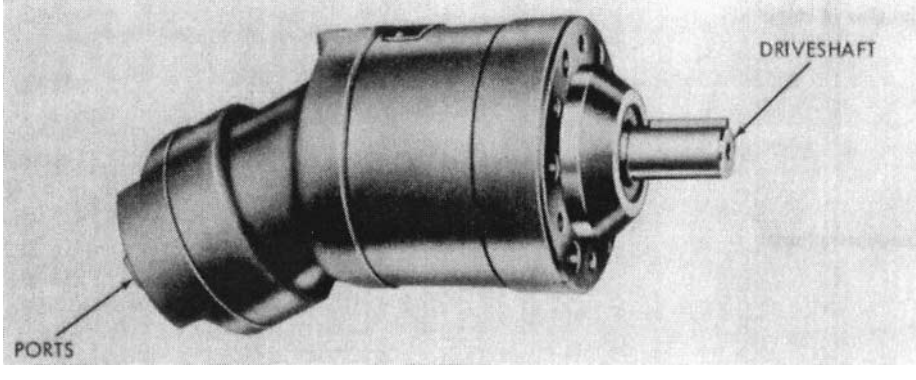


(*b*)

Figure 26 In-line piston servomotor: (*a*) operation of servomotor; (*b*) cutaway of servomotor. (Courtesy of Vickers, Inc., Troy, MI.).



(*a*)



(*b*)

Figure 27 Bent-axis piston servomotor: (*a*) operation of servomotor; (*b*) photograph of servomotor. (Courtesy of Vickers, Inc., Troy, MI.)

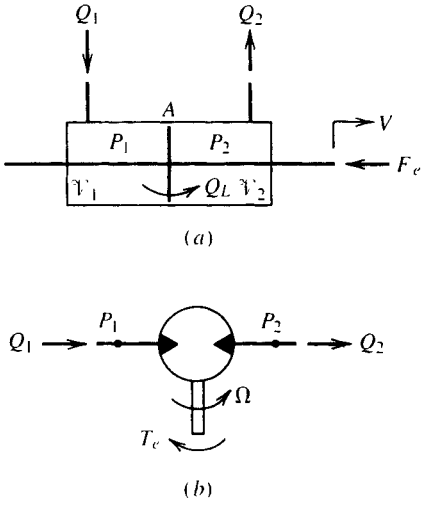


Figure 28 Nomenclature of hydraulic servomotors.

***Linear Servomotor* (*Balanced Design*)**

Force balance

$$\frac{dV}{dt} = \frac{1}{M_a}(AP_m - B_mV - F_f - F_c - F_e) \tag{38}$$

Chamber continuity

$$\rho_1 Q_1 - \frac{(\rho_1 + \rho_2)}{2} Q_L = \frac{d}{dt}(\rho_1 \mathcal{V}_1) \tag{39}$$

$$\frac{\rho_1 + \rho_2}{2} Q_L - \rho_2 Q_2 = \frac{de}{dt}(\rho_2 \mathcal{V}_2) \tag{40}$$

Equation of state

$$\frac{d\rho_1}{dt} = \frac{\rho_1}{\beta}\frac{dP_1}{dt} \tag{41}$$

$$\frac{d\rho_2}{dt} = \frac{\rho_2}{\beta}\frac{dP_2}{dt} \tag{42}$$

Chamber volume

$$\mathcal{V}_1 = \mathcal{V}_{1i} + AY \tag{43}$$

or

$$\frac{d\mathcal{V}_1}{dt} = AV$$

$$\mathcal{V}_2 = \mathcal{V}_{2i} = -AY \tag{44}$$

or

$$\frac{d\mathcal{V}_2}{dt} = -AV$$

where A = effective area of servomotor piston
B_m = viscous damping coefficient in servomotor
C_2 = leakage coefficient
F_c = force due to Coulomb friction in servomotor
F_e = external load force on servomotor piston
F_f = force due to stiction in servomotor
M_a = mass of moving parts in servomotor
P_1 = pressure at inlet
P_2 = pressure at outlet
$P_m = P_1 - P_2$ = pressure drop across servomotor
Q_1 = flow rate into servomotor
Q_2 = flow rate out of servomotor
$Q_L = C_2 P_m$ = internal leakage flow rate
V = velocity of servomotor piston
$\mathcal{V}_1$ = fluid volume under compression at the inlet
$\mathcal{V}_{1i}$ = fluid volume under compression at inlet for $Y = 0$
$\mathcal{V}_2$ = fluid volume under compression at the outlet
$\mathcal{V}_{2i}$ = fluid volume under compression at outlet for $Y = 0$
Y = linear displacement of servomotor piston from neutral position
β = fluid bulk modulus of elasticity
ρ_1 = fluid mass density at inlet
ρ_2 = fluid mass density at exit

Rotary Servomotor

Torque balance

$$\frac{d\Omega}{dt} = \frac{1}{J_a}(D_m P_m - B_r\Omega - T_f - T_c - T_e) \tag{45}$$

Chamber continuity

$$\rho_1 Q_1 - \frac{(\rho_1 + \rho_2)}{2} Q_L = \frac{d}{dt}(\rho_1 \mathcal{V}_1) \tag{46}$$

$$\frac{(\rho_1 + \rho_2)}{2} Q_L - \rho_2 Q_2 = \frac{d}{dt}(\rho_2 \mathcal{V}_2) \tag{47}$$

Equation of state

$$\frac{d\rho_1}{dt} = \frac{\rho_1}{\beta}\frac{dP_1}{dt} \tag{48}$$

$$\frac{d\rho_2}{dt} = \frac{\rho_2}{\beta}\frac{dP_2}{dt} \tag{49}$$

Chamber volume

$$\mathcal{V}_1 = \mathcal{V}_{1i} + D_m\theta \tag{50}$$

or

$$\frac{d\mathcal{V}_1}{dt} = D_m\Omega$$

$$\mathcal{V}_2 = \mathcal{V}_{2i} - D_m\theta \tag{51}$$

or

$$\frac{d\mathcal{V}_2}{dt} = -D_m\Omega$$

where B_r = viscous damping coefficient in servomotor
C_2 = leakage coefficient
D_m = displacement of servomotor
J_a = polar moment of inertia of servomotor moving parts
P_1 = pressure at inlet
P_2 = pressure at outlet
$P_m = P_1 - P_2$ = pressure drop across servomotor
Q_1 = flow rate into servomotor
Q_2 = flow rate out of servomotor
$Q_L = C_2P_m$ = internal leakage flow rate
T_c = torque due to Coulomb friction in servomotor
T_e = external load torque on servomotor
T_f = torque due to stiction in servomotor
$\mathcal{V}_1$ = fluid volume under compression at inlet
$\mathcal{V}_{1i}$ = fluid volume under compression at inlet for $\theta = 0$
$\mathcal{V}_2$ = fluid volume under compression at outlet
$\mathcal{V}_{2i}$ = fluid volume under compression at outlet for $\theta = 0$
β = fluid bulk modulus of elasticity
ρ_1 = fluid mass density at inlet
ρ_2 = fluid mass density at outlet
θ = angular displacement of servomotor
Ω = angular velocity of servomotor

Simplified Mathematical Model

A simplified mathematical model for hydraulic servomotors can be obtained by assuming that (1) stiction and Coulomb friction effects are negligible, (2) internal leakage is negligible, (3) external load force (or torque) is zero, and (4) the fluid is incompressible. The result is

$$\frac{Z(s)}{P_m(s)} = \frac{K}{\tau s + 1} \tag{52}$$

where the parameters are as defined in Table 7.

Table 7 Hydraulic Servomotor Parameters

Z	V	Ω
K	A/B_m	D_m/B_r
τ	M_a/B_m	J_a/B_r

8 HYDRAULIC MODULATORS

Two basic approaches are used to modulate the flow of a high-pressure fluid to a work-producing device (servomotor). First, modulation may be accomplished by varying the displacement of a rotary pump which supplies fluid directly to a rotary servomotor. A variation on this approach is to use a variable-displacement servomotor and a fixed-displacement pump. Such systems, referred to as pump-displacement-controlled (or motor-displacement-controlled) servoactuators, are not as commonly used in high-performance applications as are valve-controlled servoactuators. The reader is referred to Refs. 29–33 for more detailed discussion of pump-displacement-controlled servoactuators. The discussion here is limited to the second modulation approach (i.e., servoactuators that employ servovalves as modulators).

8.1 Servovalve Design and Operation

Modem servovalves employ one or more of several types of metering devices: flapper-nozzle, poppet, spool, sliding plate, rotary ''plate,'' and jet pipe. Servovalves are typically made in one-, two-, or three-stage configurations. Single- and two-stage configurations are the most common. Generally, the flapper-nozzle valve or the jet-pipe valve is used in the first stage of a two-stage servovalve. The spool-type valve is the most commonly used for single-stage servovalves and for the second stage of two-stage servovalves. Servovalves may be of the two-way, three-way, or four-way type.[30] Four-way types are used in most servosystems where bidirectional motion is required. Three-way types can be used where only unidirectional motion is required; bidirectional control can be achieved if a load biasing scheme is used. Depending on the internal design and application, servovalves may provide flow-rate control or pressure control. Special designs are available which employ flow-rate, pressure, or dynamic pressure feedback within the valve.[34,35]

Servovalves may have mechanical, hydraulic, pneumatic, or electrical input. Most servosystems used in high-performance applications today use electrohydraulic servovalves where an electrical input signal is converted to a mechanical motion through a torque motor. In single-stage valves, the torque motor actuates the control valve, which in turn modulates the flow of hydraulic fluid under pressure from a high-pressure source to a linear- or rotary-motion servomotor. In two-stage valves, the torque motor actuates the first-stage (or pilot) valve, which is typically a flapper-nozzle or jet-pipe valve. The hydraulic output from the first stage drives the second stage (typically a spool-type valve), which in turn modulates the flow from the source to the servomotor. Reference 36 is a detailed history of electrohydraulic servomechanisms with special emphasis on electrohydraulic servovalves.

Figures 29 and 30 show the design features of a modern two-stage electrohydraulic servovalve. The double-coil, double-air-gap torque motor is ''dry'' (i.e., it is in an environmentally sealed compartment isolated from hydraulic fluid by the flexure tube). The first-stage or pilot valve is a symmetrical, double-nozzle (four-way) flapper-nozzle valve. The flapper is attached to the upper (free) end of the flexure tube. The second stage is a spool valve that slides in a bushing with mating rectangular slots formed by electric discharge machining. The spool-bushing tolerance is held to 0.5 μm. Mechanical force feedback from the second-stage spool to the torque motor is provided by a cantilever spring attached to the flapper at the upper end and to the spool through a ball joint.

Figure 31 is a cross section of a two-stage electrohydraulic servovalve that employs a jet-pipe valve as the first stage. Otherwise the valve is virtually the same in design and operation as the valve shown in Figs. 29 and 30. The jet-pipe valve can pass contamination particles as large as 200 μm, whereas the flapper-nozzle valve can only pass 50-μm particles. Good fluid filtration can negate the importance of these differences.

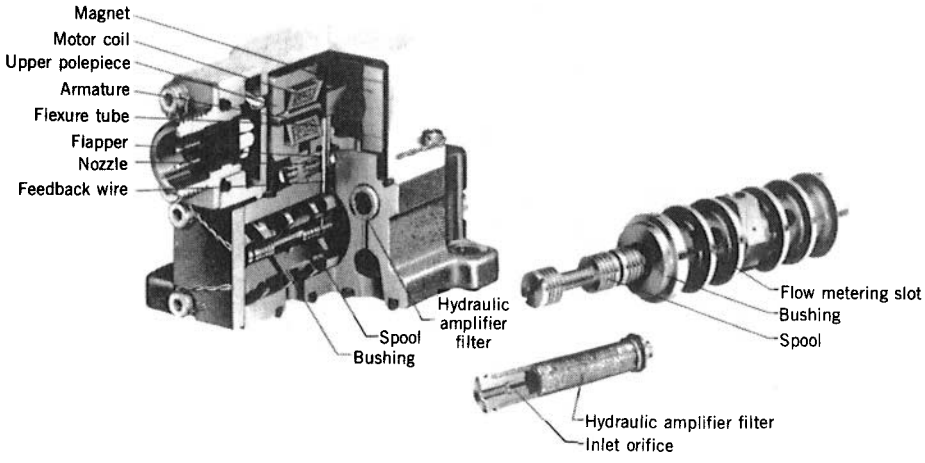


Figure 29 Design features of a two-stage electrohydraulic servovalve. (Courtesy of Moog, Inc., East Aurora, NY.)

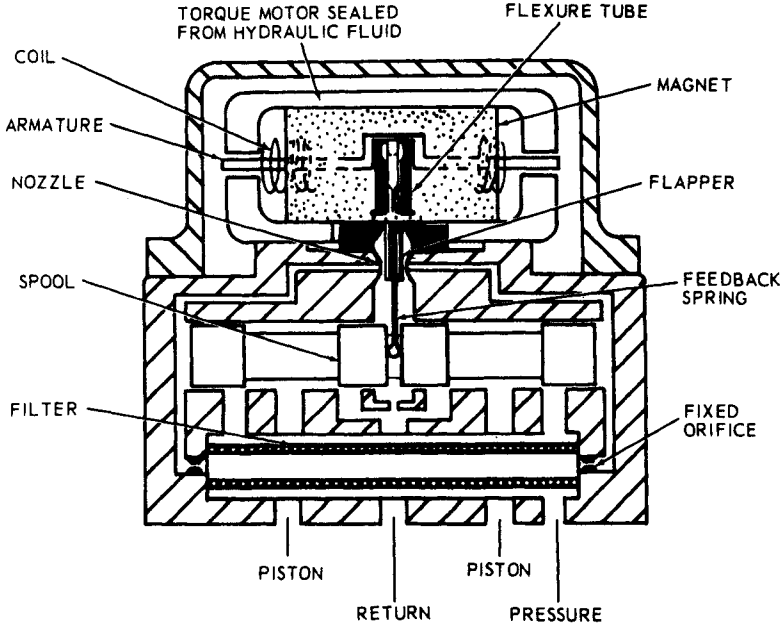


Figure 30 Cross section of two-stage electrohydraulic servovalve with a flapper-nozzle first stage and spool second stage. (Courtesy of Moog, Inc., East Aurora, NY.)

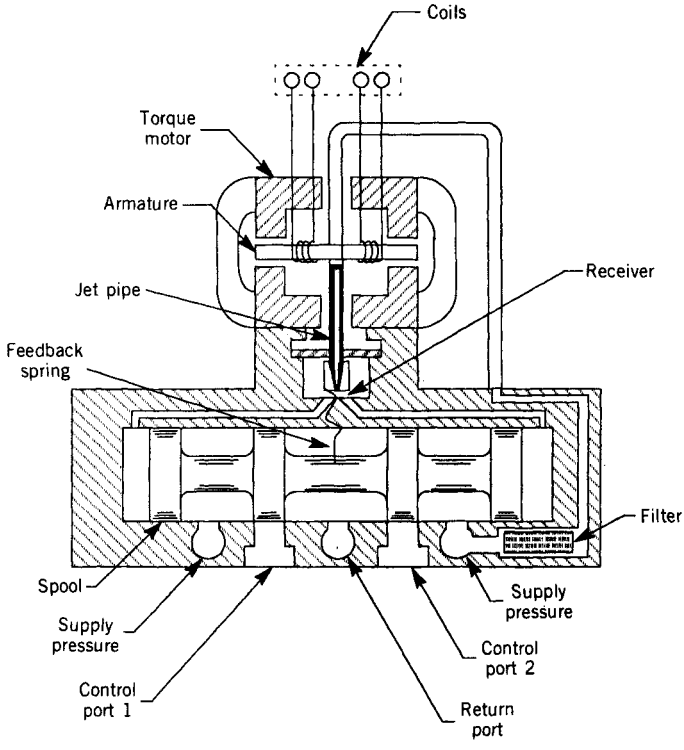


Figure 31 Cross section of a two-stage electrohydraulic servovalve with a jet-pipe first stage and spool second state. (Courtesy of Abex Corporation, Aerospace Division, Oxnard, CA.)

A cutaway diagram of a single-stage swing-plate servovalve is shown in Fig. l6.32*a*; a cross section of the valve is shown in Fig. l6.32*b*. This is an industrial valve that has a high dynamic response (natural frequency about four times that of the two-stage servovalves mentioned earlier). However, the swing-plate valve is considerably heavier than the two-stage aerospace-type valves in Figs. 30 and 31.

Table 8 shows typical performance capabilities of various types of servovalves.

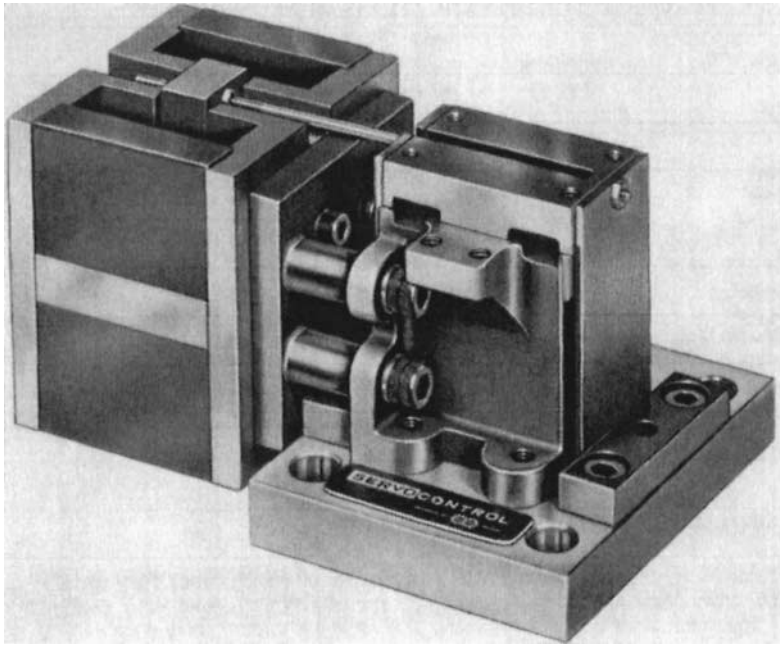
8.2 Mathematical Model of a Spool-Type Valve

Spool-type valves are the most popular due to their ease of construction. They are also easier to analyze than other types of valves. Figure 33 shows a typical spool-valve configuration and defines the important variables and parameters. The valve has three "energy ports" where energy or power flows from or to the environment of the valve. Correspondingly, the valve can be modeled using the three mathematical equations given in functional form as follows:

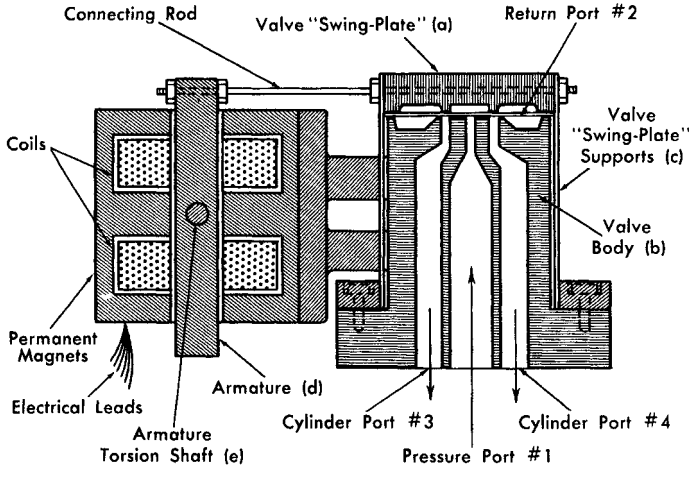
$$Q_m = f(x, P_m, P_s) \tag{53}$$

$$Q_s = f(x, P_m, P_s) \tag{54}$$

$$F_v = f(x, P_m, P_s) \tag{55}$$



(a)



(b)

Figure 32 Cross section of a single-stage, "swing-plate" electrohydraulic servovalve. (Courtesy of The Oilgear Company, Milwaukee, WI.)

Table 8 Performance Specifications of Servovalves

Valve Type	Maximum Working Pressure (psi)	Maximum Flow at 1000 psi Pressure Drop (gpm)	Frequenty at 90° Lag (Hz)	Hysteresis (%)	Resolution (%)
Spool					
One-stage	5000	3500	200	0.1	0.01
Two-stage	7000	1000	200	1	0.01
Three-stage	4500	300	200	1	0.01
Flapper-nozzle/spool					
One- and two-stage	5000	1000	500	0.2	0.01
Three-stage	5000	1000	500	1	0.01
Jet pipe/spool					
One- and two-stage	4500	300	500	2	0.1
Three-stage	4500	300	200	2	0.1
Sliding plate					
One- and two-stage	300	40	150	3	0.1

Source: From Ref. 25.

Equation (53) gives the pressure–flow–displacement characteristics of the valve. These characteristics are needed in the dynamic analysis of a servoactuator which employs the valve. Equation (54) is used to compute the required flow rate from the source and will not be considered further here. Equation (55) is used to calculate the force required to move the spool (e.g., force output requirement of the torque motor in the case of an electrohydraulic servovalve).

The steady-state pressure–flow–displacement characteristics of the spool valve are characterized by the nonlinear orifice equation.[30,37]

$$Q_m = C_d w(x + U)\sqrt{\frac{P_s - P_m}{\rho}} \tag{56}$$

where C_d = effective coefficient of discharge
P_s = supply pressure
P_m = pressure drop across the servomotor (see Fig. 33)

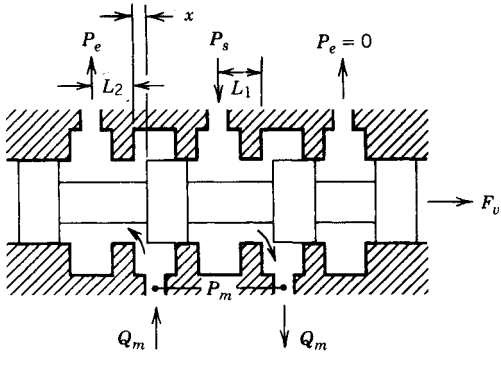


Figure 33 Spool valve nomenclature.

Q_m = flow rate to the servomotor (see Fig. 33)
U = underlap of spool with respect to sleeve (see Ref. 30); $U = 0$ for an "idealized" valve
w = circumferential width of metering ports in the valve
x = displacement of the spool from its neutral position
ρ = mass density of fluid

This model assumes that the flow rates through the metering orifices are steady, the fluid is incompressible, and the valve exhaust pressure $P_e = 0$. A linearized form of this model facilitates the dynamic analysis of a servoactuator containing the valve. The nonlinear model may be linearized by considering small changes of all variables about an initial steady-state operating point, with the result

$$\Delta Q_m = K_1 \, \Delta x - C_1 \, \Delta P_m \tag{57}$$

where

$$K_1 = \left.\frac{\partial Q_m}{\partial x}\right|_{P_{m0}, x_0} = C_d w \sqrt{\frac{P_s - P_{m0}}{\rho}} \tag{58}$$

$$C_1 = -\left.\frac{\partial Q_m}{\partial P_m}\right|_{x_0, P_{m0}} = \frac{C_d w x_0}{2\sqrt{\rho(P_s - P_{m0})}} \tag{59}$$

The terms ΔQ_m, Δx, and ΔP_m represent small changes of the corresponding variables about the steady-state operating point x_0, P_{m0}. The constants K_1 and C_1 are evaluated at the operating point. These expressions assume that the valve port shape does not vary with displacement.

The static and dynamic behavior of the valve spool [Eq. (55)] can be modeled by considering the forces which act on the spool.[30] These forces include the externally imposed force (input) as well as steady and unsteady flow forces resulting from flow through the orifices. Additional forces that may be present include the viscous damping between the spool and the sleeve and any mechanical spring forces acting on the spool (not shown in Fig. 33). The force balance equation for the spool shown in Fig. 33 is

$$F_v = m_s \ddot{x} + \frac{\mu A_s}{h} \dot{x} + \left[C_d w \sqrt{2\rho \left(\frac{P_s - P_m}{2} \right)} (L_1 - L_2) \right] \dot{x} + \left[2 C_d C_v w \left(\frac{P_s - P_m}{2} \right) \cos \theta_j \right] x \tag{60}$$

where A_s = net shear area of spool
C_d = metering orifice discharge coefficient
C_v = metering orifice velocity coefficient (see Ref. 30)
F_v = external force on spool (e.g., imposed by torque motor)
h = radial clearance between spool and sleeve (valve body)
L_1 = length of fluid column to be accelerated at inlet (see Fig. 33)
L_2 = length of fluid column to be accelerated at outlet (see Fig. 33)
m_s = mass of spool
P_m = pressure drop across servomotor
P_s = supply pressure
w = circumferential width of metering ports in valve
x = displacement of spool
$\dot{x}$ = velocity of spool

$\ddot{x}$ = acceleration of spool
ρ = mass density of fluid
μ = absolute viscosity of fluid
θ_j = effective angle of fluid jet (see Ref. 30)

The fourth term on the right-hand side of Eq. (60) is the steady flow-induced force and the third term on the right-hand side is the unsteady flow-induced force. The steady flow force is a ''springlike'' force that always opposes the motion of the spool and hence is a stabilizing force. The unsteady flow force is a ''dampinglike'' force that changes its direction of action depending on the flow direction, and hence it can be a stabilizing or destabilizing force. The valve is dynamically stable if $L_1 - L_2 > 0$. A more complete discussion of the dynamic modeling of the valve spool is given in Ref. 30.

8.3 Mathematical Models for an Electrohydraulic Servovalve

The steady-state pressure–flow characteristics for an electrohydraulic servovalve of the type shown in Fig. 30 are identical to those of the spool-type valve in the previous section except the input x is replaced by the current I. That is, in the steady state, the motion of the spool in the electrohydraulic servovalve is directly proportional to the current input to the valve. The steady-state pressure–flow–current characteristics for the ''idealized'' electrohydraulic servovalve (e.g., Fig. 30; spool matched perfectly with sleeve such that effective underlap $U = 0$) are given by the equation

$$Q_m = K_v I \sqrt{\frac{P_s - P_m}{\rho}} \tag{61}$$

where K_v = a size factor
I = current input to servovalve
P_s = supply pressure
P_m = pressure drop across the servomotor
Q_m = control flow rate to the servomotor
ρ = mass density of fluid

This model assumes that the exhaust pressure $P_e = 0$. Equation (61) may be linearized for operation about an initial steady-state operating point with the result

$$\Delta Q_m = K_1 \, \Delta I - C_1 \, \Delta P_m \tag{62}$$

where

$$K_1 = \left.\frac{\partial Q_m}{\partial I}\right|_{P_{m0}, I_0} \qquad \text{(flow sensitivity)} \tag{63}$$

$$C_1 = -\left.\frac{\partial Q_m}{\partial P_m}\right|_{I_0, P_{m0}} \qquad \text{(flow–pressure sensitivity)} \tag{64}$$

Equation (62) is valid for cases when $U \neq 0$ as well. The terms ΔQ_m, ΔI, and ΔP_m represent small changes of the corresponding variables about the initial steady-state operating point I_0, P_{m0}. The constants K_1 and C_1 are evaluated at the operating point.

Typical steady-state pressure–flow–current characteristics for an ''idealized'' electrohydraulic servovalve that employs a spool-valve second stage [governed by Eq. (61)] are shown in Fig. 34. Characteristics for other types of electrohydraulic servovalves are given in Refs. 34 and 35.

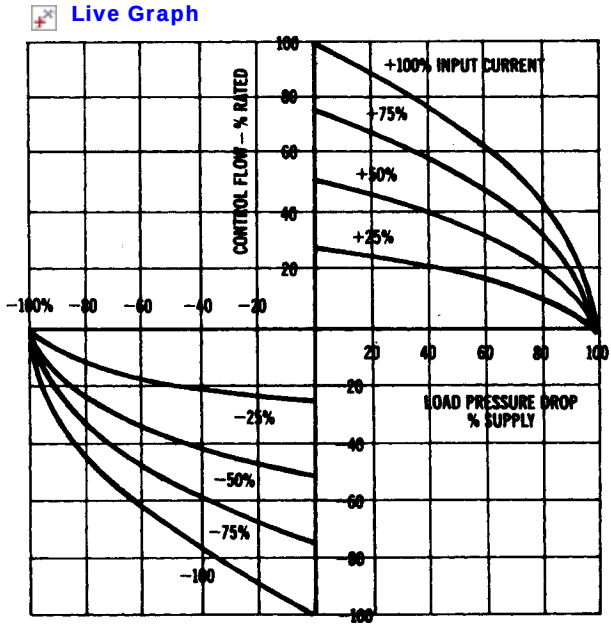


Figure 34 Typical steady-state pressure–flow characteristics of an electrohydraulic servovalve. (Courtesy of Moog Inc., East Aurora, NY.)

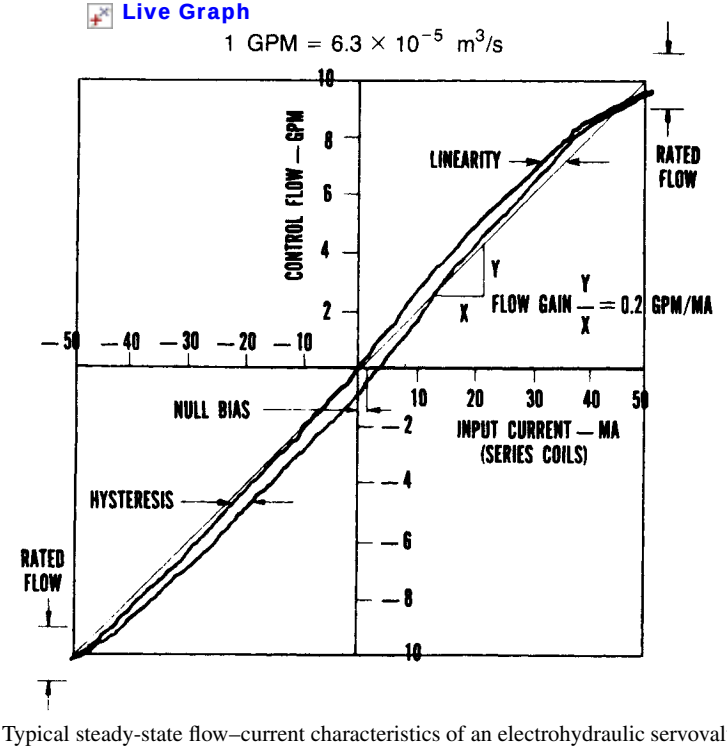


Figure 35 Typical steady-state flow–current characteristics of an electrohydraulic servovalve. (Courtesy of Moog, Inc., East Aurora, NY.)

Another important characteristic of an electrohydraulic servovalve is its hysteresis due to the characteristics of the permanent magnets in the torque motor. The hysteresis characteristic is determined from a measurement of the output flow rate as a function of the input current for a constant (usually zero) pressure drop across the valve (load pressure drop). A typical hysteresis characteristic is shown in Fig. 35. The slope of the flow–current curve is the ''flow sensitivity'' of the valve [i.e., K_1 in Eq. (63)].

It is often convenient in the dynamic analysis of servoactuators to have an approximate dynamic model for the servovalve. Experience has shown that linearized transfer functions based on empirical approximations from measured servovalve responses are adequate for most system designs. Reference 39 outlines considerations underlying the determination of approximate transfer function models for electrohydraulic servovalves. Figure 36 shows typical frequency response plots for an electrohydraulic flow control servovalve, along with approximate transfer functions. For a frequency range of 0–50 Hz, the following first-order expression has been found to be adequate for two-stage electrohydraulic servovalves:

$$\frac{\Delta Q_m(s)}{\Delta I(s)} = \frac{K_1}{\tau s + 1} \tag{65}$$

where $Q_m(s)$ = Laplace transform of control flow rate to the servomotor
$I(s)$ = Laplace transform of the current input to the servovalve
K_1 = servovalve flow sensitivity at $P_m = 0$, $I = 0$
τ = apparent servovalve time constant (s)

Typical time constants for electrohydraulic flow control servovalves are given in Table 9.

If a good approximation is desired over a wider frequency range, the following second-order model may be preferred:

$$\frac{\Delta Q_m(s)}{\Delta I(s)} = \frac{K_1}{(s/\omega_n)^2 + (2\zeta/\omega_n)s + 1} \tag{66}$$

where $\omega_n = 2\pi f_n$ = apparent natural frequency (rad/s)
ζ = apparent damping ratio (dimensionless)

Typical values of f_n and ζ for two-stage electrohydraulic flow control servovalves are given in Table 9.

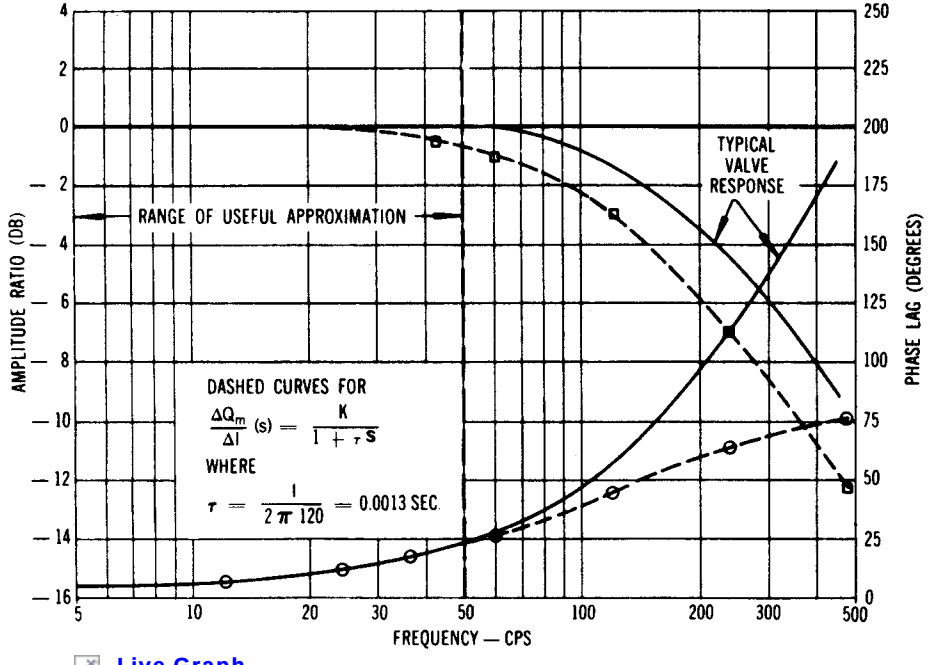
9 ELECTROMECHANICAL AND ELECTROHYDRAULIC SERVOSYSTEMS

9.1 Typical Configurations of Electromechanical Servosystems

An electrical servomotor may be combined with an electrical or electronic modulator to form an electromechanical servoactuator. The addition of a feedback transducer forms a servosystem. Figure 2 shows an electromechanical linear-motion servosystem which incorporates a rotary brushless dc servomotor and tachometer feedback; the electronic modulator is not shown.

9.2 Typical Configurations of Electrohydraulic Servosystems

A servoactuator comprising an electrohydraulic servovalve and a servomotor may be combined with an electronic servoamplifier (or modulator) and an appropriate feedback transducer to form a high-performance servosystem. Schematic diagrams of three typical electrohydraulic servosystems are shown in Fig. 37.



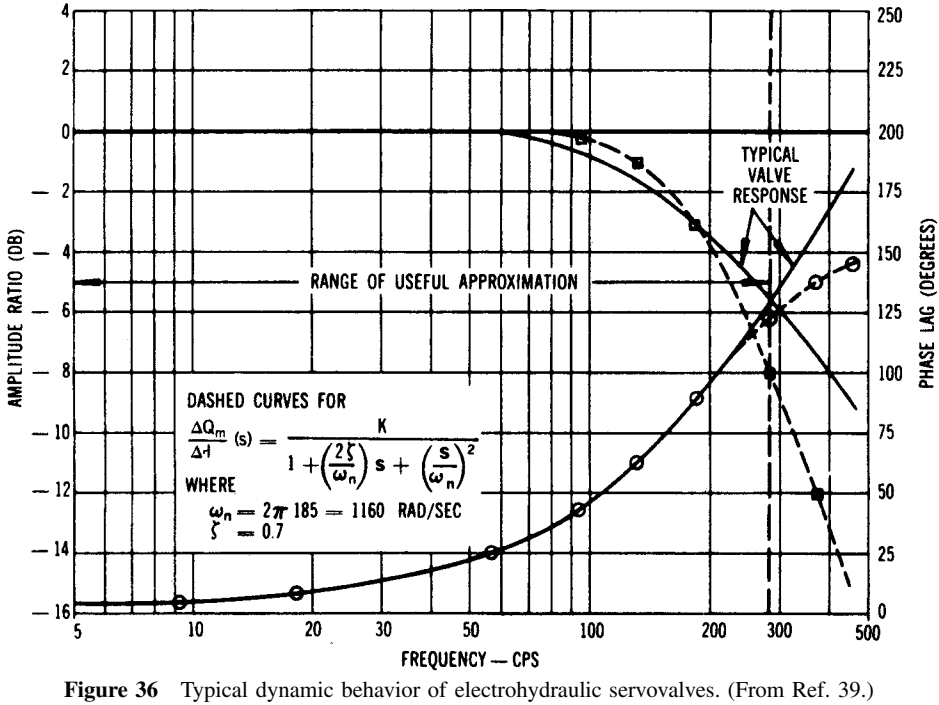


Figure 36 Typical dynamic behavior of electrohydraulic servovalves. (From Ref. 39.)

Table 9 Typical Dynamic Characteristics of Two-Stage Electrohydraulic Flow Control Servovalves

		Approximate Dynamics, 3000 psi, 100°F, Peak-to-Peak Input at 50% Rated Current		
			Second Order	
Flow Control Servovalve	Maximum Flow Capacity at 3000 psi (gpm)	First Order, τ (s)	f_n (cps)	ζ
A	2	0.0013	240	0.5
B	6	0.0015	200	0.5
C	12	0.0020	160	0.55
D	18	0.0023	140	0.6
E	30	0.0029	110	0.65

Source: From Ref. 39.

Figure 38 shows a photograph and a cross section of a high-performance servosystem which incorporates an electrohydraulic servovalve, an axial-piston servomotor, and a tachometer. The servoamplifier is not shown. Direct manifold mounting of the servovalve results in a small compressed oil volume and therefore high torsional stiffness and fast dynamic response.

Digital control is becoming an important technique for producing near-optimum performance from electrohydraulic servosystems. Figure 39 shows a block diagram and a cutaway of a fully integrated digital electrohydraulic position control system.[40] A two-stage electrohydraulic servovalve drives a linear-motion servomotor. A microcomputer and other electronics integrated within the servovalve housing drive the valve and provide signal conditioning for the position feedback transducer. A ferromagnetic digital position measurement transducer is mounted within the servomotor housing. The feedback management technique uses the microcomputer to model the system and provide digital velocity and acceleration signals without the use of separate sensors (i.e., a digital observer is used). Eight gains are required for accurate and smooth control, and these are calculated within the digital controller to generate the control signal to the torque motor.

9.3 Comparison of Electromechanical and Electrohydraulic Servosystems

Precision motion and force control can be achieved using either electromechanical or electrohydraulic servosystems. The actual choice between electromechanical and electrohydraulic must be based on a number of factors and trade-offs. Studies by Moog, Inc. have produced the following conclusions[3]:

1. Brushless motors with high-energy samarium–cobalt magnets make possible lightweight electromechanical actuators having good response and high efficiency.
2. Electromechanical actuation is currently an alternative to electrohydraulic actuation for applications requiring up to approximately 3–4 hp. Higher power electromechanical actuation systems are limited at the present time by the lack of reliable, compact, lightweight electronics.
3. Electrohydraulic actuation has a proven record in a variety of aerospace and industrial applications requiring high power levels.

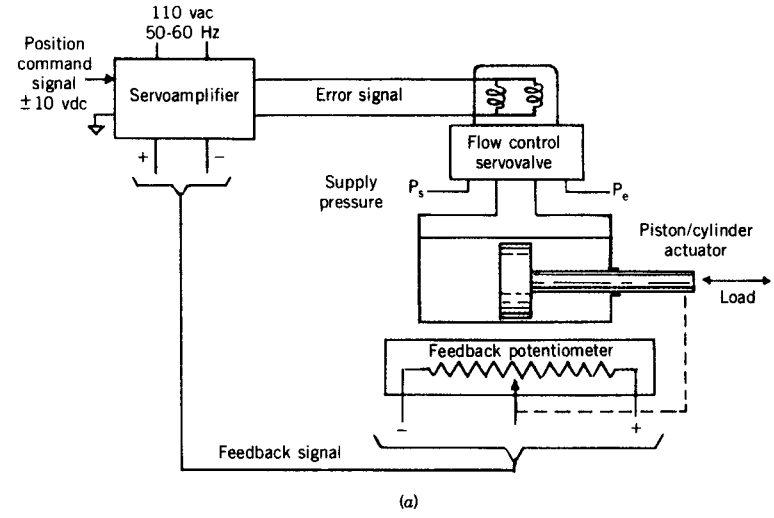
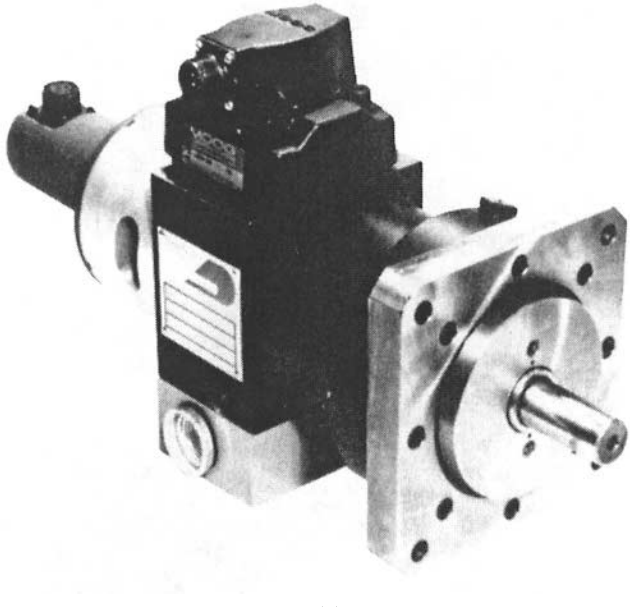
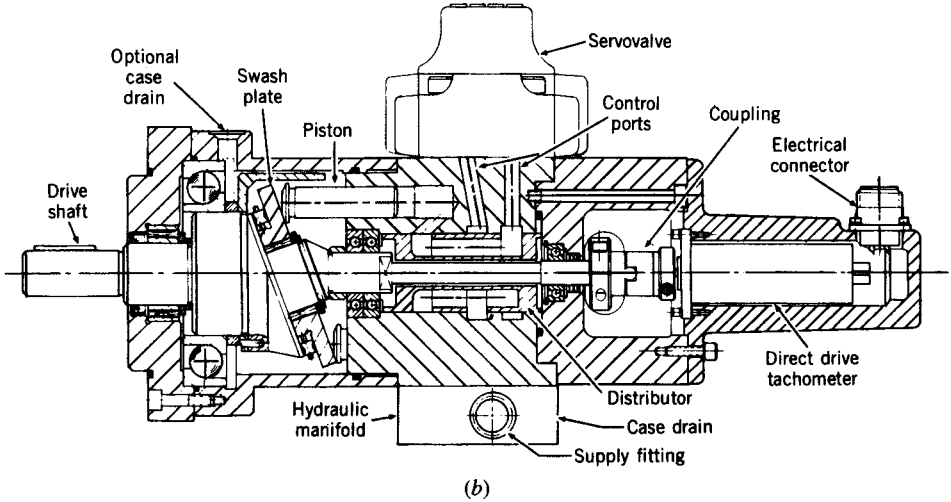


Figure 37 Typical electrohydraulic servosystems: (*a*) linear position servosystem; (*b*) rotary velocity servosystem; (*c*) force servosystem. (Courtesy of Moog, Inc., East Aurora, NY.)

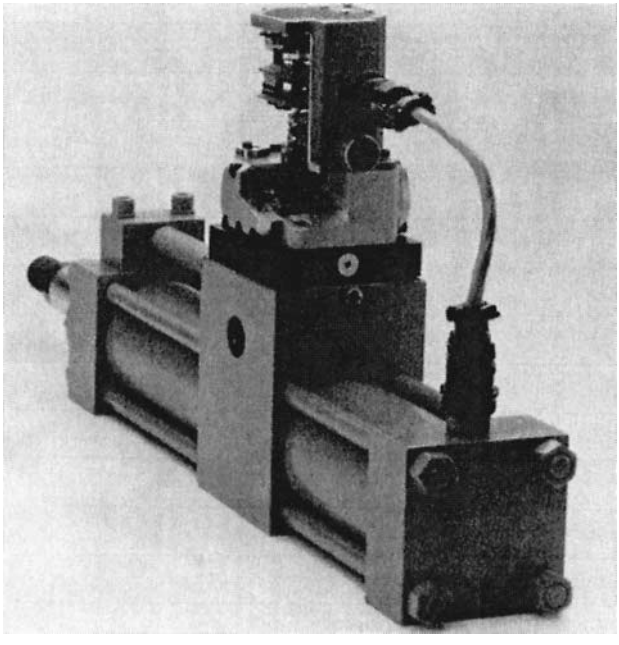


(*a*)

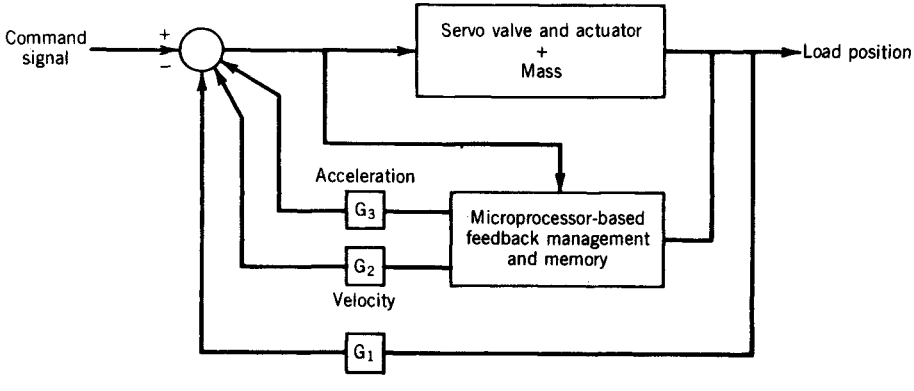


(*b*)

Figure 38 Servosystem with rotary actuator, tachometer, and electrohydraulic servovalve: (*a*) photograph of Moog–Donzelli servosystem; (*b*) cross section of Moog–Donzelli servosystem. (Courtesy of Moog, Inc., East Aurora, NY.)



(*a*)



(*b*)

Figure 39 Servosystem with linear actuator, position transducer, and microprocess-based electrohydraulic servovalve: (*a*) cutaway of servosystem; (*b*) block diagram of servosystem. (Courtesy of Vickers, Inc., Troy, MI.)

Table 10 compares advantages and disadvantages of electromechanical and electrohydraulic servosystems.[3]

10 STEADY-STATE AND DYNAMIC BEHAVIOR OF SERVOACTUATORS AND SERVOSYSTEMS

Mathematical models of the components presented in previous sections of this chapter may be combined with a load model to describe the behavior of the servosystem. The system model may be used to study the steady-state and dynamic behavior of the system for various values of system parameters and operating conditions. A number of commercially available digital simulation codes are available for determining the performance in the time or frequency domain.

The combination of a modulator and a servomotor with a load (with or without gearing) forms an open-loop system. Position or velocity feedback may be used to provide a special performance feature (e.g., use of position feedback to convert an open-loop velocity control system to a position control system) or to improve performance.

10.1 Electromechanical Servoactuators

Figure 40 shows schematically a servoactuator comprising a permanent-magnet dc servomotor and an electronic amplifier used to control the velocity of a rotary inertia load. Gearing is used to match the motor torque capability with the load requirements.

Table 10 Comparison of Electromechanical and Electrohydraulic Servosystems

Electromechanical	Electrohydraulic
Advantages	
Lower cost than electrohydraulic	Mature technology
Momentary overdrive capability	Very high reliability
Low quiescent power	Highest actuation performance
Low system weight in low-hp range	Smaller and lighter weight in high-hp range
Packaging flexibility	Continuous power output capability
Conventional or pancake motors	Continuous stall torque capability
Different types of gear reduction	Wide temperature capability
Easy check-out	High vibration and acceleration capability
Single responsibility for servoelectronics and actuators	Proven long-term storability
	Nuclear hardenable
	No EMI generation
	Simple low-power servoelectronics
Disadvantages	
More complex electronics	Usually higher cost
Communication logic for brushless motors	Generally requires more complex power conversion equipment
High-power drive with current limiting	Requires clean hydraulic fluid
Motor inertia-into-stops problems	Quiescent power loss
Overheating with high static loads	
Requires motion reduction/conversion	
Generates EMI	
More difficulty nuclear hardening	
High-power electromechanical actuation not yet proven	

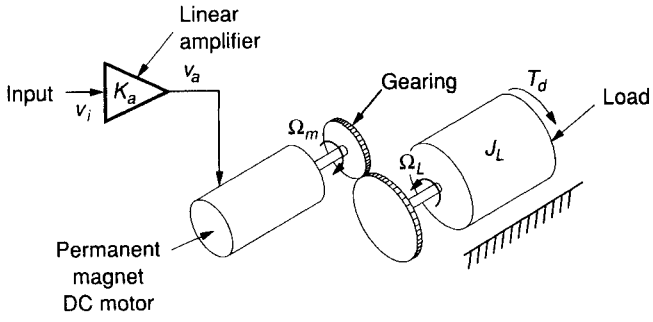


Figure 40 Schematic diagram of an electromechanical servoactuator.

A simplified dynamic model may be derived based on the following assumptions:

1. The amplifier bandwidth is considerably greater than that of the servomotor load portion of the system.
2. The gears have zero backlash and infinite stiffness.
3. The connecting shafts all have infinite stiffness.

Assumptions 2 and 3 eliminate some important dynamic effects that may need to be included in some cases.[41]

Definitions of the critical parameters and variables are as follows:

B_L = viscous damping in the load (N·m·s/rad)
J_L = polar moment of inertia of the load (N·m·s^2/rad)
K_a = voltage gain of amplifier (V/V)
K_{ac} = current gain of amplifier (A/V)
n = gear ratio, Ω_m/Ω_L, θ_m/θ_L
T_e = external load torque (N·m)
$T_d(s)$ = Laplace transform of T_d
T_{fL} = Coulomb friction torque in load (N·m)
T_m = total load torque reflected to the motor shaft (N·m)
T_L = total load torque (N·m)
v_a = voltage output of amplifier (V)
v_i = voltage input to amplifier (V)
$V_i(s)$ = Laplace transform of v_i
θ_L = angular displacement of the load (rad)
Ω_L = angular velocity of the load (rad/s)

Other parameters are as defined in Section 3.

Mathematical Model

The basic equations which describe the dynamic behavior of the servoactuator in Fig. 40 are as follows:

Amplifier equation:

$$v_a = K_a v_i \tag{67}$$

Motor equations:

- Electrical:

$$v_a = K_E\Omega_m + L_a\frac{di}{dt} + R_a i \tag{68}$$

- Torque balance:

$$K_T i = J_m\frac{d\Omega_m}{dt} + B_m\Omega_m + T_{fm} + T_m \tag{69}$$

- Gear equation:

$$n = \frac{\Omega_m}{\Omega_L} = \frac{\theta_m}{\theta_L} \tag{70}$$

- Lossless power transfer:

$$T_m\Omega_m = T_L\Omega_L \tag{71}$$

- Load torque balance:

$$T_L = J_L\frac{d\Omega_L}{dt} + B_L\Omega_L + T_{fL} + T_e \tag{72}$$

If the gearing has backlash, the relationship between θ_m and θ_L is as shown in Fig. 41. Similarly, if there is a Coulomb friction load torque, the relationship between the torque and the load velocity is as shown in Fig. 42. These nonlinear effects can be included in the model, but the resulting set of algebraic and differential equations can be studied only through digital simulation. Then the solution must be obtained for a specified input command; a general solution is not possible. It is often sufficient in analysis underlying preliminary design to simplify the model by linearizing the equations and eliminating nonlinear effects such as backlash and Coulomb friction. Such a linearized model can be very useful

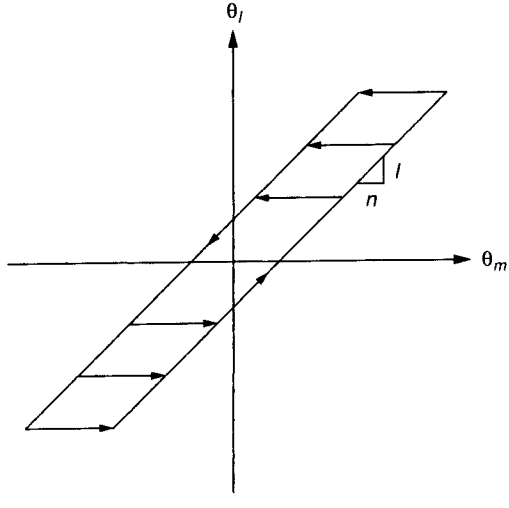


Figure 41 Relationship between θ_m and θ_L due to backlash.

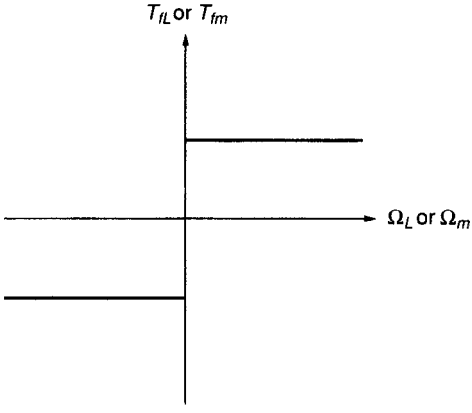


Figure 42 Coulomb friction characteristic.

in gaining an understanding of the general behavior of a system and the sensitivity of the performance to parameter changes.

Equations (67)–(72) can be linearized by assuming small variations of all variables about an initial steady-state operating point. For the system considered here, the linearized dynamic model in the Laplace domain is given by

$$\Delta\Omega_m(s) = G_1(s)\,\Delta V_i(s) - G_2(s)\,\Delta T_e(s) \tag{73}$$

where the transfer functions $G_1(s)$ and $G_2(s)$ are

$$G_1(s) = \frac{K_a K_T}{R_a B_t(\tau_e s + 1)(\tau_m s + 1) + K_T K_E} \tag{74}$$

$$G_2(s) = \frac{(R_a/n(\tau_e s + 1)}{R_a B_t(\tau_e s + 1)(\tau_m s + 1) + K_T K_E} \tag{75}$$

and where

$$\tau_e = \frac{L_a}{R_a} \qquad \tau_m = \frac{J_t}{B_t}$$

$$J_t = J_m + \frac{J_L}{n^2} \qquad B_t = B_m + \frac{B_L}{n^2}$$

A block diagram of Eq. (73) is given in Fig. 43.

In most cases the mechanical time constant (τ_m) is much greater than the electrical time constant (τ_e). In this case, the transfer functions of Eqs. (74) and (75) simplify to first-order forms as follows:

$$G_1'(s) = \frac{K_1}{\tau_1 s + 1} \tag{76}$$

$$G_2'(s) = \frac{K_2}{\tau_2 s + 1} \tag{77}$$

where

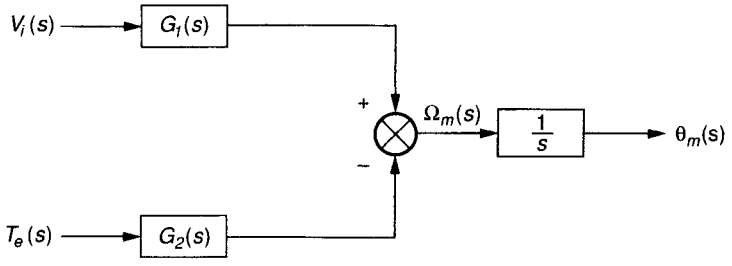


Figure 43 Block diagram of a servoactuator with voltage input.

$$K_1 = \frac{K_a K_T}{R_a B_t + K_T K_E} \tag{78}$$

$$K_2 = \frac{R_a}{n(R_a B_t + K_T K_E)} \tag{79}$$

$$\tau_1 = \tau_2 = \frac{R_a B_t \tau_m}{R_a B_t + K_T K_E}$$

If the mechanical and electrical time constants are comparable, the transfer functions can be expressed in the canonical form as

$$G_1(s) = \frac{K_1}{(s^2/\omega_n^2) + (2\zeta/\omega_n)s + 1} \tag{80}$$

$$G_2(s) = \frac{K_2(\tau_e s + 1)}{(s^2/\omega_n^2) + (2\zeta/\omega_n)s + 1} \tag{81}$$

where K_1 and K_2 are as defined in Eqs. (78) and (79), respectively, and

$$\omega_n = \sqrt{\frac{1}{\tau_e \tau_m}\left(1 + \frac{K_T K_E}{R_a B_t}\right)} \tag{82}$$

$$\zeta = \frac{1}{2}\left[\frac{\tau_e + \tau_m}{\sqrt{\tau_e \tau_m[1 + (K_T K_E/R_a B_t)]}}\right] \tag{83}$$

If a current amplifier is used instead of a voltage amplifier, the resulting linearized dynamic model of the system is given by

$$\Delta\Omega m(s) = G_3'(s)\,\Delta I(s) - G_4'(s)\,\Delta T_e(s) \tag{84}$$

where

$$G_3'(s) = \frac{K_T K_{ac}}{B_t(\tau_m s + 1)} \tag{85}$$

$$G_4'(s) = \frac{1}{B_t n(\tau_m s + 1)} \tag{86}$$

That is, the electrical time constant is not a factor if the current amplifier is used.

Numerical Example

A Magnetic Technology, Inc. dc servomotor (model 3069-237/045; see Ref. 14) is used to rotate an inertia load. System parameters are as follows:

Motor:

$B_m = 1.9$ in.·oz·s/rad (1.34×10^{-2} N·m·s/rad)

$J_m = 0.016$ in.·oz·s^2/rad (1.13×10^{-4} N·m·s^2/rad)

$K_E = 0.236$ V·s/rad

$K_T = 33.4$ in.·oz/A (0.24 N·m/A)

$L_a = 4.8$ mH

$R_a = 4.5\ \Omega$

Gearing:

$n = 3$

Load:

$B_L = 35$ in.·oz·s/rad (0.25 N·m·s/rad)

$J_L = 0.2$ in.·oz·s^2/rad (1.41×10^{-3} N·m·s^2/rad)

Amplifier:

$K_a = 8$ V/V

Substituting these parameters into Eqs. (78), (79), (82), and (83) gives the following gains and performance factors:

$$K_1 = 7.87 \text{ rad/s·V}$$

$$K_2 = 0.044 \text{ rad/in.·oz·s (6.23 rad/N·m·s)}$$

$$\omega_n = 68.5 \text{ Hz}$$

$$\zeta = 1.27$$

and from the definition for τ_e,

$$\tau_e = \frac{L_a}{R_a} = 1.07 \times 10^{-3} \text{ s}$$

Since the damping ratio (ζ) is greater than 1, the system will have an overdamped dynamic response. The transfer functions are as follows:

$$G_1(s) = \frac{7.87}{5.40 \times 10^{-6}s^2 + 5.88 \times 10^{-3}s + 1} \tag{87}$$

$$G_2(s) = \frac{0.13(1.07 \times 10^{-3}s + 1)}{5.40 \times 10^{-6}s^2 + 5.88 \times 10^{-3}s + 1} \tag{88}$$

Equations (87) and (88) can be used to determine the transient response or the frequency response.

10.2 Electromechanical Servosystems

Only servosystems including dc servomotors are considered here. The reader should consult Ref. 41 for a more comprehensive treatment of other types of electromechanical servosystems.

Figure 44 shows a closed-loop servosystem that utilizes tachometer feedback around the servoactuator discussed in the previous section. Through the use of velocity feedback, greater accuracy can be achieved than with the open-loop system.

Mathematical Models

An approximate linearized model may be derived for the servosystem by combining the open-loop system model [Eq. (73)] with the following equations:

Summation:

$$v_i = v_{\text{ref}} - v_f \tag{89}$$

Tachometer:

$$v_f = K_t \Delta_m \tag{90}$$

Amplifier:

$$v_a = K_a v_i \tag{91}$$

Equation (90) assumes that the tachometer is mounted directly on the motor shaft, which is normally the case. Reference 18 discusses cases where the tachometer is mounted in other configurations. Also, Ref. 18 presents more accurate tachometer models to account for the magnetic coupling of the tachometer to the motor field. The basic form of the tachometer model in that case is that of a high-pass filter with a phase shift that is dependent on the angular orientation of the tachometer to the motor.

Equations (73), (89), (90), and (91) may be combined to obtain the following closed-loop servosystem model:

$$\Delta\Omega_m(s) = G_3(s)\,\Delta V_i(s) - G_4(s)\Delta T_e(s) \tag{92}$$

where

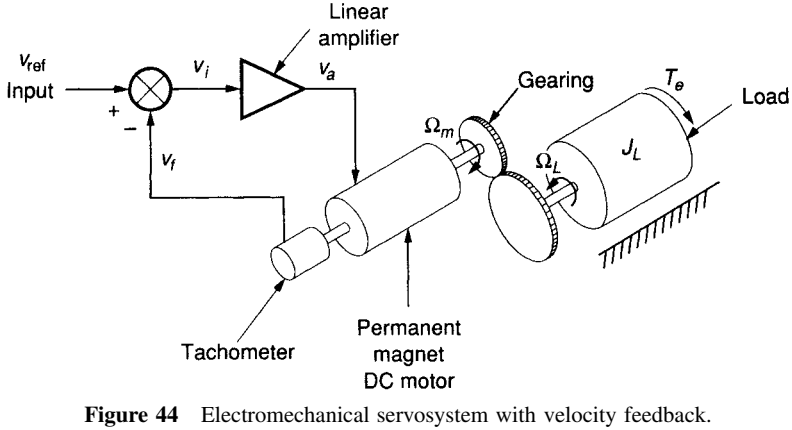


Figure 44 Electromechanical servosystem with velocity feedback.

$$G_3(s) = \frac{K_a K_T}{R_a B_t(\tau_e s + 1)(\tau_m s + 1) + K_T K_E + K_f K_a K_T} \tag{93}$$

$$G_4(s) = \frac{(R_a/n)(\tau_e s + 1)}{R_a B_t(\tau_e s + 1)(\tau_m s + 1) + K_T K_E + K_f K_a K_T} \tag{94}$$

All parameters and variables are defined in the previous section and in Fig. 44. The second-order transfer functions $G_3(s)$ and $G_4(s)$ can be expressed in canonical form as follows:

$$G_3 = \frac{K_3}{(s^2/\omega_{n1}^2) + (2\zeta_1/\omega_{n1})s + 1} \tag{95}$$

$$G_4 = \frac{K_4(\tau_e s + 1)}{(s^2/\omega_{n1}^2) + (2\zeta_1/\omega_{n1})s + 1} \tag{96}$$

where

$$K_3 = \frac{K_a K_T}{R_a B_t + K_T K_E + K_f K_a K_T} \tag{97}$$

$$K_4 = \frac{R_a}{n(R_a B_t + K_T K_E + K_f K_a K_T)} \tag{98}$$

$$\omega_{n1} = \sqrt{\frac{1}{\tau_e \tau_m}\left(1 + \frac{K_T K_E + K_f K_a K_T}{R_a B_t}\right)} \tag{99}$$

$$\zeta_1 = \frac{1}{2}\left[\frac{\tau_e + \tau_m}{\sqrt{\tau_e \tau_m\,[1 + (K_T K_E + K_f K_a K_T)/R_a B_t]}}\right] \tag{100}$$

From the expressions for the closed-loop natural frequency (ω_{n1}) and damping ratio (ζ_1), it is apparent that increasing the feedback gain (K_f) increases the speed of response but decreases the degree of stability.

As in the case with the open-loop system, if the electrical time constant is much smaller than the mechanical time constant, the second-order transfer functions of Eqs. (95) and (96) reduce to the first-order forms given below:

$$G_5(s) = \frac{K_5}{\tau_5 s + 1} \tag{101}$$

$$G_6(s) = \frac{K_6}{\tau_6 s + 1} \tag{102}$$

where

$$K_5 = K_3 \qquad \text{[see Eq. (97)]}$$

$$K_6 = K_4 \qquad \text{[see Eq. (98)]}$$

and

$$\tau_5 = \tau_6 = \frac{R_a B_i \tau_m}{R_a B_t + K_T K_E + K_f K_a K_T}$$

Similar expressions may be derived for the case with a current amplifier instead of a voltage amplifier. It is preferable to use a current amplifier where cost is not prohibitive.

Numerical Example

Consider a closed-loop electromechanical servosystem comprising the open-loop system of Section 10.1 with velocity feedback added. For the same numerical values as in the numerical example of Sec. 10.1 and with $K_f = 3$ V/krpm, the following results are obtained.

$$K_3 = 6.42 \text{ rad/s·V}$$

$$K_4 = 0.036 \text{ rad/in.·oz·s (5.10 rad/N·m·s)}$$

$$\omega_{n1} = 75.8 \text{ Hz}$$

$$\zeta_1 = 1.143$$

10.3 Electrohydraulic Servoactuators

Figure 45 is a physical representation of an electrohydraulic servoactuator used to position an inertia load. A two-stage electrohydraulic servovalve modulates the flow of hydraulic fluid to a double-acting hydraulic motor (actuator). The current input to the torque motor of the servovalve, I, is provided by an electronic servoamplifier of gain K_a.

A simplified dynamic model may be derived to relate the voltage input to the servoamplifier, E_s, to the velocity output of the load, $\dot{Y}$. The following basic assumptions simplify the analysis.

1. The amplifier bandwidth is considerably greater than that of the servovalve and the servomotor-load portions of the system.
2. The supply pressure P_s and the exhaust pressure P_e are constant.
3. The bulk modulus of elasticity and viscosity of the hydraulic fluid are constant.
4. The leakage flow rate past the actuator piston is linearly proportional to the pressure drop across the piston; that is, $Q_L = C_2 P_m$ [see Fig. 28 and Eqs. (39) and (40)].
5. All connecting passages are rigid and sufficiently short in length and large in diameter to eliminate any resistance or transmission line effects.

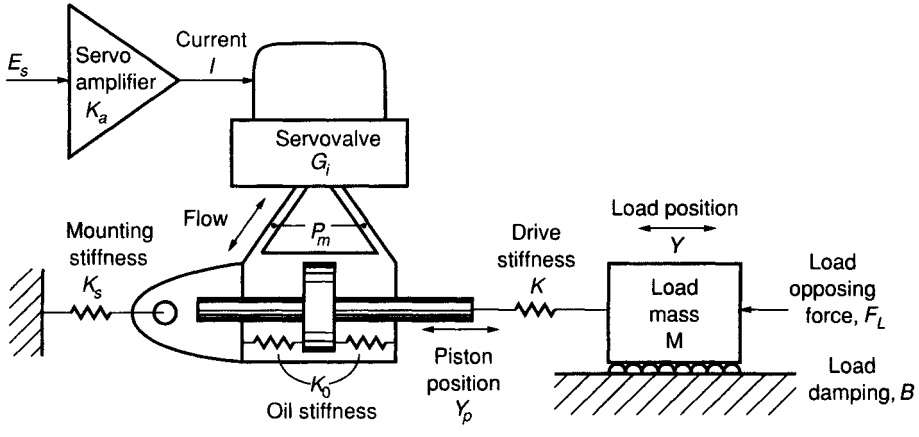


Figure 45 Physical representation of an electrohydraulci servoactuator. (Adapted from Ref. 35.)

6. The mass of the moving parts in the servomotor (M_a) and the viscous damping in the servomotor (B_m) are small compared to the mass (M) and the viscous damping (B) associated with the load.
7. The Coulomb friction and stiction forces in the servomotor and load are negligible.

Mathematical Model

The typical servoamplifier is governed by the equation

$$I = K_a E_s \tag{103}$$

Equation (61) describes the steady-state behavior of the electrohydraulic servovalve. This equation can be used in the dynamic analysis of the servoactuator if the servovalve dynamics are negligible compared to the servomotor-load dynamics. Otherwise, either Eq. (65) or (66) should be used. Equations (38)–(44) describe the dynamic behavior of the servomotor. The external load force in Eq. (38) may be expressed as follows:

$$F_e - F_L = M\frac{d^2Y}{dt^2} + B\frac{dY}{dt} + K(Y_p - Y) \tag{104}$$

The set of algebraic equations outlined above cannot be combined into a single dynamic equation or transfer function because of nonlinearities. Also, since the set of equations is rather complex, conclusions about the performance of the system cannot be drawn without actually solving the equations for a variety of conditions. A computer-based analysis is the only practical method of determining the steady-state and dynamic performance of the system unless the equations are linearized in some fashion.

A linearized model which assumes small perturbations of all variables about an initial steady-state operating condition can be very useful in quickly assessing system dynamic behavior. Such a model is particularly useful for preliminary design and as a reference when an analysis is made using the set of nonlinear describing equations.

It can be shown[45] that for the case when $\mathcal{V}_{1i} = \mathcal{V}_{2i} = \mathcal{V}_i$ (see Fig. 28) and under the assumptions listed above, the linearized model may be expressed as follows:

$$\left[\left(\frac{K_3M}{K_2B + A^2}\right)s^2 + \left(\frac{K_2M + BK_3}{K_2B + A^2}\right)s + 1\right]s(\Delta Y) = \left(\frac{K_aA}{K_2B + A^2}\right)G_1(s)(\Delta E_s) - \left(\frac{K_2 + K_3s}{K_2B + A^2}\right)(\Delta F_L) \tag{105}$$

where $K_2 = C_1 + C_2$
C_1 = servovalve pressure–flow sensitivity [see Eq. (64)]
C_2 = internal leakage flow-rate coefficient
$K_3 = A_2/K_t = A(1/K_0 + 1/K_s + 1/K)$
$K_0 = 2\beta A^2/\mathcal{V}_i$ = stiffness of the sealed chamber
K = stiffness of the load drive
K_s = stiffness of the structural mounting

and $G_i(s)$ is the transfer function for the servovalve. When the servovalve dynamics are negligible compared to the servomotor-load dynamics, $G_i(s) = K_1$ [see Eq. (63)]. When the servovalve dynamics are of the same order as the servomotor-load dynamics, $G_i(s)$ is given by the right-hand side of either Eq. (65) or Eq. (66).

Four important measures of performance can be observed from Eq. (105) without actually solving the equation. The steady-state gain or sensitivity of the servoactuator is

$$\left.\frac{\Delta \dot{Y}}{\Delta E_s}\right|_{\text{steady state; } \Delta F_L=0} = \frac{K_a K_i A}{K_2 B + A^2} \tag{106}$$

The steady-state load sensitivity of the servoactuator is

$$\left.\frac{\Delta \dot{Y}}{\Delta F_L}\right|_{\text{steady state; } \Delta E_s=0} = \frac{-K_2}{K_2 B + A^2} \tag{107}$$

Also observable from Eq. (105) are the natural frequency and the damping ratio associated with the servomotor-load portion of the system. The natural frequency is

$$\omega_{ns} = \sqrt{\frac{K_2 B + A^2}{K_3 M}} \tag{108}$$

and the damping ratio is

$$\zeta_s = \frac{K_2 M + K_3 B}{2\sqrt{K_3 M (K_2 B + A^2)}} \tag{109}$$

The valve dynamics are often negligible compared to the servomotor-load dynamics. In this case, Eq. (105) reduces to a second-order linear differential equation of the generalized form:

$$\left[\left(\frac{1}{\omega_{ns}^2}\right) s^2 + \left(\frac{2\zeta_s}{\omega_{ns}}\right) s + 1\right] s(\Delta Y) = \frac{K_a K_1 A}{K_2 B + A^2} \times \Delta E_s - \frac{K_2 + K_3 s}{K_2 B + A^2} \Delta F_L \tag{110}$$

In most cases, the term $K_2 B$ in Eqs. (105)–(110) is small compared to the term A^2. Simplified forms of these equations result.

The dynamic behavior of the open-loop system may be viewed in terms of the speed of response and the degree of damping. A fast system dynamic response requires a small value of τ and a large value of ω_{ns}. In order for ω_{ns} to be large, $K_3 M$ must be small compared to $K_2 B + A^2$. The value of M is usually fixed, but the designer often has some latitude in varying K_3. The value of K_3 can be minimized by making the volumes within the servomotor chambers small. Increasing the ram area also provides for an increase in ω_{ns}, but the effect is not as great as it first appears since $K_3 = f(\mathcal{V}_i)$ and $\mathcal{V}_i = f(A)$. Also, the actuator area is often set by such practical considerations as maximum load or acceleration requirements.

The degree of damping in the open-loop system is governed by Eq. (109). In most practical systems, $\zeta_s < 1$, and K_3, M, and A are fixed by other considerations. Then the damping may be increased by increasing the load damping B or the value of the effective leakage coefficient, K_L. The value of K_L may be increased by increasing either C_1 or C_2, that is, increasing the valve underlap or the leakage across the actuator piston. Since normally $K_2 B \ll A^2$, Eq. (107) shows that an increase in K_2 results in an increase in sensitivity to load disturbances. Likewise, an increase in the valve underlap (or the use of cross-port leakage) results in an increase in quiescent power dissipation. Clearly, there is a trade-off between degree of damping, steady-state load sensitivity, and quiescent power dissipation.

10.4 Electrohydraulic Servosystems

Figure 46 is a physical representation of a typical electrohydraulic servosystem intended to accurately position an inertia load. The addition of position feedback converts the ''rate-type'' open-loop system (servoactuator) into a position control system. The linearized model given by Eq. (110) describes the open-loop portion of this position control system, as shown in the block diagram of Fig. 47.

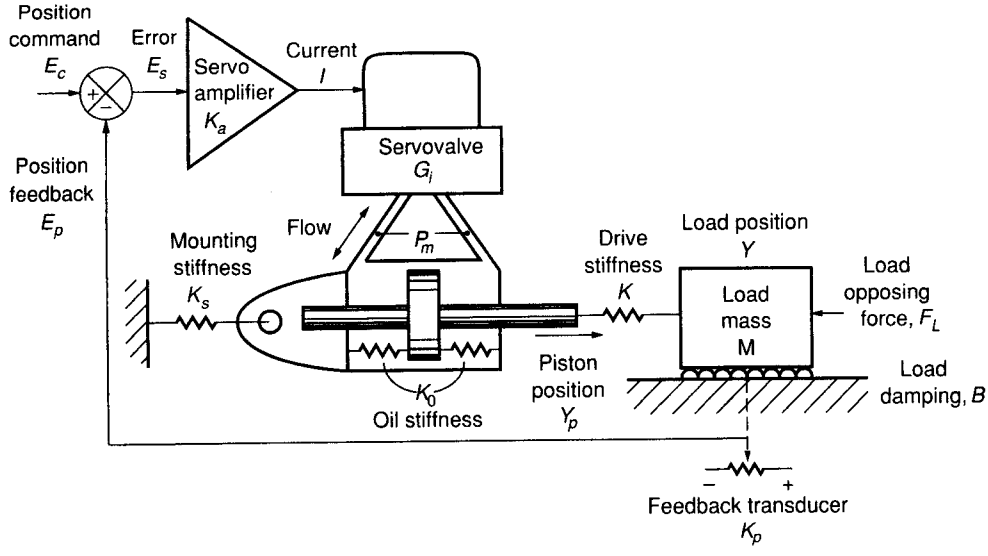


Figure 46 Physical representation of an electrohydraulic servomechanism. (From Ref. 35.)

When the change in the external load force is zero (i.e., $\Delta F_L = 0$), the dynamic model for the closed-loop system may be written as

$$\frac{\Delta Y}{\Delta E_c} = \frac{1}{K_p}\left[\frac{1}{K_{Lp}(1/\omega_{ns}^2)s^2 + (2\zeta_s/\omega_{ns})s + 1)(\tau s + 1)(s) + 1}\right] \tag{111}$$

where

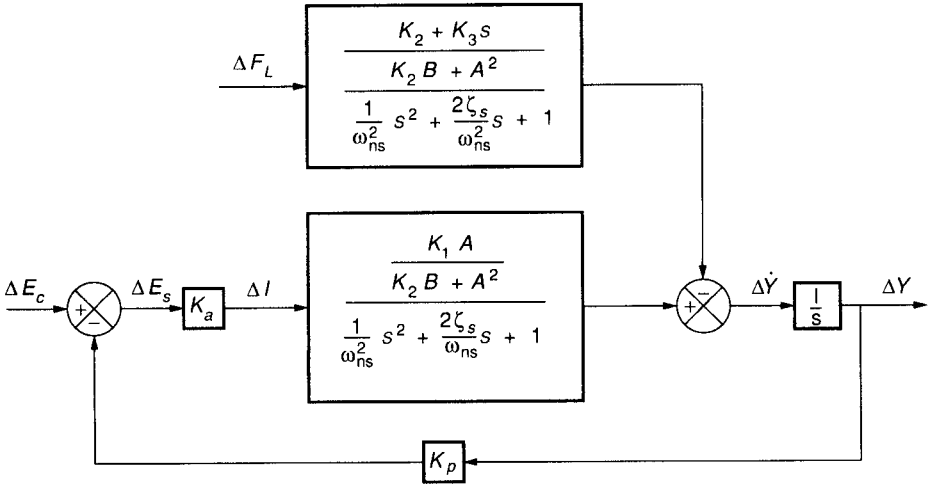


Figure 47 Block diagram of an electrohydraulic positional servomechanism.

$$K_{Lp} = \frac{K_p K_a K_1 A}{K_2 B + A^2} = \text{loop gain}$$

For the case where the servovalve dynamics are negligible compared to the servomotor-load dynamics, Eq. (111) reduces to the following third-order differential equation:

$$\frac{\Delta Y}{\Delta E_c} = \frac{1}{K_p}\left[\frac{1}{(1/K_{Lp})(1/\omega_{ns}^2)s^2 + ((2\zeta_s/\omega_{ns})s + 1s + 1)}\right] \tag{112}$$

In the steady state, Eqs. (111) and (112) both reduce to

$$\left.\frac{\Delta Y}{\Delta E_c}\right|_{\text{steady state}} = \frac{1}{K_p} \tag{113}$$

The integration in the forward loop results in a system with a zero steady-state error for a constant input and a steady-state output that is dependent only on the system input and the position feedback gain. (See Section 7 in Chapter 12 for a discussion of the following errors for systems with nonconstant inputs.) That is, the accuracy with which ΔY follows the input ΔE_c depends only on the accuracy of the feedback measurement device, and not on the accuracy of the forward loop elements.

When the change in the control input is zero (i.e., $\Delta E_c = 0$), the steady-state load sensitivity is

$$\left.\frac{\Delta Y}{\Delta F_L}\right|_{\text{steady state}} = \frac{K_2}{K_p K_a K_1 A} \tag{114}$$

That is, an increase in the feedback gain results in a decrease in the load sensitivity or an increase in the system stiffness. Likewise, an increase in the cross-port leakage in the servomotor or servovalve (i.e., increase in K_2) results in a decrease in the system stiffness.

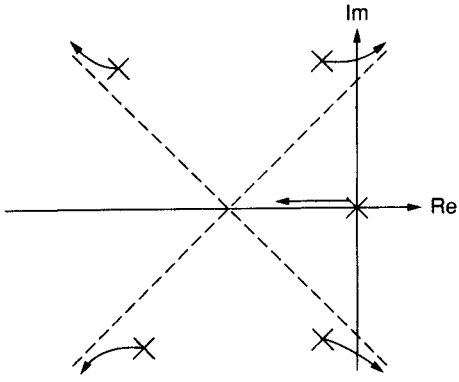
In most practical cases the roots of the quadratic in Eqs. (111) and (112) are conjugate complex (i.e., $\zeta_s < 1$), or in physical terms, this portion of the system is "underdamped." Consequently, when position feedback is employed, limitations exist in the maximum value of the position feedback gain that can be used while still ensuring system stability. Limitations also exist in the input–output sensitivity and the system stiffness to load disturbances, since these characteristics are dependent on the position feedback gain.

System relative stability can be viewed conveniently by employing the root-locus technique. Figure 48 illustrates root-locus plots for three important cases: (*a*) valve dynamics modeled by a second-order differential equation, (*b*) valve dynamics modeled by a first-order differential equation, and (*c*) negligible valve dynamics. These plots illustrate that the loop gain must be set below some value in order to ensure stability.

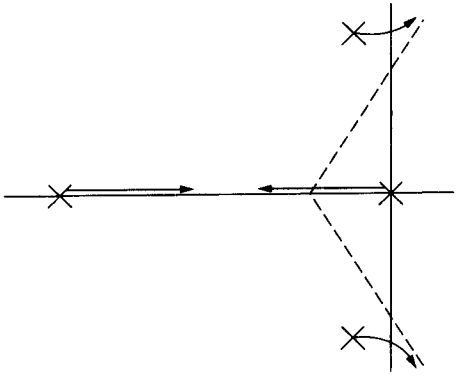
When the dynamics of the servovalve are negligible compared to the dynamics of the servomotor-load portion of the system, the system model is third order. Considerable study has been made of third-order dynamic systems. The Routh absolute stability criterion can be employed to determine the maximum value of the feedback gain that can be used and still maintain stability. For the simplified model given by Eq. (112), the maximum value of the feedback gain is

$$K_p = \frac{2\zeta_s \omega_{ns}(K_2 B + A^2)}{K_a K_1 A} \tag{115}$$

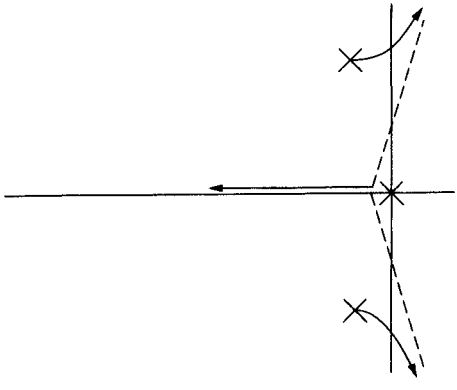
and the corresponding maximum value of the loop gain is



(*a*)



(*b*)



(*c*)

Figure 48 Typical root locus plots for an electrohydraulic positional servomechanism with and without servovalve dynamics: (*a*) with second-order servovalve model [Eq. (66)]; (*b*) with first-order servovalve model [Eq. (65)]; (*c*) with static servovalve model [Eq. (62)].

$$L_{Lp} \equiv \frac{K_p K_a K_1 A}{K_2 B + A^2} = 2\zeta_s \omega_{ns} \tag{116}$$

Equation (116) shows that the maximum value of loop gain depends only on the values of the natural frequency and damping ratio of the open-loop system.

In general, the loop gain is a critical parameter. An increase in loop gain results in a decrease in load sensitivity (or increase in stiffness), an increase in the speed of response, and a decrease in the degree of stability.

For a given electrohydraulic position control system designed to meet certain steady-state performance requirements (e.g., load sensitivity), an optimum or best value of loop gain (and therefore the best feedback gain) exists. This optimum value represents the best compromise between speed of response and degree of stability. Figure 49 illustrates responses of the system output (ΔY) to step changes in the system input (ΔE_c) for four different values of the loop gain [Eq. (112)].

A comprehensive study of Eq. (112) by Meyfarth[46] has shown that the optimum response characteristics to a step input signal are obtained when

$$\zeta_s = 0.5 \tag{117}$$

$$K_{Lp} = 0.34\omega_{ns} \tag{118}$$

In many practical casess, the open-loop system damping ratio (ζ_s) is well below 0.5. The resulting load resonance places severe limitations on the maximum level of loop gain that can be used and therefore limitations on the quality of steady-state and dynamic performance that can be achieved with the closed-loop system. That is, it may not be possible to simultaneously satisfy the steady-state load sensitivity (or stiffness) and dynamic performance requirements without special enhancements to the system.

10.5 Hydraulic Compensation

One of the features of electrohydraulic servosystems is the ease with which electronic feedback and forward-loop compensation networks can be employed to produce improved dy-

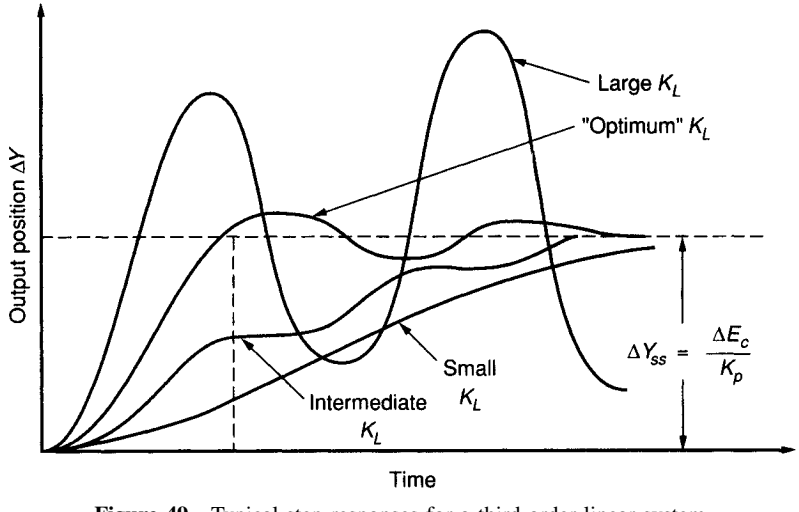


Figure 49 Typical step responses for a third-order linear system.

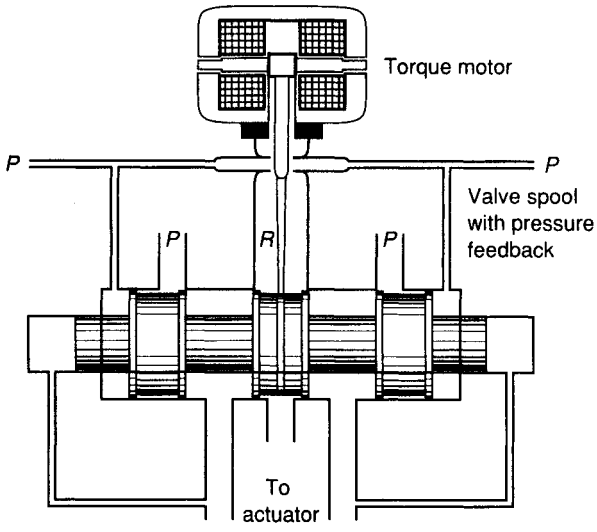


Figure 50 Electrohydraulic servovalve with pressure feedback. (From Ref. 35.)

namic performance. Such techniques are discussed in Chapter 15. The following discussion is limited to techniques for improving the damping within the hydraulic portion of the system; these techniques minimize the need to consider other electronic compensation techniques.

Techniques for improving Damping

Three well-known techniques may be employed to introduce additional damping into the open-loop system. First, *underlap* may be introduced into the servovalve, thereby increasing

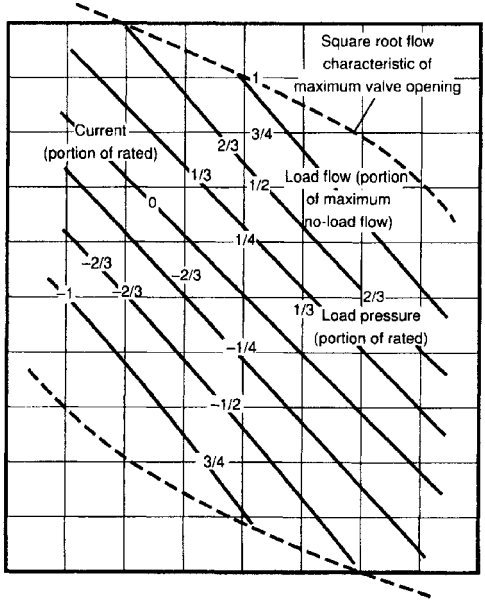


Figure 51 Pressure–flow–current characteristics of an electrohydraulic servovalve with pressure feedback. (From Ref. 35.)

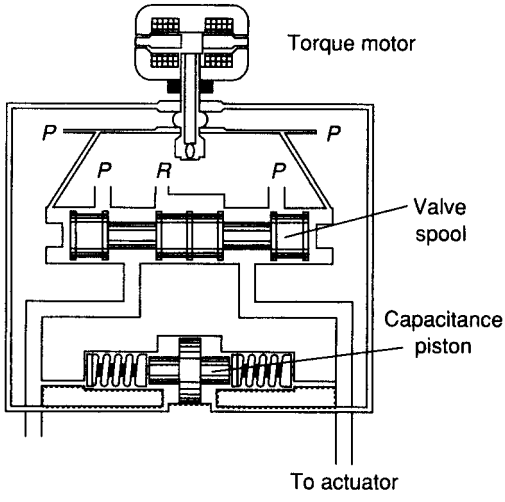


Figure 52 Electrohydraulic servovalve with dynamic pressure feedback. (From Ref. 35.)

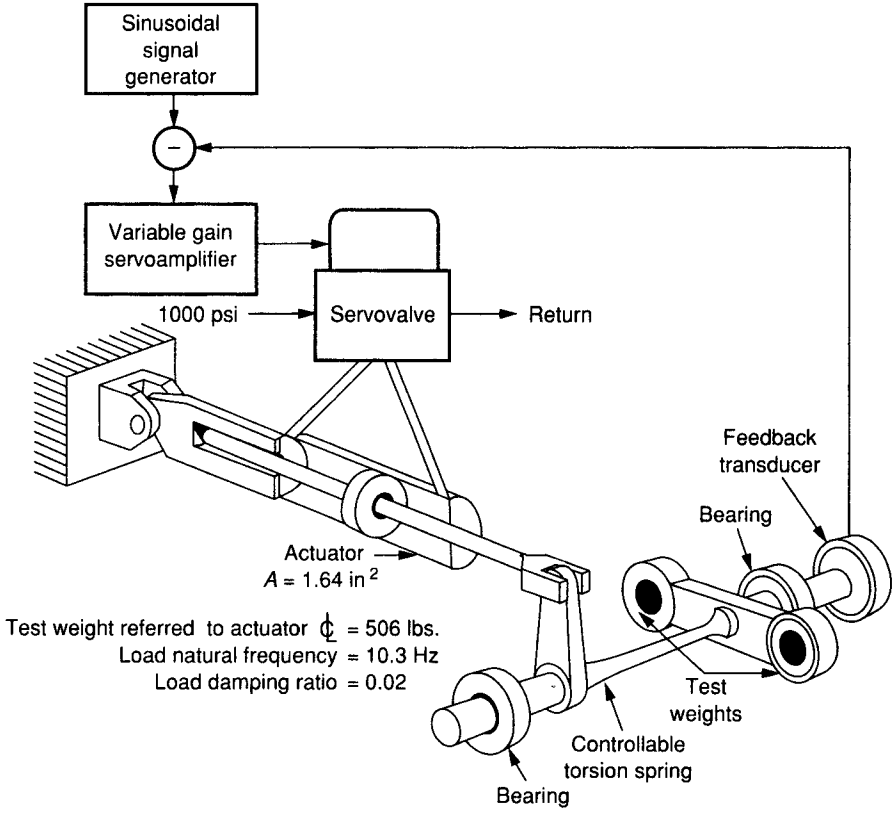


Figure 53 Pictorial diagram of experimental test setup. (From Ref. 35.)

the valve flow–pressure sensitivity [see Eq. (64)]. Second, a leakage path may be provided across the servomotor (i.e., increased value of C_2 in the equation for leakage flow rate across the piston. $Q_L = C_2 P_m$). Finally, load force (or load pressure) feedback may be provided around the servovalve–servomotor. The first and second techniques are simple and flexible but often undesirable because they result in decreased steady-state stiffness and increased steady-state power dissipation. The third technique also results in decreased steady-state stiffness but avoids the problem of increased steady-state power dissipation. All three techniques result in an effective modification of the pressure–flow–current characteristics of the servovalve.

Load force (or pressure) feedback is generally preferred in high-performance systems. This feature may be implemented electrically, that is, through feedback of the measured force directly to the servoamplifier. This electrical feedback approach results in a significant increase in system complexity and often a reduction in reliability. These problems can be avoided by direct use of the load pressure itself to reposition the servovalve spool. Figure 50 shows a servovalve in which load pressure is fed back to stub shafts located at the ends of the valve spool.

Experimentally determined steady-state flow–pressure–current characteristics for this "pressure feedback servovalve" are shown in Fig. 51. Clearly, pressure feedback results in

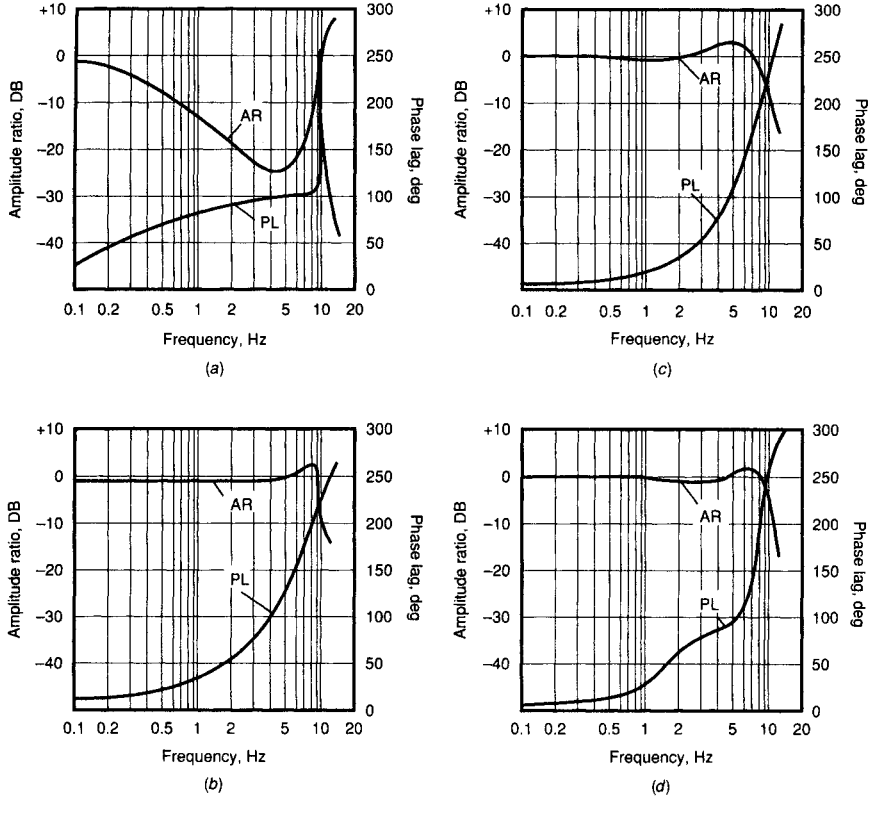


Figure 54 Measured frequency responses for electrohydraulic servosystem with different servovalves: (*a*) measured system response with flow control servovalve; (*b*) measured system response with flow control servovalve and bypass orifice; (*c*) measured system response with pressure feedback servovalve; (*d*) measured system response with servovavle. (From Ref. 35.)

Table 11 Comparative Performance of Various Electrohydraulic Position Servomechanisms

Servo Configuration	Bandwidth (±2 dB), Hz	90° Phase Lag, Hz	Static Load Stiffness, lb/in.
Flow control servovalve	0.15	0.37	9,000
Flow control servovalve with bypass orifice	8.8	5	5,100
Flow control servovalve with pressure feedback	8.8	5	2,500
DPF servovalve	9.2	5	60,000

Source: From Ref. 35.

a reshaping of the characteristics from those of the conventional servovalve (see Fig. 34). In particular, the flow-pressure sensitivity [see Eq. (64)] or slope of the characteristic curves (C_1) is increased in the vicinity of $I = 0$, $P_m = 0$ when pressure feedback is used. But an increase in this slope results in an increase in K_2 and therefore the load sensitivity [see Eq. (114)].

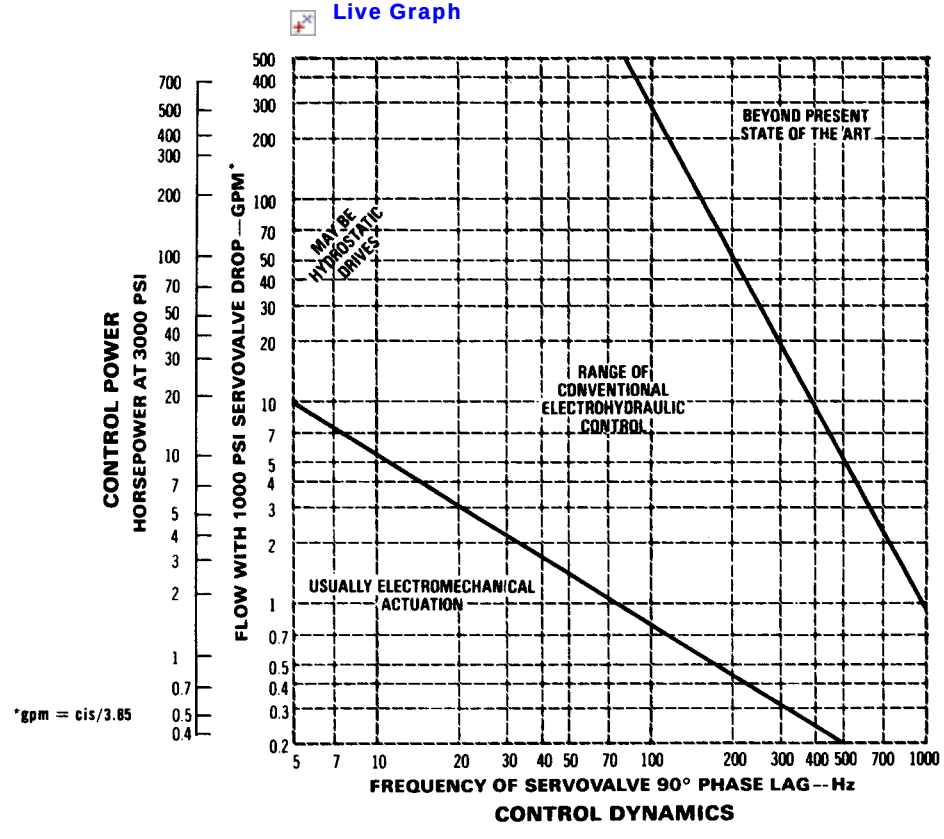


Figure 55 Range of control for electrohydraulic servomechanisms. (From Ref. 36. Courtesy of Moog, Inc., East Aurora, NY.)

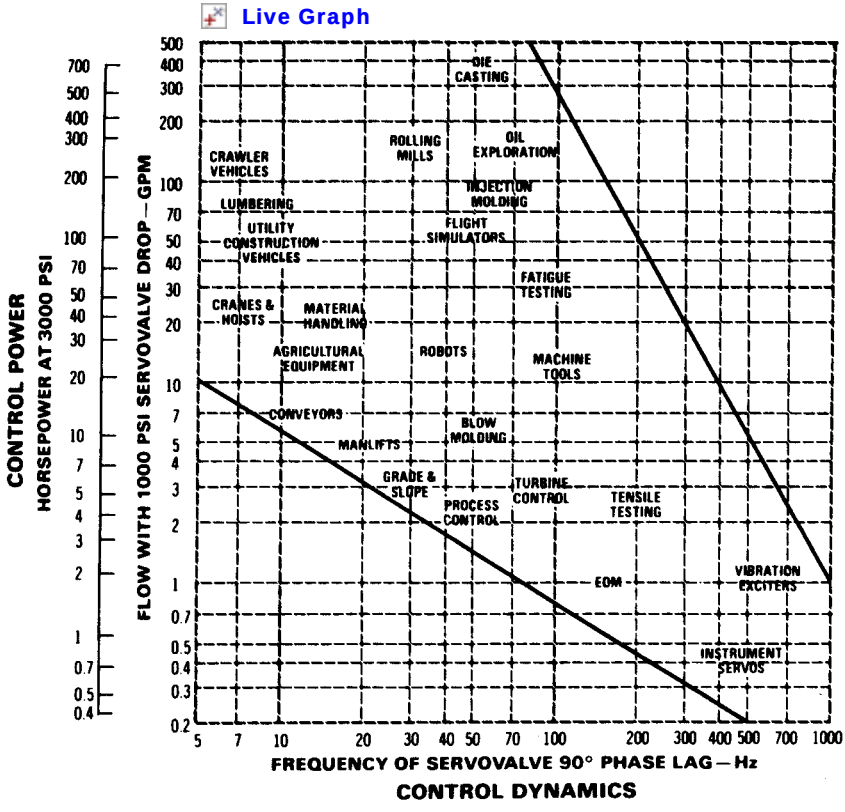


Figure 56 Spectrum of industrial applications of electrohydraulic servomechanisms. (Courtesy of Moog, Inc., East Aurora, NY.)

The *dynamic pressure feedback* (DPF) servovalve combines the best features of the conventional valve (see Fig. 30) and the pressure feedback servovalve (Fig. 50). The DPF servovalve shown in Fig. 52 is similar to the conventional servovalve except for the addition of a high-frequency-pass network (hydraulic resistance and capacitance circuit) to achieve dynamic pressure feedback. Static load pressure feedback is eliminated in this design. The design and application of the DPF servovalve is discussed in detail in Ref. 35.

Examples

A comparative study of the performance of a position control system (see Fig. 53) with different servovalves was conducted by Moog, Inc.[35] The system considered had a load resonant frequency of 10.3 Hz and a damping ratio of 0.02. Tests were conducted with four different servovalves: (a) a conventional flow control servovalve (Fig. 30), (b) a flow control servovalve with a bypass orifice, (c) a flow control servovalve with load pressure feedback (Fig. 50), and (d) a flow control servovalve with dynamic pressure feedback (Fig. 52). In each test the amplifier gain was adjusted such that the peak amplitude ratio was 1.25 (or +2 dB). In cases (b), (c), and (d) the damping was controlled to give an equivalent load damping ratio of 0.6. Measured performance results are given in Fig. 54 and Table 11. When a conventional flow control servovalve is used as in case (a), the low value of loop gain

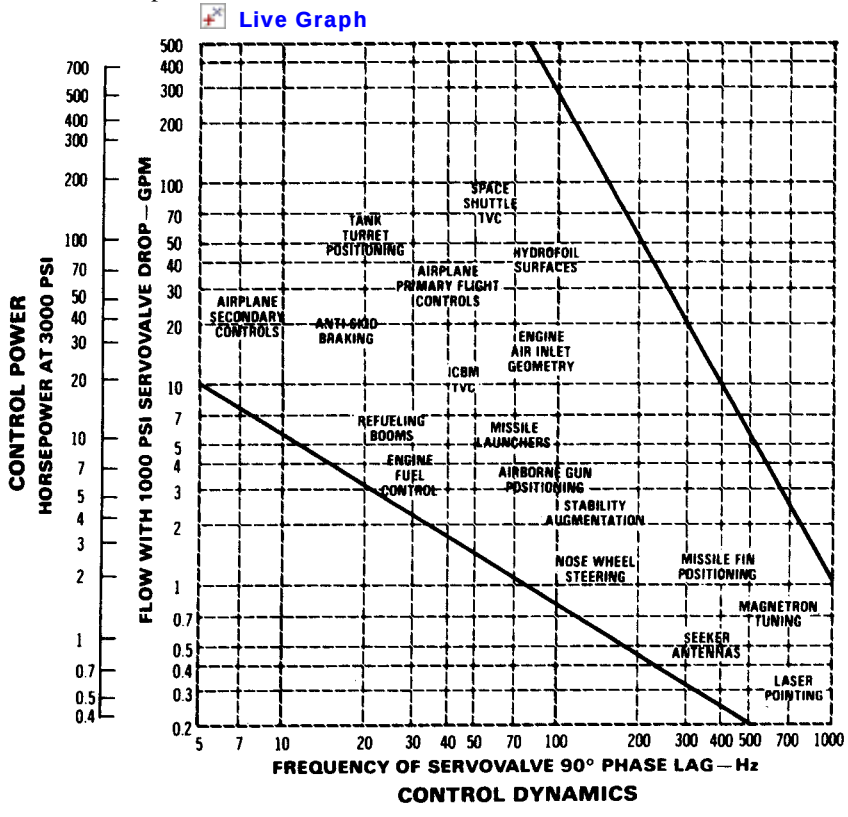


Figure 57 Spectrum of aerospace applications of electrohydraulic servomechanisms. (Courtesy of Moog, Inc., East Aurora, NY.)

required to produce stability results in significantly poorer dynamic performance. But only case (d), with a dynamic pressure feedback servovalve, combines good dynamic performance with a significant improvement in static stiffness to external load disturbances.

10.6 Range of Control for Electrohydraulic and Electromechanical Servosystems

Two principal parameters characterize the range of control for most electrohydraulic servomechanisms[36]: power level and dynamic response. Figure 55 is a graph of control power versus control dynamics showing three dominant ranges of control for electrohydraulic servomechanisms. The middle region of the graph represents the range where electrohydraulic servomechanisms traditionally have dominated applications. Yet developments of high-effeciency and high-speed-of-response rare earth servomotors have led to increased numbers of electromechanical servomechanism applications in parts of this region. For applications requiring low power levels and low dynamic response, electromechanical solutions are generally preferred. There remains a region involving high power level and high dynamic response where neither electrohydraulic nor electromechanical solutions are available.

Areas of typical applications of electrohydraulic servosystems are plotted on the control power versus control dynamics graphs of Figs. 56 and 57. Future needs for both electro-

mechanical and electrohydraulic servomechanisms are lower cost, higher energy efficiency, and higher dynamic response.

REFERENCES

1. G. S. Brown and D. P. Campbell, *Principles of Servomechanisms,* Wiley, New York, 1948.
2. M. F. Marx and T. D. Lewis, ''Electromagnetic Force Motor Design Using Rare Earth-Cobalt 1 Permanent Magnets,'' NAECON 1977 RECORD, National Aerospace & Electronics Conference, pp. 1119–1126.
3. M. A. Davis, ''High Performance Electromechanical Servoactuation Using Brushless DC Motors,'' Technical Bulletin 150, Moog Inc., East Aurora, NY, April 1984.
4. ''Electrical and Electronics 1986,'' *Machine Design* **58**(12), 6–48 (1986).
5. B. C. Kuo and J. Tal, *Incremental Motion Control—DC Motors and Control Systems,* Vol. I, SRL Publishing, Champaign, IL, 1978.
6. J. B. Leonard, ''Electromechanical Primary Flight Control Activation Systems for Fighter/Attack Aircraft,'' Paper No. 821435, Society of Automotive Engineers, Troy, MI, 1982.
7. B. Sawyer and J. T. Edge, ''Design of a Somarium Cobalt Brushless DC Motor for Electromechanical Automator Applications,'' NAECON 1977 RECORD, National Aerospace & Electronics Conference, pp. 1108–1112.
8. M. J. Cronin, ''Design Aspects of Systems in All-Electric Aircraft,'' Paper No. 821436, Society of Automotive Engineers, Troy, MI, 1982.
9. *DC Motors, Speed Controls, Servo Systems,* 5th ed., Electro-Craft Corp., Hopkins, MN, 1980.
10. *Speed and Position Control Systems Distributor Catalog,* Robbins Myers, Inc., Hopkins, MN, Form No. MM-7400-00, January 1988.
11. E. Aha, ''Brushless DC Motors—A Tutorial Study,'' *Motion,* March/April 1987, pp. 20–26.
12. S. Meshkat, ''Servo System Design—A Tutorial Study. Vectorial Control of Brushless DC Motors and AC Induction Motors,'' *Motion,* September/October 1986, pp. 19–23.
13. R. Benzer, ''Single-Chip Brushless Motor Controller,'' *Machine Design,* June 9, 1988, pp. 140–144.
14. *Motion Control Engineering Handbook—DC Servo/Tachometers/Brushless DC,* Magnetic Technology, Inc., Canoga Park, CA, 1985.
15. *Direct Drive Engineering Handbook—DC Torque Motors/Tachometers/Brushless DC,* Magnetic Technology, Inc., Canoga Park, CA, 1985.
16. B. K. Hose, ''Adjustable Speed AC Drives—A Technology Status Review,'' *Proceedings of the IEEE* **70**(2), (1982).
17. A. Kusko and D. G. Galler, ''Survey of Microprocessors in Industrial Motor Drive Systems,'' *IEEE, Industry Applications Society,* 1982, pp. 435–438.
18. J. E. Gibson and F. B. Tuteur, *Control System Components,* McGraw-Hill, New York, 1958, pp. 276–304.
19. B. C. Kuo, *Theory and Applications of Step Motors,* West Publishing, New York, 1974.
20. B. C. Kuo, *Incremental Motion Control—Step Motors and Control Systems,* Vol. II, SRL Publishing, Champaign, IL, 1979.
21. ''1.8 deg. PM Hybrid Stepper Motors and Controls,'' Catalog ST-l, Bodine Electric, Chicago, IL, 1981.
22. B. H. Carlisle, ''Stepping Motors: Edging into Servomotor Territory,'' *Machine Design* **58**(26), 88–100 (1986).
23. M. A. Lewis, ''Design Strategies for High-Performance Incremental Servos,'' in *Proceedings of the Sixth Annual Symposium on Incremental Motion Control Systems and Devices,* B. C. Kuo (ed.), University of Illinois, Urbana, IL, 1977, pp. 141–151.
24. ''Motor Selector, DC Motor Selection and Servo System—Design Software for the IBM PC and Compatibles,'' Par Tech Engineering, Windham, ME.
25. *Machine Design,* Fluid Power Reference Issue, September 17, 1987.
26. R. P. Lambeck, *Hydraulic Pumps and Motors—Selection and Application for Hydraulic Power Control Systems,* Marcel Dekker, New York, 1983.

27. *Fluid Power Design Engineers Handbook,* Parker-Hannifin Corp., Cleveland, OH, 1973.
28. G. B. Keller, *Hydraulic System Analysis,* Industrial Publishing, Cleveland, OH, 1969.
29. H. E. Merritt, *Hydraulic Control Systems,* Wiley, New York, 1967.
30. J. F. Blackburn, G. Reethof, and J. L. Shearer, *Fluid Power Control,* MIT Press, Cambridge, MA, 1960.
31. E. Lewis and H. Stern, *Design of Hydraulic Control Systems,* McGraw-Hill, New York, 1962.
32. M. Guillon, *Hydraulic Servo Systems,* Plenum, New York, 1969.
33. J. Watton, *Fluid Power Systems,* Prentice-Hall International, Hertfordshire, 1989.
34. *Electrohydraulic Servomechanisms in Industry,* Moog, Inc., East Aurora, NY (undated).
35. L. H. Geyer, ''Controlled Damping through Dynamic Pressure Feedback,'' Technical Bulletin 101, Moog, Inc., East Aurora, NY, April 1972.
36. R. H. Maskrey and W. J. Thayer, ''A Brief History of Electrohydraulic Servomechanisms,'' *ASME Transactions, Journal of Dynamic Systems, Measurement and Control* **100** (1978).
37. K. N. Reid, ''Fluid Power Control I,'' Course Notes, School of Mechanical and Aerospace Engineering, Oklahoma State University, Stillwater, OK, 1987.
38. *Industrial Hydraulics Manual,* No. 935100-A, Vickers, Inc., Troy, MI, copyright by Sperry Rand Corp., 1st ed., 1970.
39. W. J. Thayer, ''Transfer Functions for Moog Servovalves,'' Technical Bulletin 103, Moog Inc., East Aurora, NY, January 1965.
40. G. J. Blickley, ''Servo Valve Becomes Digital Actuator,'' *Control Engineering,* June 1986, pp. 76–77.
41. E. B. Canfield, *Electromechanical Control Systems and Devices,* Wiley, New York, 1965, pp. 143–197.
42. T. P. Neal, ''Performance Estimation for Electrohydraulic Control Systems,'' Technical Bulletin 126, Moog, Inc., East Aurora, NY, November 1974.
43. *Stepper Motors: Permanent Magnet 7.5° Step Angle,* Catalog No. STM-REM 987-5M-RL, Crouzet Control, Inc., Schaumburg, IL, 1987.
44. W. E. Wilson, ''Performance Criteria for Positive-Displacement Pumps and Fluid Motors,'' *Transaction of the ASME,* May 1986.
45. J. L. Shearer, ''Dynamic Characteristics of Valve-Controlled Hydraulic Servomotors,'' *ASME Transactions* **76,** 895–903 (1954).
46. P. F. Meyfarth, ''Analytical Comparison of the Linear and Bang-Bang Control of Pneumatic Servomechanisms,'' Thesis, Department of Mechanical Engineering, Massachusetts Institute of Technology, Cambridge, MA, 1958.
47. P. F. Meyfarth, ''Dynamic Response Plots and Design Charts for Third-Order Linear Systems,'' Research Memorandum 7401-3, Massachusetts Institute of Technology, Dynamic Anaysis and Control Laboratory, Cambridge, MA, September 1958.

BIBLIOGRAPHY

Chitayat, A., ''Brushless DC Linear Motors,'' *Motion,* September/October 1987, pp. 22–23.
Fitzgerald, A., and C. Kingley, *Electric Machinery,* McGraw-Hill, New York, 1961.
Humphrey, W. M., *Introduction to Servomechanical System Design,* Prentice-Hall, Englewood Cliffs, NJ, 1973.
Koopman, G., ''Operating Characteristics of 2-phase Servomotors,'' *Transactions of the AIEE* **68,** 319–329 (1949).
Kusko, A., *Solid-State DC Motor Drives,* MIT Press, Cambridge, MA, 1969.
Marinko, J. A.,''PWM Servo-Amplifiers: A Tutorial Study,'' *Motion,* July/August 1987, pp. 3–8.
Mazurkiewicz, J., ''Brushless Motors and Brushless Motor Controllers,'' *Motion,* November/December 1986, pp. 14–19.
Meshkat, S., ''Vectorial Control of Brushless DC Motors and AC Induction Motors,'' *Motion,* September/October 1986, pp. 19–23, .

Persson, E. K., ''Brushless DC Motors in High-Performance Servo Systems,'' in *Proceedings, Fourth Annual Symposium on Incremental Motion Control Systems and Devices,* B. C. Kuo (ed.), University of Illinois, Urbana, IL, 1975, pp. T1–T16.

Proceedings, Conference on Small Electrical Machines, Institution of Electrical Engineers, London, March 30–31, 1976.

Puchstein, L., and Conrad, *AC Machines,* 3rd ed., Wiley, New York, 1954.

Schept, B., ''Servo System Design—A Tutorial Study,'' Part 3 of 8, in *Motion,* 4th Quarter, 1985, pp. 22–30.

Small and Special Electrical Machines, Publication No. 202, Institution of Electrical Engineers, London, September 1981.

TaI, J., ''Quantization Errors in Digital Servo Systems,'' in *Motion,* September/October 1986, pp. 10–13.

Yeaple, F., *Fluid Power Design Handbook,* Marcel Dekker, New York, 1984.